Industrial Crops & Products 246 (2026) 123380

Contents lists available at ScienceDirect

Industrial Crops & Products

journal homepage: www.elsevier.com/locate/indcrop

Integrated evaluation of *Chrysanthemum* × *morifolium* (Ramat.) Hemsl. essential oil, compared with α-terpineol, β-pinene, borneol, and camphor: *In vitro* and *in situ* antibacterial activity against selected microorganisms and insecticidal effects on bruchine beetles

Miroslava Kačániová [a,b,*], Minhang Qiao [a], Guiguo Zhang [c,d], Alessandro Bianchi [e,f], Joel Horacio Elizondo-Luevano [g], Anis Ben Hsouna [h,i], Rania Ben Saad [h], Zhaojun Ban [j], Li Li [k], Jian Lou [j], Maciej Irenuesz Kluz [b], Stefania Garzoli [l,**]

[a] *Institute of Horticulture, Faculty of Horticulture and Landscape Engineering, Slovak University of Agriculture, Trieda Andreja Hlinku 2, Nitra 94976, Slovakia*
[b] *School of Medical & Health Sciences, VIZJA University, Okopowa 59, Warszawa 01043, Poland*
[c] *Department of Animal Nutrition, Shandong Agricultural University, Taian City 271018, China*
[d] *China-South Korea International Joint Laboratory of Functional Polysaccharides in Shandong Province, Taian City 271018, China*
[e] *Department of Agriculture, Food and Environment, University of Pisa, Via del Borghetto 80, Pisa 56124, Italy*
[f] *Department of Pharmacy, University of Pisa, via Bonanno Pisano 6, Pisa 56126, Italy*
[g] *Laboratory of Natural Sciences. Biomolecular Innovation Group, Faculty of Agronomy, Universidad Autónoma de Nuevo León, Cd. Gral, Escobedo, Nuevo León 66050, Mexico*
[h] *Laboratory of Biotechnology and Plant Improvement, Centre of Biotechnology of Sfax, B.P "1177", Sfax 3018, Tunisia*
[i] *Department of Environmental Sciences and Nutrition, Higher Institute of Applied Sciences and Technology of Mahdia, University of Monastir, Monastir, Tunisia*
[j] *School of Biological and Chemical Engineering Zhejiang University of Science and Technology, Zhejiang Provincial Key Laboratory of Chemical and Biological Processing Technology of Farm Products, Zhejiang Provincial Collaborative Innovation Center of Agricultural Biological Resources Biochemical Manufacturing, Hangzhou 310023, China*
[k] *Key Laboratory for Agro-Products Postharvest Handling of Ministry of Agriculture and Rural Affairs, College of Biosystems Engineering and Food Science, Zhejiang University, Hangzhou 310058, China*
[l] *Department of Chemistry and Technologies of Drug, Sapienza University, P. le Aldo Moro, 5, Rome 00185, Italy*

ARTICLE INFO

Keywords:
Chrysanthemum × *morifolium* (Ramat.) Hemsl.
Essential oil
α-terpineol
β-pinene
Borneol
Camphor
Antimicrobial activity
Biofilm
MALDI-TOF MS
Food model systems
Insecticidal activity

ABSTRACT

The present study evaluated the antimicrobial, antibiofilm, *in situ* food model, and insecticidal activities of *Chrysanthemum* × *morifolium* (Ramat.) Hemsl. white essential oil (CMEO) in comparison with its major constituents α-terpineol, β-pinene, endo-borneol, and camphor. CMEO was chemically characterized by GC–MS and contained mainly α-terpineol, capric acid, β-pinene, α-pinene, and camphene, together accounting for almost the entire identified fraction. *In vitro*, CMEO showed broader and stronger antimicrobial effects than all the tested constituents against a panel of Gram-negative and Gram-positive bacteria and *Candida* spp., as reflected by markedly lower MIC_{50}/MIC_{90} values, particularly for *Yersinia enterocolitica* and *Candida albicans*. In vapor phase tests on apple, pear, parsley, and Hokkaido pumpkin slices, CMEO produced high and concentration-dependent growth inhibition in all microorganisms, including a biofilm-forming *Salmonella enterica* strain, whereas the individual constituents showed only limited or inconsistent activity, particularly at lower concentrations. Crystal violet assays showed that CMEO inhibited established *Salmonella enterica* biofilms with MIC_{50} = 2.46 mg/mL and MIC_{90} = 2.64 mg/mL, while the individual constituents required markedly higher concentrations, with α-terpineol showing the strongest activity among them (MIC_{50} = 1.38–3.60 mg/mL). MALDI-TOF MS profiles and MSP dendrograms confirmed clear and time-dependent differences between planktonic and surface-attached

* Corresponding author at: Institute of Horticulture, Faculty of Horticulture and Landscape Engineering, Slovak University of Agriculture, Trieda Andreja Hlinku 2, Nitra 94976, Slovakia.
** Corresponding author.
E-mail addresses: m.kacaniova@vizja.pl (M. Kačániová), qomohoo@163.com, 19863818523@163.com (M. Qiao), zhanggg@sdau.edu.cn (G. Zhang), alessandro.bianchi@phd.unipi.it (A. Bianchi), joel.elizondolv@uanl.edu.mx (J.H. Elizondo-Luevano), benhsounanis@gmail.com (A. Ben Hsouna), raniabensaad@gmail.com (R. Ben Saad), banzhaojun@zust.edu.cn (Z. Ban), lili1984@zju.edu.cn (L. Li), 106018@zust.edu.cn (J. Lou), m.kluz@vizja.pl (M.I. Kluz), stefania.garzoli@uniroma1.it (S. Garzoli).

https://doi.org/10.1016/j.indcrop.2026.123380
Received 24 February 2026; Received in revised form 27 April 2026; Accepted 28 April 2026
Available online 5 May 2026

cells on wood and stainless steel, with more pronounced shifts in the presence of CMEO. In insecticidal assays, CMEO caused high mortality of *Callosobruchus maculatus* and *Megabruchidius dorsalis* down to 25–12.5%, whereas the individual constituents showed only moderate effects, with α-terpineol being the most active (LC_{50} = 24.74% for *C. maculatus*; LC_{90} = 32.62% for *M. dorsalis*). Overall, the data demonstrate that CMEO consistently outperforms tested individual constituents across all models, confirming that no single constituent alone accounts for the observed biological activity of the oil.

1. Introduction

Chrysanthemum × *morifolium* (Ramat.) Hemsl., known in traditional Chinese medicine as "Juhua", is one of the most important medicinal and ornamental species of the genus Chrysanthemum (Asteraceae). In China, it has been cultivated for more than 3000 years, and its dried inflorescences have traditionally been used to treat inflammation, fever, headaches, ocular disorders, and hypertension, commonly in the form of chrysanthemum tea or oil (Youssef et al., 2020). Modern phytochemical and pharmacological research supports its traditional use, revealing that the genus *Chrysanthemum* is a rich source of flavonoids, terpenoids, polysaccharides, and unsaturated fatty acids responsible for a broad range of biological activities, including antioxidant, antimicrobial, anti-inflammatory, anticancer, antiallergic, anti-obesity, immunomodulatory, hepatoprotective, and nephroprotective effects (Hadizadeh et al., 2022).

The essential oil (EO) extracted from the inflorescences of *C.* × *morifolium* exhibits a complex chemical composition that has been extensively characterized through GC/MS analysis. One study identified 55 volatile compounds accounting for 98.98% of the total oil composition (Youssef et al., 2020). Camphor is consistently reported as the major constituent (approximately 14.56%), followed by curcumene, τ-eudesmol, pentacosane, borneol, and copaene (Youssef et al., 2020). A similar composition was observed in the cultivar *C.* × *morifolium* cv. Fubaiju, where camphor again dominated, accompanied by substantial proportions of 1,8-cineole, β-curcumene, bornyl acetate, α-zingiberene, β-elemene, α-bisabolol, borneol, and eugenol (Zhan et al., 2021). Phytochemical profiling of 23 genotypes further revealed industrially relevant concentrations of α-pinene, camphene, eucalyptol, cis-chrysanthenol, (1S)-camphor, and endo-borneol (Gajbhiye et al., 2025). Common components across EO samples included α-pinene, myrcene, α-humulene, β-caryophyllene, spathulenol, and caryophyllene oxide (Kuang et al., 2018). Notably, significant variability occurs across cultivars: yellow *C.* × *morifolium* contained up to 51% terpenoids, whereas red and pink cultivars exhibited only about 15% (Sharma et al., 2023), which may substantially influence the biological properties of each oil.

The antimicrobial activity of *C.* × *morifolium* EO has been demonstrated in several *in vitro* studies. The oil showed promising antibacterial effects against *Escherichia coli*, *Staphylococcus aureus*, *Salmonella* Enteritidis, *Pseudomonas aeruginosa*, and *Bacillus subtilis* (Kuang et al., 2018). Among these, *P. aeruginosa* displayed the greatest sensitivity with an inhibition zone of 20.43 mm, while *E. coli* exhibited a zone of 12.29 mm (Kuang et al., 2018). Comparative studies with EO from *C. indicum* revealed moderate activity against Gram-positive bacteria, though *C. indicum* generally demonstrated stronger antibacterial effects. *C.* × *morifolium* EO exhibited MIC values of 62.5 μg/mL against *B. subtilis*, *Streptococcus agalactiae*, and *Streptococcus pyogenes*, while activity against Gram-negative bacteria and fungi was weaker (MIC > 500 μg/mL) (Youssef et al., 2020). MIC values of chrysanthemum extracts ranged from 5 to 10 mg/mL for *S. enterica* and *Bacillus cereus*, and 10–20 mg/mL for *S. aureus* and *E. coli* (Hodaei et al., 2021). Applications in food safety have also been explored: antimicrobial formulations containing *C.* × *morifolium* EO demonstrated potent inhibitory effects against *Aeromonas hydrophila*, *Salmonella choleraesuis*, *S. enterica*, *Shigella sonnei*, *Vibrio parahaemolyticus*, *V. vulnificus*, *B. subtilis*, *L. monocytogenes*, and *S. aureus* (Jung, 2009; Sun et al., 2010). These effects are attributed to dominant components such as camphor and 1, 8-cineole, but also to the combined contribution of multiple terpenoids and phenolic compounds.

α-Terpineol, the dominant oxygenated monoterpene of CMEO (20.1%), exerts antibacterial effects primarily through disruption of cell membrane integrity, impairing of electron transport and collapsing the proton motive force, with activity against foodborne pathogens decreasing in the order *E. coli* O157:H7 > *S. typhimurium* > *L. monocytogenes* > *S. aureus* (Li et al., 2014; Yang et al., 2023). β-Pinene, a bicyclic monoterpene present in numerous essential oils, exhibits significant standalone antimicrobial activity. Only the positive enantiomers of α- and β-pinene are biologically active, while their negative counterparts show no detectable antimicrobial effects even at concentrations up to 20 mg/mL (Silva et al., 2012). MIC values for β-pinene against bacteria and fungi range from 117 to 4150 μg/mL (Silva et al., 2012). Synthetic β-pinene derivatives, such as bis-hydronopyl compounds, have displayed remarkable antifungal potency; for example, bis-hydronopyl dimethylammonium bromide exhibited an EC_{50} of 0.538 μg/mL against *Colletotrichum acutatum*, outperforming carbendazim (Feng et al., 2021a). Endo-Borneol (7.0%) and camphor (6.3%), both oxygenated monoterpenes present in CMEO, have been documented to disrupt bacterial membranes and inhibit respiratory chain function; borneol was found more effective than camphor against *S. aureus* in disc diffusion assays, and EOs rich in camphor and borneol demonstrated insecticidal activity against *C. maculatus* (Chen et al., 2013; El Abdali et al., 2022).

Several studies also highlight a relationship between pinene content and antibiofilm or antimicrobial properties of EO. *Cuminum cyminum* L. EO, rich in terpineol, carene, and pinene, inhibited *Salmonella* spp., and its antimicrobial efficacy correlated positively with the concentration of aldehydes (particularly cuminaldehyde) and terpene compounds (primarily α-pinene and β-pinene) (Palomares-Navarro et al., 2022). This EO (cuminaldehyde 44.2%, β-pinene 15.1%, γ-terpinene 14.4%, p-cymene 14.2%) exerted strong effects against Gram-positive and Gram-negative bacteria, including *Salmonella typhimurium*, twelve *Vibrio* species, and yeast strains (Ghannay et al., 2022). *Citrus limon* (L.) EO (limonene 60.7%, β-pinene 12.6%, γ-terpinene 10.3%) demonstrated strong antibiofilm activity against *S. enterica*, with MIC and crystal violet assays confirming its capacity to inhibit and disrupt biofilms, while MALDI-TOF MS analyses revealed alterations in bacterial protein profiles on glass and stainless steel surfaces (Kačániová et al., 2024). β-Pinene also reduced biofilm mass of drug-resistant *Enterococcus faecalis*, and other EO rich in α-pinene and borneol, such as rosemary oil, showed antimicrobial activity at low concentrations (Vidaković Knežević et al., 2025).

Beyond antimicrobial properties, α-terpineol, β-pinene, camphor, and borneol also exhibit notable insecticidal activity. EO from *Juniperus recurva* Buch.-Ham. ex D. Don, containing 39.18% 2-β-pinene, showed strong fumigant toxicity against *Callosobruchus maculatus* and *C. chinensis* (Gupta et al., 2023). Terpenes such as α-pinene and β-caryophyllene have demonstrated repellent, insecticidal, antioviposition, and egg-hatching inhibitory effects against *C. chinensis*, reducing adult preference during oviposition tests and causing dose-dependent fumigant and contact toxicity (Chaubey, 2014). α-Pinene and geraniol acted as repellents at LC_{50} and LC_{95} levels, while other isolated compounds exhibited contact toxicity, reduced population growth (*trans*-anethole), decreased oviposition and emergence (geraniol, eugenol), and repellent

actions (geraniol, α-pinene) toward *C. maculatus* (Barbosa et al., 2021). High toxicity of *Nigella sativa* L. EO has been linked to its content of o-cymene, cyclofenchene, β-pinene, and carvacrol (Matos et al., 2020). EO rich in carvacrol and monoterpenoids such as α-pinene, thymol, and limonene exhibited strong fumigant activity against various stored-product pests (Et-tazy et al., 2025). Pinene monoterpenes from *Eucalyptus* spp. L'Hér., *Rosmarinus officinalis* L., *Pinus* spp. L., and *Lavandula officinalis* Chaix possess antiviral, antibacterial, fungicidal, and insecticidal properties and are widely used in the food and fragrance industries (Ribeiro et al., 2025; Said-Al Ahl et al., 2024). Sharifian et al. also reported the efficacy of *Artemisia vulgaris* L. EO, dominated by α-pinene, against bean weevils (*Callosobruchus* spp.) (Ribeiro et al., 2025).

Despite the extensive phytochemical and *in vitro* antimicrobial characterization of *C.* × *morifolium* essential oil, no studies to date have evaluated its *in situ* antimicrobial efficacy, either on food-contact materials, biotic or abiotic surfaces, or within realistic contamination models. Existing research has focused exclusively on laboratory-based assays, while *in situ* evaluations have been reported only for essential oils of other botanical origins containing similar terpenoid constituents, such as limonene-, α-pinene–, or β-pinene–rich oils. A comparable research gap also exists for the *in situ* insecticidal activity of *C.* × *morifolium* EO, as published studies address only fumigant or contact toxicity of other terpenoid-rich essential oils or isolated monoterpenes toward bruchine beetles. Consequently, no integrated study has simultaneously examined both the antimicrobial and insecticidal properties of *C.* × *morifolium* EO under *in situ* conditions, nor compared them directly with α-terpineol, β-pinene, endo-borneol, and camphor as major constituents. These constituents were selected because they represent the dominant oxygenated and hydrocarbon monoterpene fractions of CMEO and each possesses documented independent antimicrobial and insecticidal activity. To the best of our knowledge, this is the first study to simultaneously evaluate the antimicrobial and insecticidal activity of CMEO and its major individual constituents α-terpineol, β-pinene, endo-borneol, and camphor under both *in vitro* and *in situ* conditions. Importantly, the most abundant constituent of an essential oil is not necessarily its principal bioactive component, as minor or moderate constituents may carry a disproportionate share of the biological effect through synergistic interactions with other oil components (Kong et al., 2025).

This gap highlights the novelty and scientific relevance of the present work, which provides the first comprehensive in situ assessment of these bioactivities. The aim of this study is to perform an integrated evaluation of *Chrysanthemum* × *morifolium* essential oil (CMEO) and its major constituents α-terpineol, β-pinene, endo-borneol, and camphor by (i) characterizing the chemical composition of CMEO using GC-MS and (ii) comparing the *in vitro* and *in situ* antibacterial activity against a selected panel of microorganisms, as well as the insecticidal efficacy against bruchine beetles. This comparative approach seeks to clarify whether the biological activity of the whole essential oil can be attributed to individual constituents or to their combined contribution, thereby contributing to the development of natural antimicrobial and insecticidal agents.

2. Material and methods

2.1. Characterization of the essential oil

The analyses were carried out using white chrysanthemum essential oil (*C.* × *morifolium* Ramat Hemsl., white chrysanthemum flower oil) supplied by GuiLin Four Seasons Sunshine (Guilin, China), Batch No. 202240529. The quality parameters of the oil, provided in its official specification sheet, were used to characterize the basic physicochemical properties of the material. According to the quality certificate, the oil exhibits a yellow-green to light-brown colour and a liquid physical state. Its odour is described as characteristic of white chrysanthemum, without foreign or off notes. The relative density (25/25 °C) ranges between 0.936 and 1.000, and the refractive index (20 °C) between 1.490 and 1.523. The oil is fully miscible in three volumes of 95% ethanol (*v/v*), producing a clear solution. The specification lists an acid value ≤ 50 and an ester value ≥ 50, which aligns with the parameters typical for terpenoid-rich essential oils. The declared major constituents include camphor, isoborneol, α-terpineol, bornyl acetate, and α-curcumene, along with other terpenoids commonly found in this botanical species. The oil was stored as recommended, in a cool, dry, and well-ventilated environment, protected from contaminants and sources of heat. It was supplied in clean aluminium containers or amber glass bottles, and the manufacturer specifies a shelf-life of 36 months for unopened product.

The components α-terpineol ($\geq$ 96%), β-pinene ($\geq$ 99%), (-)-borneol (97%), and (±)-camphor (96%) were purchased at the stated purity from Sigma-Aldrich (Merck), Darmstadt, Germany.

2.2. Volatile profile analysis of CMEO by GC–MS

The volatile composition of *C.* × *morifolium* essential oil (CMEO) was determined by gas chromatography coupled with mass spectrometry (GC-MS). Analyses were carried out on a Clarus 500 system (PerkinElmer, Waltham, MA, USA) equipped with both a flame ionization detector (FID) and a mass spectrometric detector. Separation of volatile compounds was achieved on a VF-5ms capillary column (Varian Factor Four, 60 m × 0.25 mm i.d., film thickness 1.0 μm). The oven temperature was initially set at 60 °C, then increased at a rate of 6 °C/min to 220 °C, and maintained at this final temperature for 20 min. Helium was used as the carrier gas at a constant flow rate of 1.0 mL/min (Monacci et al., 2025).

Identification of individual components was based on comparison of the recorded mass spectra with those included in the Wiley 2.2 and NIST 11 mass spectral libraries. In addition, linear retention indices (LRIs) were calculated by co-injection of a homologous series of n-alkanes (C_8-C_{25}) under identical chromatographic conditions, and the obtained values were compared with reference data. The relative abundance of each constituent was calculated from the peak areas in the total ion chromatogram and expressed as a percentage of the total identified composition. No internal standards were used, and no response factor corrections were applied. All measurements were performed in triplicate to ensure analytical reliability and reproducibility.

2.3. In vitro antimicrobial assessment of CMEO and its major constituents

2.3.1. Bacterial and yeast strains and culture maintenance

The antibacterial and antifungal activities of CMEO, (-)-α-terpineol, β-pinene, (-)-borneol, and (±)-camphor were evaluated against a representative panel of reference microorganisms. The Gram-positive bacteria included *Enterococcus faecalis* (CCM 4224), *Listeria monocytogenes* (CCM 4699), and *Staphylococcus aureus* (CCM 4223). The Gram-negative panel comprised *Escherichia coli* (CCM 3954), *Salmonella enterica* subsp. *enterica* (CCM 3807), and *Yersinia enterocolitica* (CCM 7204^T). The yeast strains used in this study were *Candida albicans* (CCM 8261), *C. glabrata* (CCM 8270), *C. krusei* (CCM 8271), *C. parapsilosis* (CCM 8260), and *C. tropicalis* (CCM 8264).

Bacterial strains were routinely maintained and propagated in Mueller-Hinton broth (MHB; Oxoid, Basingstoke, UK), whereas yeasts were cultured in Sabouraud Dextrose broth (SDB; Oxoid). All cultures were incubated for 24 h, at 37 °C for bacteria and 25 °C for yeasts. Prior to each assay, the inoculum density was adjusted to the 0.5 McFarland turbidity standard, corresponding to approximately 1.5×10^8 CFU/mL, to ensure consistency and reproducibility across experiments. For antibiofilm assays, biofilm-forming isolates of *S. enterica*, distinct from the reference strain, were obtained from milk samples. These isolates were confirmed as *S. enterica* by molecular identification based on sequencing and subsequently used as biofilm-producing test strains.

2.3.2. Disc diffusion-based screening of antimicrobial activity

The initial screening of the antimicrobial activity of CMEO and (-)-α-terpineol, β-pinene, (-)-borneol, and (±)-camphor were carried out using a disc diffusion assay. Sterile paper discs (6 mm in diameter; Oxoid, Basingstoke, UK) were loaded with 10 μL of each test substance at the required concentrations and placed onto the surface of Mueller-Hinton agar for bacterial strains or Sabouraud Dextrose agar for yeast strains. Prior to disc application, each plate was uniformly inoculated with 100 μL of microbial suspension adjusted to the 0.5 McFarland standard (1.5×10^8 CFU/mL).

The inoculated plates were incubated for 24 h at 37 °C for bacteria and 24 h at 25 °C for yeasts. After incubation, the diameters of the inhibition zones (mm) surrounding each disc were measured and taken as indicators of antimicrobial efficacy. The size of the clear zones was qualitatively interpreted as reflecting weak, moderate, or strong antimicrobial responses.

Discs treated with the corresponding solvent served as negative controls, whereas standard antimicrobial agents were used as positive controls: cefoxitin for Gram-positive bacteria, gentamicin for Gram-negative bacteria, and fluconazole for yeasts (all from Oxoid, Basingstoke, UK). The assay followed the procedure described by Kačániová et al. (2021), with minor modifications to account for the hydrophobic and volatile nature of CMEO and the tested constituents. All experimental variants were performed at least in triplicate, and the results were expressed as mean values ± standard deviation.

2.3.3. Broth microdilution assay for MIC_{50} and MIC_{90} determination

The minimum inhibitory concentrations (MIC_{50} and MIC_{90}) of CMEO and (-)-α-terpineol, β-pinene, (-)-borneol, and (±)-camphor were determined by a broth microdilution assay in sterile 96-well microtiter plates. Each well contained 50 μL of a standardized microbial suspension (0.5 McFarland) mixed with 50 μL of a twofold serial dilution of the tested compound. Dilutions were prepared in Mueller–Hinton broth (MHB; Oxoid, Basingstoke, UK) for bacterial strains and in Sabouraud Dextrose broth (SDB; Oxoid, Basingstoke, UK) for yeasts. All microbial suspensions were adjusted to approximately 1.5×10^8 CFU/mL, corresponding to the 0.5 McFarland standard.

The tested concentration range of CMEO and (-)-α-terpineol, β-pinene, (-)-borneol, and (±)-camphor was 10.0–0.00485 mg/mL, following a procedure previously optimized for essential oils and their constituents (Kačániová et al., 2023b). For each assay, sterile broth without inoculum served as a negative control, whereas broth inoculated with the test microorganism but without any test compound was used as a positive growth control.

Microplates were incubated for 24 h at 37 °C for bacteria and 25 °C for yeasts. Microbial growth was subsequently evaluated spectrophotometrically at 570 nm using a GloMax microplate reader (Promega, Madison, WI, USA). MIC_{50} and MIC_{90} were defined as the lowest concentrations of CMEO or the tested constituents that resulted in 50% and 90% inhibition of visible growth, respectively, compared with the untreated control wells. All measurements were performed in triplicate to ensure reliability and reproducibility. Final MIC_{50} and MIC_{90} values were calculated using Probit analysis to obtain accurate inhibition thresholds.

2.4. In situ antimicrobial performance of CMEO and its major constituents in food model systems

The *in situ* antimicrobial activity of CMEO and the tested constituents was evaluated using fresh food matrices (apple, pear, parsley, and Hokkaido pumpkin) to simulate realistic contamination scenarios. Sterile Petri dishes (60 mm in diameter) were prepared by pouring Mueller–Hinton agar (for bacteria) or Sabouraud Dextrose agar (for yeasts) and allowing the medium to solidify. Commercial produce was thoroughly washed, cut into uniform slices approximately 0.5 cm thick, and air-dried under aseptic conditions before being placed directly onto the agar surface.

Each slice was inoculated with 10 μL of a standardized microbial suspension adjusted to the 0.5 McFarland standard (1.5×10^8 CFU/mL). To promote uniform colonization, several shallow punctures were made in the surface of the slice using a sterile pipette tip, and the inoculum was carefully distributed into these punctures.

Vapor phase treatment was performed by attaching sterile filter-paper discs to the inner surface of the Petri dish lids. The discs were impregnated with ethyl acetate solutions of CMEO or the tested constituents at concentrations of 500, 250, 125, and 62.5 μL/L. Discs treated with ethyl acetate alone served as negative controls. The dishes were tightly sealed with Parafilm to minimize volatilization and incubated for seven days at 37 °C. All experimental variants were conducted in triplicate.

After incubation, microbial growth on the surface of the food matrices was assessed using conventional culture-based methods. Semi-quantitative analysis of growth inhibition was subsequently performed with ImageJ software (NIH, Bethesda, MD, USA), following a modified procedure described by Kačániová et al. (2020). This approach enabled an objective evaluation of the *in situ* antimicrobial performance of CMEO and the tested constituents under conditions representative of food storage environments.

2.5. Evaluation of antibiofilm properties

2.5.1. Crystal violet microtiter assay for quantification of biofilm inhibition

The antibiofilm effects of CMEO and the tested constituents were examined using a crystal violet microtiter plate assay adapted from Kačániová et al. (2025). Standardized bacterial suspensions were inoculated into Mueller–Hinton broth (MHB) dispensed in sterile 96-well microtiter plates, and CMEO or the tested constituents were added as twofold serial dilutions within the concentration range 10.0–0.0048 mg/mL. The plates were incubated under static conditions for 24 h at 37 °C to allow biofilm development.

Following incubation, planktonic cells were carefully removed, and the wells were gently rinsed with sterile phosphate-buffered saline (PBS) to eliminate non-adherent bacteria. The surface-associated biofilm was stained with 0.1% (w/v) crystal violet for 15 min, after which excess dye was removed by repeated washing with distilled water, and the plates were air-dried. The bound crystal violet was then solubilized with 95% ethanol, and absorbance was measured at 570 nm.

The minimum biofilm inhibitory concentration (MBIC) was defined as the lowest concentration of CMEO or the tested constituents that completely prevented visible biofilm formation. $MBIC_{50}$ and $MBIC_{90}$, corresponding to 50% and 90% reductions in biofilm biomass relative to untreated controls, were calculated using Probit analysis to obtain precise inhibition thresholds. All antibiofilm experiments were performed in three independent replicates.

2.5.2. MALDI-TOF MS profiling of biofilm responses to CMEO and its major constituents treatment

The impact of CMEO and the tested constituents on the structural and compositional characteristics of *S. enterica* biofilms was examined using matrix-assisted laser desorption/ionization time-of-flight mass spectrometry (MALDI-TOF MS; Bruker Daltonics, Bremen, Germany). A biofilm-forming *S. enterica* isolate was cultivated in 20 mL of Mueller-Hinton broth (MHB) inoculated with 100 μL of a standardized 0.5 McFarland suspension. Biofilms were allowed to develop on sterile stainless-steel and wood coupons placed in polypropylene tubes according to the method of Kačániová et al. (2024). Cultures were supplemented with 0.1% (*v/v*) CMEO or 0.1% (*v/v*) the tested constituents, while untreated cultures served as controls. Incubations proceeded at 37 °C with agitation at 170×g for 3, 7, and 14 days. At each sampling interval, the sessile biomass was gently removed from the coupon surfaces, and planktonic cells were collected from the surrounding medium.

Mass spectra were acquired using a Microflex LT mass spectrometer

operating in linear positive-ion mode over an *m/z* range of 2000–20,000. Spectral preprocessing, peak alignment, and feature extraction were carried out in Biotyper software (Bruker Daltonics). Comparative analyses were performed to evaluate spectral differences between treated and identify treatment-related shifts in the mass spectral profiles of *S. enterica* biofilms. Hierarchical clustering using Euclidean distance was applied to visualize similarity patterns and to identify treatment-related shifts in the mass spectral fingerprints of *S. enterica* biofilms. All MALDI-TOF MS analyses were performed on samples prepared in three independent biological replicates.

2.6. Insecticidal activity of CMEO and its major constituents against stored-product beetles

The insecticidal potential of CMEO and its major constituents was evaluated against the stored-product pests *Callosobruchus maculatus* (Fabricius, 1775) and *Megabruchidius dorsalis* (Fåhraeus, 1839). Groups of 100 adults of each species were placed in sterile 90 mm Petri dishes lined with filter paper. The filter papers were treated with 100 µL of the test solutions prepared in 0.1% (*v/v*) polysorbate 80 (Tween 80; Sigma-Aldrich, St. Louis, MO, USA) to obtain final concentrations of 100, 50, 25, 12.5, 6.25, and 3.125% (*v/v*). The dishes were sealed with Parafilm to limit volatilization of the tested substances and maintained at room temperature (22–25 °C) for 24 h. After the exposure period, the numbers of live and dead adults were recorded, and mortality was expressed as a percentage. Filter papers treated with 0.1% Tween 80 alone served as negative controls. All assays were performed in three independent replicates to ensure reproducibility of the results.

2.7. Statistical analysis

Statistical processing and figure generation were carried out using JMP Student Edition 18.2 (SAS Institute, Cary, NC, USA). Results are reported as mean values accompanied by their standard deviation (SD), with each analysis performed in triplicate. Before conducting the inferential analyses, compliance with ANOVA assumptions was confirmed: residual normality was examined through the Shapiro-Wilk test, while variance homogeneity was verified using Bartlett's test. Since these assumptions were satisfied, a one-way ANOVA was employed to evaluate differences among treatments. When the model indicated significant effects ($p \leq 0.05$), Tukey's HSD procedure was applied for post hoc comparisons.

Instead, *In situ* data were analysed using a three-way analysis of variance (ANOVA) to evaluate the effects of essential oil type (5 levels), concentration (4 levels), and microorganism (12 levels) on antimicrobial activity. The experimental design was fully factorial, including all interaction terms (Essential Oil × Concentration × Microorganism). Each experimental condition was performed in triplicate (n = 3), and replicates were treated as independent observations. Prior to analysis, data were inspected for consistency and completeness, and no missing values were observed after dataset restructuring. The assumptions of ANOVA were evaluated by assessing the normality of residuals (Shapiro–Wilk test) and homogeneity of variances (Levene's test). Residual diagnostics indicated no substantial deviations from model assumptions. The ANOVA model was fitted using a general linear model approach. Statistical significance was determined at $p < 0.05$. In addition to F-values and *p*-values, effect sizes were calculated using eta squared (η^2) to estimate the proportion of total variance explained by each factor, and partial eta squared (partial η^2) to assess the magnitude of each effect independently of other factors. When significant effects were observed, the interaction structure of the model was carefully interpreted to avoid misleading conclusions based solely on main effects.

3. Results

3.1. Chemical composition of CMEO

The GC-MS analysis of CMEO revealed a chemically diverse profile composed primarily of monoterpenes, oxygenated monoterpenes, and medium-chain fatty acids, accounting for 99.9% of the total identified constituents (Table 1). The EO was dominated by α-terpineol (20.1%), capric acid (13.4%), β-pinene (12.3%), α-pinene (11.8%) and camphene (8.7%), indicating a strong representation of monoterpene hydrocarbons and oxygenated monoterpenoids. Additional notable compounds included endo-borneol (7.0%), camphor (6.3%), linalool (5.9%), and 5-heptene-2-one, 6-methyl- (4.4%), all of which may contribute to the antimicrobial and bioactive properties observed in subsequent assays. Minor monoterpenes such as p-cymene (0.1%), γ-terpinene (0.1%), limonene (0.6%), and 1,8-cineole (2.4%) were present in lower proportions but may still contribute to the overall biological activity of the EO. Sesquiterpenes, including β-elemene (0.4%), β-caryophyllene (0.7%), β-eudesmene (0.2%), and caryophyllene oxide (0.1%), were also detected, contributing to the structural complexity of the EO. Trace amounts (tr) of compounds such as cis-linalool oxide and humulene epoxide, as well as low levels of esters like linalyl acetate (1.9%) and isoamyl and isobornyl decanoates (0.1% and 1.0%, respectively), further enriched the chemical profile. Overall, the composition is consistent with a terpenoid-rich EO, with β-pinene and α-pinene representing the major monoterpene hydrocarbons, while α-terpineol, linalool, and borneol constitute the dominant oxygenated monoterpenes. The relatively high proportion of capric acid distinguishes this

Table 1
Chemical composition of CMEO (percentage mean values ± SD).

N.	Compound	LRI^{calc}	LRI^{lit}	%
1	tricyclene	918	922	1.8 ± 0.08
2	*α*-pinene	938	942	11.8 ± 0.22
3	camphene	950	953	8.7 ± 0.16
4	6-methyl-5-heptene-2-one	983	986	4.4 ± 0.11
5	*β*-pinene	968	970	12.3 ± 0.07
6	*p*-cymene	1022	1026	0.1 ± 0.02
7	limonene	1030	1031	0.6 ± 0.03
8	1,8-cineole	1036	1033	2.4 ± 0.10
9	γ-terpinene	1065	1062	0.1 ± 0.02
10	*cis*-linalool oxide	1072	1070	tr
11	linalool	1105	1102	5.9 ± 0.13
12	camphor	1122	1126	6.3 ± 0.14
13	*δ*-terpineol	1152	1147	0.2 ± 0.02
14	endo-borneol	1158	1160	7.0 ± 0.15
15	*α*-terpineol	1190	1193	20.1 ± 1.67
16	linalyl acetate	1248	1252	1.9 ± 0.07
17	capric acid	1350	1353	13.4 ± 1.12
18	*β*-elemene	1395	1393	0.4 ± 0.03
19	*β*-caryophyllene	1428	1431	0.7 ± 0.03
20	humulene	1475	1473	0.2 ± 0.02
21	*β*-eudesmene	1486	1481	0.2 ± 0.02
22	nerolidol	1571	1565	0.2 ± 0.02
23	caryophyllene oxide	1582	1580	0.1 ± 0.02
24	humulene epoxide	1588	1593	tr
25	isoamyl decanoate	1655	1653	0.1 ± 0.02
26	isobornyl decanoate	2081	2087	1.0 ± 0.06
	TOTAL			**99.9**
	Monoterpenes			*37.3*
	Oxygenated Monoterpenes			*33.2*
	Sesquiterpenes			*1.7*
	Oxygenated Sesquiterpenes			*0.1*
	Monoterpenoids			*2.4*
	Monoterpene ketone			*6.3*
	Fatty esters			*1.1*
	Fatty acids			*13.4*
	Others			*4.4*

The components are reported according to their elution order on apolar column; LRI^{calc}: Linear Retention Indices measured on apolar column; LRI^{lit} Linear Retention indices from literature; tr: percentage mean values ≤ 0.1%.

EO from typical chrysanthemum chemotypes and may contribute to its biological activity.

3.2. Initial antimicrobial assessment by disc diffusion method

CMEO showed the significantly larger inhibition zones (Table 2) against the Gram-negative bacteria *S. enterica*, *Y. enterocolitica* and *E. coli*, with mean inhibition zones ranging from about 12–14 mm. This indicates that CMEO is most effective against these enteric Gram-negative species.

Among the Gram-positive bacteria, *L. monocytogenes* and *E. faecalis* were moderately sensitive (8–10 mm), whereas *S. aureus* showed only weak inhibition (7 mm), suggesting a lower susceptibility of staphylococci to this EO. Within the yeasts, *C. albicans* and *C. parapsilosis* exhibited moderate inhibition (8–9 mm), while *C. glabrata*, *C. krusei* and *C. tropicalis* were less affected, with inhibition zones mostly below 8 mm, indicating a more tolerant phenotype towards CMEO (Table 2). Interestingly, the biofilm-forming *S. enterica* strain still displayed measurable inhibition (10 mm), only slightly lower than the planktonic reference strain. This suggests that the volatile components of CMEO can partly counteract the increased tolerance typically associated with biofilm growth. Overall, CMEO exerted broad-spectrum but generally mild-to-moderate antimicrobial activity, with the highest efficacy against Gram-negative enteric bacteria and somewhat lower effects on Gram-positive bacteria and yeasts.

α-Terpineol showed the strongest activity among the tested constituents (Table 2). The largest inhibition zones were recorded against *S. enterica* (8.67 mm) and *E. coli* (7.67 mm), followed by the biofilm-forming *S. enterica* strain (7.33 mm), *Y. enterocolitica* and *L. monocytogenes* (6.67 mm each), and *E. faecalis* (6.33 mm). *S. aureus* showed the lowest susceptibility among Gram-positive bacteria (5.33 mm). Within the yeast panel, *C. glabrata* was the most sensitive (5.67 mm), followed by *C. albicans* (5.33 mm), while *C. krusei*, *C. parapsilosis*, and *C. tropicalis* showed the lowest response (4.67 mm).

For β-pinene, the largest inhibition zones were observed against the Gram-negative bacteria *S. enterica*, *E. coli* and *Y. enterocolitica* (roughly 6–7 mm), as well as the biofilm-forming *S. enterica* isolate (about 6–7 mm) (Table 2). This indicates that β-pinene is most active against enteric Gram-negative species, although the absolute inhibition is weaker.

Borneol exhibited weaker activity than α-terpineol (Table 2). The highest inhibition zones were observed against *S. enterica* (7.33 mm) and *Y. enterocolitica* (6.67 mm), while *E. coli* and *E. faecalis* showed inhibition zones of 6.33 mm each. *L. monocytogenes* showed 5.67 mm and *S. aureus* remained the least susceptible Gram-positive bacterium (4.67 mm). Among yeasts, *C. glabrata* was the most sensitive (5.67 mm), whereas *C. albicans*, *C. krusei*, and *C. tropicalis* showed the lowest response (3.67 mm). The biofilm-forming *S. enterica* strain showed an inhibition zone of 6.33 mm.

Camphor showed the weakest activity among the tested constituents (Table 2). Inhibition zones against Gram-negative bacteria ranged from 5.67 mm (*E. coli*, *Y. enterocolitica*) to 6.67 mm (*S. enterica*). Among Gram-positive bacteria, *L. monocytogenes* showed 5.67 mm, *E. faecalis* 5.33 mm, and *S. aureus* was the least affected (4.67 mm). The yeast panel was generally poorly sensitive, with inhibition zones ranging from 3.67 to 4.67 mm. The biofilm-forming *S. enterica* strain showed an inhibition zone of 5.67 mm. Compared to all tested constituents, CMEO exhibited a generally stronger antimicrobial effect across the tested panel (Table 2). For Gram-negative bacteria, CMEO produced visibly larger inhibition zones against *E. coli*, *S. enterica* and *Y. enterocolitica*, indicating that the whole EO is more effective than any of its individual constituents. A similar pattern was seen for Gram-positive bacteria: although all tested agents affected *E. faecalis*, *L. monocytogenes* and *S. aureus*, the responses were consistently more pronounced with CMEO, while the individual constituents caused only weak to moderate inhibition, particularly in *S. aureus*. The difference was even more evident in yeasts. CMEO inhibited *C. albicans*, *C. glabrata*, *C. krusei*, *C. parapsilosis* and *C. tropicalis* more effectively, whereas the individual constituents produced only slight to moderate suppression of growth. For the biofilm-forming *S. enterica* isolate, all tested agents retained measurable activity, but CMEO achieved the strongest inhibitory effect. Overall, these observations indicate that the antimicrobial potential of CMEO arises from the combined contribution of multiple constituents, resulting in higher efficacy against both bacterial and yeast targets, including the biofilm-forming *S. enterica* strain.

3.3. In vitro inhibitory potency of CMEO expressed as MIC_{50} and MIC_{90}

The MIC results (Table 3 and Table 4) showed that CMEO exhibited its strongest antimicrobial effect against *Y. enterocolitica*, which displayed very low values of MIC_{50} = 0.49 mg/mL and MIC_{90} = 0.71 mg/mL, representing the highest sensitivity among all tested microorganisms.

High susceptibility was also observed in *C. albicans*, where MIC_{50} was approximately 0.48 mg/mL and MIC_{90} around 0.68 mg/mL, confirming notable antifungal activity of the EO. On the opposite end of the spectrum, *C. parapsilosis* showed the weakest response, with MIC_{50} exceeding 6.38 mg/mL and MIC_{90} reaching about 6.77 mg/mL, indicating low sensitivity to CMEO (Table 3 and Table 4). Similarly, *C. glabrata* required markedly higher concentrations, with MIC_{50} around 3.52 mg/mL. Overall, *Y. enterocolitica* and *C. albicans* emerged as the most sensitive microorganisms, whereas *C. parapsilosis* showed the lowest susceptibility. These differences reflect variations in cell wall composition and inherent resistance mechanisms across the tested species toward terpenoid-rich EOs.

α-Terpineol showed the strongest inhibitory activity among the tested constituents (Table 3 and Table 4). The lowest MIC_{50} values were recorded against *C. albicans* (1.38 mg/mL) and *Y. enterocolitica*

Table 2
Antimicrobial activity (expressed as inhibition zone in mm) of CMEO, β-pinene, α-terpineol, borneol, and camphor evaluated by disc diffusion method.

Class	Microorganism	CMEO	β-Pinene	α-Terpineol	Borneol	Camphor
G-negative bacteria	*E. coli*	$12.33 \pm 0.59^{a,A}$	$6.33 \pm 0.58^{ab,C}$	$7.67 \pm 0.59^{ab,B}$	$6.33 \pm 0.58^{ab,C}$	$5.67 \pm 0.58^{ab,C}$
	S. enterica	$13.67 \pm 0.58^{a,A}$	$7.33 \pm 0.58^{a,C}$	$8.67 \pm 0.58^{a,B}$	$7.33 \pm 0.59^{a,C}$	$6.67 \pm 0.58^{a,C}$
	Y. enterocolitica	$13.33 \pm 0.58^{a,A}$	$6.33 \pm 0.59^{ab,B}$	$6.67 \pm 0.58^{bcd,B}$	$6.67 \pm 0.59^{a,B}$	$5.67 \pm 0.59^{ab,B}$
BFB	Biofilm forming *S. enterica*	$10.33 \pm 0.58^{b,A}$	$6.67 \pm 0.58^{ab,BC}$	$7.33 \pm 0.58^{abc,B}$	$6.33 \pm 0.57^{ab,C}$	$5.67 \pm 0.59^{ab,C}$
G-positive bacteria	*E. faecalis*	$8.33 \pm 0.58^{cde,A}$	$5.67 \pm 0.58^{abc,B}$	$6.33 \pm 0.58^{bcde,B}$	$6.33 \pm 0.58^{ab,B}$	$5.33 \pm 0.58^{abc,B}$
	L. monocytogenes	$9.67 \pm 0.58^{bc,A}$	$5.33 \pm 0.59^{bc,C}$	$6.67 \pm 0.59^{bcd,B}$	$5.67 \pm 0.59^{ab,BC}$	$5.67 \pm 0.59^{ab,BC}$
	S. aureus	$7.33 \pm 0.57^{de,A}$	$4.33 \pm 0.57^{cd,B}$	$5.33 \pm 0.57^{de,B}$	$4.67 \pm 0.59^{bc,B}$	$4.67 \pm 0.59^{bc,B}$
Yeast	*C. albicans*	$8.67 \pm 0.59^{bcd,A}$	$4.33 \pm 0.58^{cd,BC}$	$5.33 \pm 0.58^{de,B}$	$3.67 \pm 0.57^{c,C}$	$4.67 \pm 0.58^{bc,BC}$
	C. glabrata	$7.67 \pm 0.59^{de,A}$	$5.33 \pm 0.58^{bc,B}$	$5.67 \pm 0.59^{cde,B}$	$5.67 \pm 0.58^{ab,B}$	$4.67 \pm 0.58^{bc,B}$
	C. krusei	$6.67 \pm 0.58^{e,A}$	$3.33 \pm 0.57^{d,C}$	$4.67 \pm 0.58^{e,B}$	$3.67 \pm 0.59^{c,BC}$	$3.67 \pm 0.58^{c,BC}$
	C. parapsilosis	$8.33 \pm 0.57^{cde,A}$	$4.33 \pm 0.58^{cd,B}$	$4.67 \pm 0.58^{e,B}$	$4.67 \pm 0.57^{bc,B}$	$3.67 \pm 0.59^{c,B}$
	C. tropicalis	$7.33 \pm 0.58^{de,A}$	$4.33 \pm 0.57^{cd,B}$	$4.67 \pm 0.57^{e,B}$	$3.67 \pm 0.59^{c,B}$	$3.67 \pm 0.58^{c,B}$

Data are the mean (± standard deviation) of 3 replicates. [a–e] Different superscript lowercase letters indicate statistically significant differences within each column ($p \leq 0.05$). [A–C] Different superscript uppercase letters indicate statistically significant differences within each row ($p \leq 0.05$). CMEO= *C.* × *morifolium* essential oil.

Table 3
Minimal inhibitory concentration (MIC_{50}) expressed in mg/mL of CMEO, β-pinene, α-terpineol, borneol, and camphor.

Class	Microorganism	MIC_{50}				
		CMEO	β-Pinene	α-Terpineol	Borneol	Camphor
G-negative bacteria	*E. coli*	$2.285 \pm 0.166^{c,D}$	$4.323 \pm 0.055^{c,B}$	$3.596 \pm 0.029^{b,C}$	$4.582 \pm 0.058^{c,A}$	$4.754 \pm 0.060^{c,A}$
	S. enterica	$2.456 \pm 0.190^{c,D}$	$5.692 \pm 0.232^{b,B}$	$3.415 \pm 0.139^{b,C}$	$6.034 \pm 0.245^{b,A}$	$6.262 \pm 0.255^{b,A}$
	Y. enterocolitica	$0.489 \pm 0.126^{e,C}$	$3.488 \pm 0.251^{d,A}$	$2.093 \pm 0.150^{f,B}$	$3.697 \pm 0.266^{d,A}$	$3.849 \pm 0.265^{d,A}$
BFB	Biofilm forming *S. enterica*	$2.460 \pm 0.086^{c,C}$	$4.392 \pm 0.160^{c,B}$	$2.635 \pm 0.095^{def,C}$	$4.656 \pm 0.169^{c,AB}$	$4.825 \pm 0.165^{c,A}$
G-positive bacteria	*E. faecalis*	$1.409 \pm 0.125^{d,C}$	$3.535 \pm 0.304^{d,A}$	$2.121 \pm 0.183^{ef,B}$	$3.748 \pm 0.322^{d,A}$	$3.892 \pm 0.335^{d,A}$
	L. monocytogenes	$1.449 \pm 0.186^{d,D}$	$4.464 \pm 0.188^{c,B}$	$2.679 \pm 0.113^{cde,C}$	$4.733 \pm 0.198^{c,AB}$	$4.910 \pm 0.207^{c,A}$
	S. aureus	$2.345 \pm 0.012^{c,C}$	$4.486 \pm 0.242^{c,A}$	$2.692 \pm 0.145^{cd,B}$	$4.756 \pm 0.258^{c,A}$	$4.946 \pm 0.260^{c,B}$
Yeast	*C. albicans*	$0.484 \pm 0.171^{e,B}$	$1.743 \pm 0.209^{e,A}$	$1.379 \pm 0.498^{g,A}$	$1.847 \pm 0.222^{e,A}$	$1.916 \pm 0.236^{e,A}$
	C. glabrata	$3.522 \pm 0.348^{b,B}$	$5.527 \pm 0.310^{b,A}$	$3.317 \pm 0.186^{b,B}$	$5.858 \pm 0.328^{b,A}$	$6.109 \pm 0.359^{b,A}$
	C. krusei	$3.410 \pm 0.060^{b,C}$	$5.312 \pm 0.066^{b,B}$	$3.187 \pm 0.040^{bcd,D}$	$5.630 \pm 0.071^{b,A}$	$5.818 \pm 0.064^{b,A}$
	C. parapsilosis	$6.378 \pm 0.168^{a,C}$	$8.444 \pm 0.350^{a,B}$	$5.064 \pm 0.211^{a,D}$	$8.950 \pm 0.372^{a,AB}$	$9.227 \pm 0.275^{a,A}$
	C. tropicalis	$3.367 \pm 0.010^{b,D}$	$5.369 \pm 0.059^{b,C}$	$3.223 \pm 0.038^{bc,D}$	$5.691 \pm 0.063^{b,B}$	$5.906 \pm 0.065^{b,A}$

Data are the mean (± standard deviation) of 3 replicates. $^{a–g}$ Different superscript lowercase letters indicate statistically different values within the column ($p \leq 0.05$). $^{A–D}$ Different superscript uppercase letters indicate statistically different values within the row ($p \leq 0.05$). CMEO= *C.* × *morifolium* essential oil.

Table 4
Minimal inhibitory concentration (MIC_{90}) expressed in mg/mL of CMEO, β-pinene, α-terpineol, borneol and camphor.

Class	Microorganism	MIC_{90}				
		CMEO	β-Pinene	α-Terpineol	Borneol	Camphor
G-negative bacteria	*E. coli*	$2.529 \pm 0.167^{c,D}$	$4.604 \pm 0.060^{c,B}$	$3.866 \pm 0.085^{b,C}$	$4.926 \pm 0.046^{bcd,A}$	$5.039 \pm 0.174^{d,A}$
	S. enterica	$2.780 \pm 0.099^{c,D}$	$5.998 \pm 0.203^{b,B}$	$3.662 \pm 0.171^{b,C}$	$5.668 \pm 1.379^{bc,B}$	$6.662 \pm 0.371^{b,A}$
	Y. enterocolitica	$0.714 \pm 0.062^{e,C}$	$3.750 \pm 0.307^{d,A}$	$2.362 \pm 0.211^{de,B}$	$3.925 \pm 0.206^{d,A}$	$4.214 \pm 0.319^{e,A}$
BFB	Biofilm forming *S. enterica*	$2.643 \pm 0.124^{c,C}$	$4.696 \pm 0.104^{c,B}$	$2.894 \pm 0.135^{cd,C}$	$4.962 \pm 0.237^{bcd,AB}$	$5.195 \pm 0.148^{d,A}$
G-positive bacteria	*E. faecalis*	$1.790 \pm 0.184^{d,C}$	$3.770 \pm 0.270^{d,A}$	$2.432 \pm 0.200^{d,B}$	$4.045 \pm 0.368^{d,A}$	$4.143 \pm 0.400^{e,A}$
	L. monocytogenes	$1.775 \pm 0.262^{d,D}$	$4.663 \pm 0.280^{c,B}$	$2.939 \pm 0.147^{cd,C}$	$4.663 \pm 0.280^{cd,B}$	$5.209 \pm 0.196^{d,A}$
	S. aureus	$2.637 \pm 0.228^{b,C}$	$4.748 \pm 0.180^{c,B}$	$2.939 \pm 0.142^{cd,C}$	$5.029 \pm 0.287^{bcd,AB}$	$5.341 \pm 0.308^{cd,A}$
Yeast	*C. albicans*	$0.677 \pm 0.191^{e,B}$	$1.951 \pm 0.168^{e,A}$	$1.724 \pm 0.559^{e,A}$	$2.289 \pm 0.050^{e,A}$	$2.369 \pm 0.278^{f,A}$
	C. glabrata	$3.795 \pm 0.100^{b,C}$	$5.681 \pm 0.232^{b,B}$	$3.668 \pm 0.122^{b,C}$	$6.287 \pm 0.453^{b,AB}$	$6.697 \pm 0.234^{b,A}$
	C. krusei	$3.740 \pm 0.108^{b,C}$	$5.813 \pm 0.113^{b,B}$	$3.619 \pm 0.039^{b,C}$	$5.919 \pm 0.074^{bc,B}$	$6.152 \pm 0.152^{b,A}$
	C. parapsilosis	$6.769 \pm 0.100^{a,C}$	$8.843 \pm 0.078^{a,B}$	$5.344 \pm 0.309^{a,D}$	$9.248 \pm 0.363^{a,AB}$	$9.611 \pm 0.247^{a,A}$
	C. tropicalis	$3.647 \pm 0.217^{b,C}$	$5.672 \pm 0.095^{b,B}$	$3.554 \pm 0.084^{bc,C}$	$5.939 \pm 0.152^{bc,AB}$	$6.075 \pm 0.082^{bc,A}$

Data are the mean (± standard deviation) of 3 replicates. $^{a–f}$ Different superscript lowercase letters indicate statistically different values within the column ($p \leq 0.05$). $^{A–D}$ Different superscript uppercase letters indicate statistically different values within the row ($p \leq 0.05$). CMEO= *C.* × *morifolium* essential oil.

(2.09 mg/mL), indicating the highest sensitivity of these microorganisms. *E. coli* and *S. enterica* showed MIC_{50} values of 3.60 and 3.42 mg/mL, respectively. Among Gram-positive bacteria, *L. monocytogenes* was the most sensitive (MIC_{50} = 2.68 mg/mL), while *S. aureus* required higher concentrations (MIC_{50} = 2.69 mg/mL). *C. parapsilosis* showed the lowest susceptibility among yeasts, with MIC_{50} = 5.06 mg/mL and MIC_{90} = 5.34 mg/mL.

β-Pinene demonstrated overall weaker antimicrobial activity compared to CMEO and the other tested constituents, with notably higher MIC values across all tested microorganisms (Table 3 and Table 4). Among bacteria, the strongest inhibitory effect was observed against *Y. enterocolitica*, with MIC_{50} values around 3.49 mg/mL and MIC_{90} approximately 3.75 mg/mL, making it the most sensitive bacterial species in this panel. In contrast, *S. enterica* required clearly higher concentrations, with MIC_{50} near 5.69 mg/mL and MIC_{90} around 5.99 mg/mL, reflecting substantially reduced susceptibility. Within Gram-positive bacteria, *E. faecalis* showed moderate sensitivity, with MIC_{50} around 3.54 mg/mL, whereas *S. aureus* displayed relatively low susceptibility, with MIC_{50} approximately 4.49 mg/mL, confirming that staphylococci are less responsive to β-pinene. For yeasts (Table 3 and Table 4), *C. albicans* emerged as the most sensitive species, with MIC_{50} around 1.74 mg/mL and MIC_{90} near 1.95 mg/mL. However, other *Candida* species, such as *C. parapsilosis*, exhibited much higher tolerance, with MIC_{50} reaching 8.44 mg/mL, representing the weakest response among all tested organisms. Overall, β-pinene showed moderate to weak antimicrobial potency, with activity most pronounced against *Y. enterocolitica* and *C. albicans*, and the lowest effectiveness observed in *C. parapsilosis* and *S. enterica*.

Borneol exhibited weaker inhibitory activity than α-terpineol. The lowest MIC_{50} values were recorded against *C. albicans* (1.85 mg/mL) and *Y. enterocolitica* (3.70 mg/mL). Among Gram-negative bacteria, *E. coli* showed MIC_{50} = 4.58 mg/mL and *S. enterica* MIC_{50} = 6.03 mg/mL. Among Gram-positive bacteria, *E. faecalis* showed MIC_{50} = 3.75 mg/mL and *S. aureus* MIC_{50} = 4.76 mg/mL. *C. parapsilosis* was the least susceptible yeast, with MIC_{50} = 8.95 mg/mL and MIC_{90} = 9.25 mg/mL (Table 3 and Table 4).

Camphor showed the weakest inhibitory activity among the tested constituents. The lowest MIC_{50} values were recorded against *Y. enterocolitica* (3.85 mg/mL) and *E. coli* (4.75 mg/mL). Among Gram-positive bacteria, *S. aureus* showed MIC_{50} = 1.92 mg/mL, while *E. faecalis* showed MIC_{50} = 4.91 mg/mL and *L. monocytogenes* MIC_{50} = 4.95 mg/mL. Among yeasts, *C. albicans* was the most sensitive (MIC_{50} = 6.11 mg/mL), while *C. krusei* showed the lowest susceptibility (MIC_{50} = 9.23 mg/mL and MIC_{90} = 9.61 mg/mL).These findings confirm that no single constituent alone accounts for the inhibitory effects produced by the whole EO. CMEO consistently showed stronger antimicrobial effects than all tested constituents across the whole panel of test organisms. For Gram-negative bacteria, inhibition by CMEO was clearly more pronounced, especially in *Y. enterocolitica*, *E. coli* and *S. enterica*, where the individual constituents produced only modest suppression of growth. A similar trend was observed in Gram-positive bacteria: although both CMEO and the tested constituents affected *E. faecalis*, *L. monocytogenes* and *S. aureus*, the responses to the individual constituents were visibly weaker, with *S. aureus* remaining particularly tolerant. Among yeasts, *C. albicans* was the most susceptible species to both CMEO and the tested constituents, but CMEO again outperformed all, while the remaining *Candida* spp., especially *C. parapsilosis* and *C. glabrata*, responded only weakly to all individual constituents. Taken

together, these findings indicate that the antimicrobial potential of CMEO reflects the combined contribution of several constituents within the EO.

3.4. In situ antimicrobial activity

3.4.1. In situ vapor phase antimicrobial effects on apple slices

The three-way ANOVA (Table 5) revealed highly significant main effects of microorganism, essential oil, and concentration on antimicrobial activity ($p < 0.001$ for all factors). Among these, concentration ($F = 332.40$, $\eta p^2 = 0.675$) and microorganism ($F = 104.95$, $\eta p^2 = 0.706$) showed the strongest effects, followed by oil ($F = 148.46$, $\eta p^2 = 0.553$).

All interaction terms were also statistically significant. The microorganism × essential oil interaction ($F = 20.54$, $\eta p^2 = 0.653$) and microorganism × concentration interaction ($F = 29.19$, $\eta p^2 = 0.667$) indicate that both oil efficacy and dose–response relationships are strongly dependent on the microbial species.

The essential oil × concentration interaction was significant ($F = 5.82$, $\eta p^2 = 0.127$), although with a smaller effect size, suggesting that the relative effectiveness of oils varies moderately across concentrations. The three-way interaction was also significant ($F = 6.23$, $\eta p^2 = 0.632$), indicating a complex interplay among all factors (Table 5).

The results demonstrate that antimicrobial activity in the apple matrix is governed by both strong main effects and substantial interaction effects, indicating a highly complex system. Concentration emerges as a major driver of antimicrobial efficacy, confirming a strong dose-dependent response. At the same time, microorganism identity plays an equally important role, highlighting variability in susceptibility among species. Oil type also significantly affects antimicrobial activity, reflecting differences in chemical composition and mode of action. However, the strong interaction terms suggest that the effectiveness of each oil cannot be generalized and depends on both the microbial target and the applied concentration. The significant microorganism-dependent interactions indicate that both oil performance and dose–response behavior vary across species, emphasizing the need for tailored antimicrobial strategies. Although the oil × concentration interaction shows a smaller effect size, its significance suggests that the relative ranking of oils changes across concentrations, which is relevant for practical applications. The presence of a strong three-way interaction confirms that antimicrobial efficacy in this matrix is influenced by the combined effects of all factors, reflecting a complex and dynamic system.

In situ apple model (Table S1), CMEO exhibited strong antimicrobial efficacy, particularly against Gram-negative bacteria. At a concentration of 500 μL/L, *Y. enterocolitica* showed an inhibition of 84.94%, while at 62.5 μL/L the inhibition remained at 57.15%. For *E. coli*, CMEO produced an inhibition of 65.40% at 500 μL/L and 33.90% at 62.5 μL/L.

Table 5
Three-way ANOVA evaluating the effects of microorganism, essential oil, and concentration on antimicrobial response in apple matrix.

Variable	df	Sum of Squares	F	*p*-value	η^2	ηp^2
Microorganism	11	3368.31	104.95	< 0.001	0.160	0.706
Essential Oil	4	1732.56	148.46	< 0.001	0.082	0.553
Concentration	3	2909.43	332.40	< 0.001	0.138	0.675
Microorganism × Essential Oil	44	2636.37	20.54	< 0.001	0.125	0.653
Microorganism × Concentration	33	2810.37	29.19	< 0.001	0.133	0.667
Essential Oil × Concentration	12	203.92	5.82	< 0.001	0.010	0.127
Microorganism × Essential Oil × Concentration	132	2400.76	6.23	< 0.001	0.114	0.632
Residual	480	1400.45			0.066	

Effect sizes are reported as eta squared (η^2) and partial eta squared (ηp^2).

S. enterica reached inhibition levels of 76.34% at 500 μL/L and 41.22% at 62.5 μL/L.

Among Gram-positive bacteria, *E. faecalis* was the most sensitive strain, with inhibition values of 94.78% (500 μL/L) and 37.60% (62.5 μL/L). *L. monocytogenes* demonstrated an inhibition of 76.19% at 500 μL/L, decreasing to 15.55% at 62.5 μL/L. Within the yeast group, *C. albicans* showed the highest susceptibility, with CMEO reducing growth by 84.36% at 500 μL/L and 26.82% at 62.5 μL/L. In contrast, *C. parapsilosis* exhibited lower sensitivity, with inhibition values of 66.51% at 500 μL/L and 35.96% at 62.5 μL/L. The biofilm-forming strain of *S. enterica* was less affected than the planktonic reference strain, yet CMEO still demonstrated relevant activity: inhibition was 76.26% at 500 μL/L and 34.63% at 62.5 μL/L (Table S1).

α-Terpineol showed the strongest inhibitory activity among the tested constituents on apple slices (Table S1). Among Gram-negative bacteria, *Y. enterocolitica* was the most sensitive, with inhibition of 41.80% at 500 μL/L and 9.29% at 62.5 μL/L. *S. enterica* reached 40.95% inhibition at 500 μL/L and 11.88% at 62.5 μL/L, while *E. coli* showed inhibition of 41.57% at 500 μL/L and 9.86% at 62.5 μL/L. Among Gram-positive bacteria, *E. faecalis* showed inhibition of 38.75% at 500 μL/L and 9.86% at 62.5 μL/L, while *L. monocytogenes* reached 44.90% at 500 μL/L and 4.68% at 62.5 μL/L. *S. aureus* showed inhibition of 44.56% at 500 μL/L and 9.61% at 62.5 μL/L. Within the yeast group, *C. albicans* was the most sensitive, with inhibition of 36.91% at 500 μL/L and 7.60% at 62.5 μL/L. The biofilm-forming *S. enterica* strain showed inhibition of 42.63% at 500 μL/L and 8.81% at 62.5 μL/L.

In the apple matrix, β-pinene exhibited weaker antimicrobial activity than CMEO, yet still demonstrated a clear concentration-dependent inhibitory effect. Among Gram-negative bacteria, *S. enterica* was the most sensitive strain. At 500 μL/L (Table S1), β-pinene achieved 39.09% inhibition, whereas at 62.5 μL/L the inhibition decreased to 10.33%. The response of *E. coli* was more moderate, with inhibition values of 36.35% at 500 μL/L and 8.66% at 62.5 μL/L. *Y. enterocolitica* showed the lowest sensitivity within this group, as inhibition reached only 31.24% at 500 μL/L and dropped to 4.29% at 62.5 μL/L. Among Gram-positive bacteria, *L. monocytogenes* was the most affected species, with inhibition levels of 39.05% at 500 μL/L and 3.89% at 62.5 μL/L. *E. faecalis* reached 33.70% inhibition at 500 μL/L, decreasing to 8.57% at 62.5 μL/L. In contrast, *S. aureus* responded relatively weakly across all concentrations; inhibition at 500 μL/L was 38.90%, while at 62.5 μL/L it remained at 8.38%. Within the yeast group (Table S1), *C. albicans* exhibited the highest susceptibility. β-pinene reduced its growth by 32.09% at 500 μL/L and by 6.70% at 62.5 μL/L. *C. glabrata* showed a comparable pattern, with inhibition values of 39.08% at 500 μL/L and 7.54% at 62.5 μL/L. The response of *C. parapsilosis* was more variable, but inhibition still reached 35.30% at 500 μL/L and 8.35% at 62.5 μL/L. The biofilm-forming *S. enterica* strain displayed the lowest overall sensitivity. At 500 μL/L, inhibition reached 37.07%, whereas at 62.5 μL/L it decreased to 7.66%, confirming that β-pinene has limited capacity to penetrate or disrupt biofilm structures compared with CMEO.

Borneol showed weaker inhibitory activity than α-terpineol on apple slices (Table S1). Among Gram-negative bacteria, *E. coli* showed inhibition of 35.28% at 500 μL/L and 8.23% at 62.5 μL/L, *S. enterica* reached 38.20% at 500 μL/L and 9.90% at 62.5 μL/L, and *Y. enterocolitica* showed 30.09% at 500 μL/L and 5.21% at 62.5 μL/L. Among Gram-positive bacteria, *E. faecalis* showed inhibition of 32.46% at 500 μL/L and 8.26% at 62.5 μL/L, *L. monocytogenes* reached 37.61% at 500 μL/L and 3.75% at 62.5 μL/L, and *S. aureus* showed 37.33% at 500 μL/L and 8.05% at 62.5 μL/L. Within the yeast group, *C. albicans* was the most sensitive, with inhibition of 30.92% at 500 μL/L and 6.37% at 62.5 μL/L. The biofilm-forming *S. enterica* strain showed inhibition of 35.70% at 500 μL/L and 5.17% at 62.5 μL/L.

Camphor showed the weakest inhibitory activity among the tested constituents on apple slices (Table S1). Among Gram-negative bacteria, *E. coli* showed inhibition of 34.85% at 500 μL/L and 8.30% at 62.5 μL/L, *S. enterica* reached 37.47% at 500 μL/L and 9.07% at 62.5 μL/L, and

Y. enterocolitica showed 29.94% at 500 µL/L and 4.13% at 62.5 µL/L. Among Gram-positive bacteria, *E. faecalis* showed inhibition of 32.30% at 500 µL/L and 8.22% at 62.5 µL/L, *L. monocytogenes* reached 37.43% at 500 µL/L and 3.73% at 62.5 µL/L, and *S. aureus* showed 37.29% at 500 µL/L and 8.03% at 62.5 µL/L. Within the yeast group, *C. albicans* showed inhibition of 30.77% at 500 µL/L and 6.34% at 62.5 µL/L. The biofilm-forming *S. enterica* strain showed inhibition of 35.53% at 500 µL/L and 5.99% at 62.5 µL/L.

On apples, CMEO exhibited clearly stronger in situ antimicrobial activity than all tested constituents. At all tested concentrations, CMEO more effectively inhibited the growth of Gram-negative bacteria (*E. coli*, *S. enterica*, *Y. enterocolitica*), Gram-positive bacteria (*E. faecalis*, *L. monocytogenes*, *S. aureus*), as well as yeasts, particularly *C. albicans*. The biofilm-forming strain of *S. enterica* was also inhibited more distinctly by CMEO than by any individual constituent. Overall, CMEO demonstrates a more potent and consistent in situ effect on apples, supporting the notion that the biological activity of the EO arises from the overall contribution of multiple constituents, rather than from any single component alone.The heatmap analysis in apple model (Fig. 1) revealed a clear concentration-dependent increase in antimicrobial activity for CMEO and its individual components against all tested microorganisms. In particular, CMEO exhibited the strongest inhibitory effect, with values exceeding 60% at higher concentrations (250–500 µL/L) for most strains, and reaching peak inhibition levels in *E. faecalis, Y. enterocolitica*, and several *Candida* species.

Among the tested compounds, α-terpineol showed a comparatively higher antimicrobial activity than β-pinene, borneol, and camphor, especially at elevated concentrations, suggesting a more pronounced contribution to the overall bioactivity of the essential oil. In contrast, β-pinene, borneol, and camphor displayed moderate inhibition levels, generally remaining below the 60% threshold, indicating a weaker individual antimicrobial potential.

Gram-positive bacteria, particularly *E. faecalis* and *S. aureus*, appeared more susceptible to treatment compared to Gram-negative strains, although notable inhibition was also observed in *S. enterica* and *Y. enterocolitica* at higher concentrations. Additionally, biofilm-forming *S. enterica* showed increased resistance at lower concentrations but became significantly inhibited as the concentration increased.

Yeast strains of the genus *Candida* exhibited a variable response, with *C. albicans* and *C. glabrata* showing higher susceptibility compared to *C. tropicalis*, which remained the least affected species across all treatments.

Overall, these findings suggest that CMEO possesses strong antimicrobial properties, likely due to synergistic interactions among its constituents, with α-terpineol playing a key role in enhancing its efficacy.

3.4.2. *In situ vapor phase antimicrobial effects on pear slices*

A three-way ANOVA (Table 6) revealed highly significant main effects of microorganism, essential oil, and concentration on antimicrobial activity ($p < 0.001$ for all factors). Among these, microorganism identity exhibited a particularly strong effect ($F = 147.66$, $\eta p^2 = 0.772$),

Table 6
Three-way ANOVA evaluating the effects of microorganism, essential oil, and concentration on antimicrobial response in pear matrix.

Variable	df	Sum of Squares	F	*p*-value	η^2	ηp^2
Microorganism	11	7214.48	147.66	< 0.001	0.185	0.772
Essential Oil	4	3105.16	174.77	< 0.001	0.079	0.593
Concentration	3	1546.81	116.08	< 0.001	0.040	0.420
Microorganism × Essential Oil	44	9680.34	49.53	< 0.001	0.248	0.820
Microorganism × Concentration	33	4685.86	31.97	< 0.001	0.120	0.687
Essential Oil × Concentration	12	67.59	1.27	0.234	0.002	0.031
Microorganism × Essential Oil × Concentration	132	4795.97	8.18	< 0.001	0.123	0.692
Residual	480	2132.08			0.055	

Effect sizes are reported as eta squared (η^2) and partial eta squared (ηp^2).

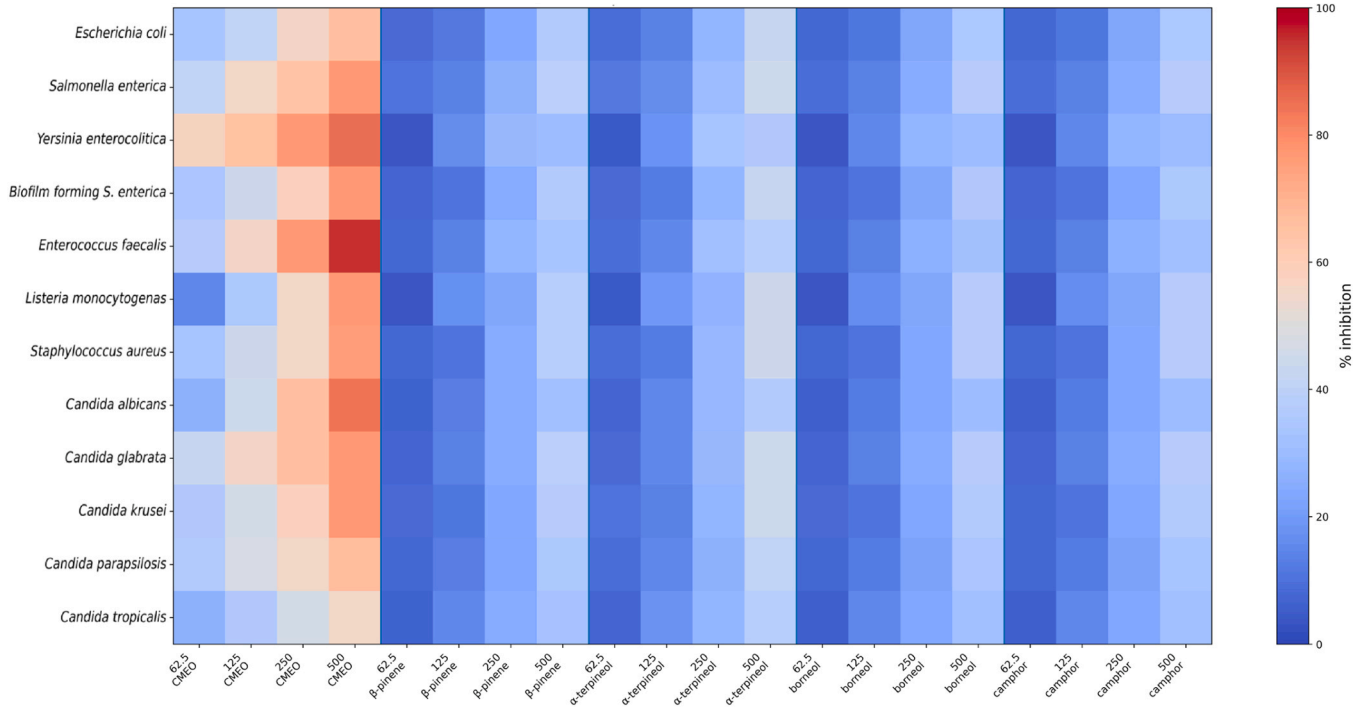

Fig. 1. Heatmap representing in situ analysis of the inhibition of microbial growth (%) by the vapor phase of CMEO and its main components (β-pinene, α-terpineol, borneol, and camphor) against selected microorganisms in apple samples at increasing concentrations (62.5–500 µL/L). Values are expressed as mean percentages of inhibition obtained from three independent replicates. Color gradient ranges from blue (low inhibition) to red (high inhibition).

indicating substantial variability in susceptibility across the tested microbial species.

Oil type also significantly influenced antimicrobial response ($F = 174.77$, $\eta p^2 = 0.593$), confirming marked differences in efficacy among the tested compounds. Concentration showed a strong and significant effect ($F = 116.08$, $\eta p^2 = 0.420$), supporting a clear dose–response relationship.

Significant two-way interactions were observed between microorganism and oil ($F = 49.53$, $\eta p^2 = 0.820$) (Table 6), and between microorganism and concentration ($F = 31.97$, $\eta p^2 = 0.687$), indicating that both the effectiveness of specific oils and the dose–response patterns depend strongly on the microbial target.

In contrast, the interaction between oil and concentration was not statistically significant ($F = 1.27$, $p = 0.234$, $\eta p^2 = 0.031$), suggesting that the relative efficacy of the oils remains broadly consistent across concentration levels.

Importantly, the three-way interaction among microorganism, oil, and concentration was highly significant ($F = 8.18$, $\eta p^2 = 0.692$), indicating a complex interplay among these factors in determining antimicrobial activity.

The strong main effect of concentration confirms a pronounced dose-dependent antimicrobial activity, which is consistent with the expected pharmacodynamic behavior of essential oils and their constituents. However, the relatively lower effect size compared to microorganism-related factors suggests that microbial susceptibility plays a more dominant role than dosage alone. The significant effect of oil type highlights the importance of chemical composition in determining antimicrobial efficacy. This likely reflects differences in bioactive compounds such as monoterpenes and oxygenated derivatives, which vary in their mechanisms of action and membrane permeability.

The highly significant microorganism × oil interaction indicates that specific oils exhibit selective antimicrobial activity depending on the target organism. This is particularly relevant when considering structural differences between Gram-positive and Gram-negative bacteria, as well as yeasts, which can influence compound uptake and sensitivity.

Similarly, the microorganism × concentration interaction suggests that dose–response relationships are not uniform across species, reinforcing the need for organism-specific optimization of antimicrobial treatments.

The absence of a significant oil × concentration interaction suggests that increasing concentration enhances antimicrobial activity in a broadly consistent manner across oils, without substantially altering their relative effectiveness.

Finally, the significant three-way interaction underscores the complexity of antimicrobial responses, indicating that the combined effects of oil type and concentration vary depending on the microbial species. This highlights the necessity of multifactorial approaches when evaluating antimicrobial agents.

In the pear model (Table S2), CMEO showed clear concentration-dependent inhibition across most tested microorganisms. Among Gram-negative bacteria, *E. coli* exhibited strong suppression, with 66.39% inhibition at 500 μL/L, decreasing to 35.81% at 62.5 μL/L. *S. enterica* showed moderate sensitivity (about 55.79% at 500 μL/L and 25.82% at 62.5 μL/L), while *Y. enterocolitica* ranked among the most susceptible Gram-negative strains, with inhibition reaching 75.25% at 500 μL/L and 46.71% at 62.5 μL/L.

Among Gram-positive species (Table S2), *S. aureus* responded particularly well to CMEO, with inhibition of 84.92% at the highest tested dose and 25.72% at the lowest. *E. faecalis* showed inhibition of 75.13% at 500 μL/L, dropping to 16.03% at 62.5 μL/L, whereas *L. monocytogenes* reached 74.56% and 26.59% at the same respective concentrations. Within the yeast panel, *C. albicans* was among the more sensitive species. CMEO achieved 64.49% inhibition at 500 μL/L and 35.87% at 62.5 μL/L. *C. glabrata* exhibited unusually high inhibition across all concentrations, with values from 75.42% (500 μL/L) to 73.95% (62.5 μL/L), indicating substantial susceptibility even at low doses. *C. parapsilosis* also showed notable inhibition (65.29–33.97% across the tested range). The biofilm-forming *S. enterica* strain responded strongly to CMEO as well. Inhibition reached 74.78% at 500 μL/L and remained considerable (44.12%) even at 62.5 μL/L, demonstrating that CMEO is effective not only against planktonic cells but also against biofilm-associated populations in a fruit matrix.

α-Terpineol showed the strongest inhibitory activity among the tested constituents on pear slices. Among Gram-negative bacteria, *E. coli* showed inhibition of 42.10% at 500 μL/L and 8.56% at 62.5 μL/L, *S. enterica* reached 40.00% at 500 μL/L and 8.10% at 62.5 μL/L, and *Y. enterocolitica* showed 39.77% at 500 μL/L and 9.07% at 62.5 μL/L. Among Gram-positive bacteria, *E. faecalis* showed inhibition of 41.15% at 500 μL/L and 5.76% at 62.5 μL/L, *L. monocytogenes* reached 42.13% at 500 μL/L and 7.68% at 62.5 μL/L, and *S. aureus* showed 36.62% at 500 μL/L and −6.07% at 62.5 μL/L. Within the yeast group, *C. albicans* showed inhibition of 29.43% at 500 μL/L and −8.57% at 62.5 μL/L, *C. glabrata* reached 33.30% at 500 μL/L and −9.59% at 62.5 μL/L, *C. krusei* showed 32.81% at 500 μL/L and −6.24% at 62.5 μL/L, *C. parapsilosis* reached 30.22% at 500 μL/L and −8.57% at 62.5 μL/L, and *C. tropicalis* showed 33.67% at 500 μL/L and −8.21% at 62.5 μL/L. The biofilm-forming *S. enterica* strain showed inhibition of 40.10% at 500 μL/L and 9.74% at 62.5 μL/L.

On pear, β-pinene showed a weaker inhibitory effect compared to CMEO, with activity appearing mainly at the highest concentration (Table S2). In *E. coli*, inhibition at 500 μL/L reached 36.63%, while at 62.5 μL/L it decreased to 8.62%. A similar pattern was observed in *S. enterica*, where β-pinene achieved 35.28% inhibition at 500 μL/L and only 6.79% at 62.5 μL/L. *Y. enterocolitica* responded slightly better at the highest concentration (35.48% at 500 μL/L), but inhibition dropped to 5.01% at 62.5 μL/L. Among Gram-positive bacteria, *L. monocytogenes* was the most sensitive to β-pinene, showing 36.64% inhibition at 500 μL/L, while at 62.5 μL/L inhibition decreased to 6.68%. *S. aureus* exhibited 31.23% inhibition at 500 μL/L, dropping to 6.43% at the lowest concentration. Yeasts showed the lowest sensitivity to β-pinene (Table S2). *C. albicans* was inhibited by only 26.12% at 500 μL/L, whereas at 62.5 μL/L the value reached −6.94%, indicating enhanced growth rather than suppression. *C. glabrata* behaved similarly, with inhibition of 29.19% at 500 μL/L and −6.61% at 62.5 μL/L. Likewise, *C. krusei* showed 27.25% inhibition at 500 μL/L and −6.16% at 62.5 μL/L, while *C. tropicalis* reached 27.11% and −6.04%, respectively. The biofilm-forming *S. enterica* strain was inhibited only partially by β-pinene. At 500 μL/L, inhibition reached 34.87%, whereas at 62.5 μL/L it dropped to 8.03%, confirming the limited effect of β-pinene in this food matrix.

Borneol showed weaker inhibitory activity than α-terpineol on pear slices (Table S2). Among Gram-negative bacteria, *E. coli* showed inhibition of 36.01% at 500 μL/L and 7.17% at 62.5 μL/L, *S. enterica* reached 32.00% at 500 μL/L and 6.73% at 62.5 μL/L, and *Y. enterocolitica* showed 33.31% at 500 μL/L and 5.22% at 62.5 μL/L. Among Gram-positive bacteria, *E. faecalis* showed inhibition of 33.02% at 500 μL/L and 3.05% at 62.5 μL/L, *L. monocytogenes* reached 35.94% at 500 μL/L and 6.40% at 62.5 μL/L, and *S. aureus* showed 30.10% at 500 μL/L and 25.02% at 62.5 μL/L. Within the yeast group, *C. albicans* showed inhibition of 26.31% at 500 μL/L and −7.60% at 62.5 μL/L, *C. glabrata* reached 27.90% at 500 μL/L and −8.00% at 62.5 μL/L, *C. krusei* showed 26.25% at 500 μL/L and −5.23% at 62.5 μL/L, *C. parapsilosis* reached 25.19% at 500 μL/L and −5.44% at 62.5 μL/L, and *C. tropicalis* showed 22.97% at 500 μL/L and −6.85% at 62.5 μL/L. The biofilm-forming *S. enterica* strain showed inhibition of 33.34% at 500 μL/L and 8.16% at 62.5 μL/L.

Camphor showed the weakest inhibitory activity among the tested constituents on pear slices (Table S2). Among Gram-negative bacteria, *E. coli* showed inhibition of 35.10% at 500 μL/L and 7.13% at 62.5 μL/L, *S. enterica* reached 33.82% at 500 μL/L and 6.51% at 62.5 μL/L, and *Y. enterocolitica* showed 34.02% at 500 μL/L and 4.34% at 62.5 μL/L. Among Gram-positive bacteria, *E. faecalis* showed inhibition of 32.80%

at 500 μL/L and 7.30% at 62.5 μL/L, *L. monocytogenes* reached 33.29% at 500 μL/L and 6.02% at 62.5 μL/L, and *S. aureus* showed 30.53% at 500 μL/L and 11.64% at 62.5 μL/L. Within the yeast group, *C. albicans* showed inhibition of 24.53% at 500 μL/L and −5.06% at 62.5 μL/L, *C. glabrata* reached 27.76% at 500 μL/L and −8.00% at 62.5 μL/L, *C. krusei* showed 27.77% at 500 μL/L and −5.21% at 62.5 μL/L, *C. parapsilosis* reached 22.81% at 500 μL/L and −7.14% at 62.5 μL/L, and *C. tropicalis* showed 28.07% at 500 μL/L and −6.85% at 62.5 μL/L. The biofilm-forming *S. enterica* strain showed inhibition of 30.78% at 500 μL/L and 8.27% at 62.5 μL/L.

On pear slices, CMEO again displayed a clearly stronger antimicrobial effect than all tested constituents across all tested microorganisms. CMEO maintained inhibitory activity even at lower concentrations, while the individual constituents exerted a noticeable effect mainly at the highest dose, with inhibition rapidly decreasing as the concentration dropped. Gram-negative bacteria responded substantially better to CMEO, whereas the individual constituents produced only modest suppression. Gram-positive bacteria followed the same pattern, with CMEO consistently outperforming all tested constituents. In yeasts, the difference was even more pronounced: CMEO reduced growth across the entire concentration range, whereas several *Candida* species exhibited minimal inhibition or even slight stimulation of growth in the presence of the individual constituents. The biofilm-forming *S. enterica* strain was also inhibited more effectively by CMEO, confirming that the EO retains functional antimicrobial activity within the pear matrix, while no single constituent alone is sufficient to achieve comparable effects.

The heatmap analysis of pear samples (Fig. 2) revealed a clear concentration-dependent increase in antimicrobial activity for CMEO and its individual components across all tested microorganisms. CMEO exhibited the strongest inhibitory effect, with values frequently exceeding 60% at higher concentrations (250–500 μL/L), confirming its superior efficacy compared to the isolated compounds.

Among the tested microorganisms, *Y. enterocolitica, S. aureus*, and *E. faecalis* showed the highest susceptibility to CMEO, reaching inhibition levels above 75% at the maximum concentration. Notably, *C. glabrata* displayed consistently high inhibition values across all CMEO concentrations, suggesting a marked sensitivity even at lower doses.

In contrast, the individual components (β-pinene, α-terpineol, borneol, and camphor) exhibited a more moderate antimicrobial activity. Among them, α-terpineol demonstrated relatively higher efficacy, particularly at increasing concentrations, reaching inhibition values above 40% for several strains. The remaining compounds showed similar trends, with gradual increases in activity but generally lower effectiveness compared to CMEO.

Interestingly, negative or near-zero inhibition values were observed for some *Candida* species (e.g., *C. albicans*, *C. glabrata*, and *C. tropicalis*) at lower concentrations of the individual components, suggesting a possible stimulatory or negligible effect under these conditions. However, this trend was progressively reversed at higher concentrations.

Overall, Gram-positive bacteria appeared slightly more susceptible than Gram-negative strains, although a strong inhibitory effect of CMEO was observed across both groups. These findings support the hypothesis that the whole essential oil exerts enhanced antimicrobial activity due to synergistic interactions among its constituents, which are not fully replicated when the compounds are tested individually.

3.4.3. *In situ vapor phase antimicrobial effects on parsley slices*

The three-way ANOVA (Table 7) revealed highly significant main effects of microorganism, oil, and concentration on antimicrobial activity ($p < 0.001$ for all factors). Among these, microorganism identity ($F = 141.29$, $\eta p^2 = 0.764$) and concentration ($F = 458.46$, $\eta p^2 = 0.741$) exhibited the strongest effects, indicating that both microbial susceptibility and dosage play dominant roles in determining antimicrobial response.

Oil type also had a statistically significant effect ($F = 13.77$, $\eta p^2 = 0.103$), although with a comparatively smaller effect size, suggesting that differences among oils are less pronounced than differences among microorganisms or concentration levels.

All interaction terms were statistically significant. The microorganism × oil interaction ($F = 27.40$, $\eta p^2 = 0.715$) (Table 7) and

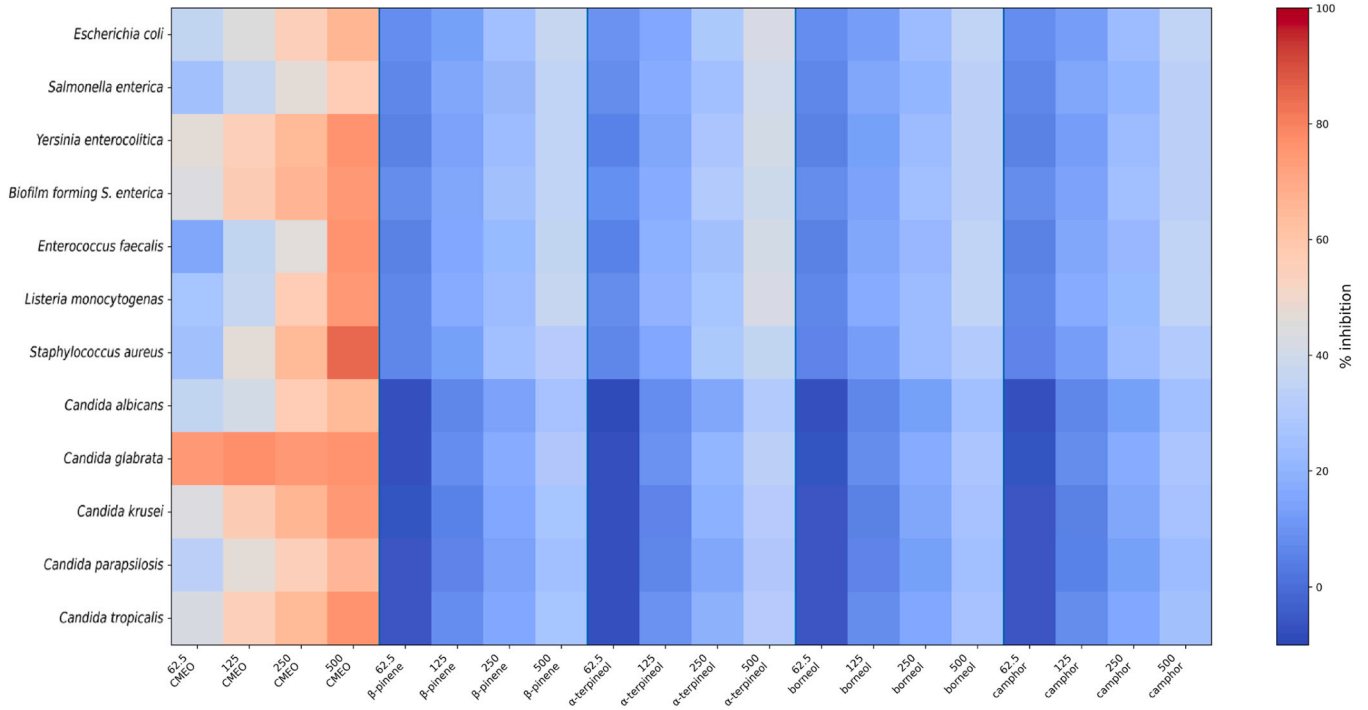

Fig. 2. Heatmap representing In situ analysis of the inhibition of microbial growth (%) by the vapor phase of CMEO and its main components (β-pinene, α-terpineol, borneol, and camphor) against selected microorganisms in pear samples at increasing concentrations (62.5–500 μL/L). Values are expressed as mean percentages of inhibition obtained from three independent replicates. Color gradient ranges from blue (low inhibition) to red (high inhibition).

Table 7
Three-way ANOVA evaluating the effects of microorganism, essential oil, and concentration on antimicrobial response in parsley matrix.

Variable	df	Sum of Squares	F	*p*-value	η^2	ηp^2
Microorganism	11	7218.13	141.29	< 0.001	0.254	0.764
Essential Oil	4	255.89	13.77	< 0.001	0.009	0.103
Concentration	3	6387.60	458.46	< 0.001	0.224	0.741
Microorganism × Essential Oil	44	5598.16	27.40	< 0.001	0.197	0.715
Microorganism × Concentration	33	2674.54	17.45	< 0.001	0.094	0.545
Essential Oil × Concentration	12	1239.00	22.23	< 0.001	0.044	0.357
Microorganism × Essential Oil × Concentration	132	2095.92	3.42	< 0.001	0.074	0.485
Residual	480	2229.26			0.078	

Effect sizes are reported as eta squared (η^2) and partial eta squared (ηp^2).

microorganism × concentration interaction ($F = 17.45$, $\eta p^2 = 0.545$) indicate that both the effectiveness of oils and dose–response patterns vary depending on the microbial species.

The essential oil × concentration interaction was also significant ($F = 22.23$, $\eta p^2 = 0.357$), demonstrating that the relative efficacy of oils changes across concentration levels. Additionally, the three-way interaction ($F = 3.42$, $\eta p^2 = 0.485$) was significant, confirming a complex interplay among microorganism, oil, and concentration (Table 7).

The results highlight concentration as a major determinant of antimicrobial activity, with a very large effect size confirming a strong dose–response relationship. This suggests that increasing concentration substantially enhances antimicrobial efficacy across all tested conditions. Microorganism identity also plays a critical role, reflecting inherent differences in susceptibility among microbial species. These differences likely arise from variations in cell wall structure, membrane composition, and metabolic activity, particularly when comparing bacteria and yeasts. Although oil type was statistically significant, its relatively small effect size suggests that its influence is secondary compared to microorganism and concentration. This indicates that, while chemical composition is important, it may not be the primary driver of antimicrobial variability in this dataset. The significant oil × concentration interaction represents a key finding, indicating that the effectiveness of individual oils is not constant across doses. This suggests that some oils may exhibit enhanced activity only at higher concentrations, while others may reach a plateau earlier.

The strong microorganism-dependent interactions further emphasize that antimicrobial efficacy cannot be generalized across species. Instead, the results support a targeted approach, where both the choice of oil and the applied concentration should be optimized for specific microorganisms. Finally, the significant three-way interaction confirms the complexity of the system, demonstrating that antimicrobial activity is governed by the combined effects of chemical composition, dosage, and microbial characteristics.

In the parsley model (Table S3), among Gram-negative bacteria, *E. coli* exhibited strong suppression, with 77.08% inhibition at 500 μL/L, decreasing to 45.92% at 62.5 μL/L. *S. enterica* showed moderate sensitivity, reaching 76.40% at 500 μL/L and 43.78% at 62.5 μL/L, while *Y. enterocolitica* ranked among the more responsive strains, with inhibition of 75.03% at 500 μL/L and 44.97% at 62.5 μL/L. Among Gram-positive bacteria, *S. aureus* responded particularly well to CMEO, exhibiting 87.60% inhibition at 500 μL/L and 55.64% at 62.5 μL/L (Table S3).

E. faecalis reached 76.38% at 500 μL/L, decreasing to 44.86% at 62.5 μL/L, while *L. monocytogenes* displayed inhibition of 86.81% and 55.90%, respectively. Within the yeast panel, *C. albicans* showed substantial susceptibility, with inhibition values of 86.27% at 500 μL/L and 56.60% at 62.5 μL/L. *C. glabrata* remained consistently inhibited across all concentrations, ranging from 86.93% to 55.64%, while *C. parapsilosis* showed inhibition between 86.34% and 56.56%. *C. tropicalis* demonstrated similar behaviour, with inhibition decreasing from 87.04% to 55.67%. The biofilm-forming *S. enterica* strain responded strongly to CMEO as well, with 77.67% inhibition at 500 μL/L and 15.93% at 62.5 μL/L (Table S3), indicating that the EO maintains relevant activity even against biofilm-associated cells in the parsley matrix.

α-Terpineol showed the strongest inhibitory activity among the tested constituents on parsley (Table S3). Among Gram-negative bacteria, *E. coli* showed inhibition of 44.01% at 500 μL/L and 10.07% at 62.5 μL/L, *S. enterica* reached 44.56% at 500 μL/L and 11.47% at 62.5 μL/L, and *Y. enterocolitica* showed 41.50% at 500 μL/L and 8.71% at 62.5 μL/L. Among Gram-positive bacteria, *E. faecalis* showed inhibition of 43.04% at 500 μL/L and 9.06% at 62.5 μL/L, *L. monocytogenes* reached 37.99% at 500 μL/L and 5.72% at 62.5 μL/L, and *S. aureus* showed 38.21% at 500 μL/L and 6.41% at 62.5 μL/L. Within the yeast group, *C. albicans* showed inhibition of 37.07% at 500 μL/L and 7.52% at 62.5 μL/L, *C. glabrata* reached 38.02% at 500 μL/L and 6.41% at 62.5 μL/L, *C. krusei* showed 40.00% at 500 μL/L and 4.73% at 62.5 μL/L, *C. parapsilosis* reached 37.09% at 500 μL/L and 8.95% at 62.5 μL/L, and *C. tropicalis* showed 37.29% at 500 μL/L and 4.96% at 62.5 μL/L. The biofilm-forming *S. enterica* strain showed inhibition of 41.11% at 500 μL/L and 6.11% at 62.5 μL/L.

In the parsley model (Table S3), β-pinene exhibited an overall weaker *in situ* antimicrobial effect than CMEO, with consistently lower activity across all tested concentrations. Among Gram-negative bacteria, *E. coli* showed only mild inhibition, reaching 38.27% at 500 μL/L and decreasing to 7.57% at 62.5 μL/L. *S. enterica* responded similarly, with inhibition of 37.43% at 500 μL/L and 8.04% at 62.5 μL/L. *Y. enterocolitica* was among the more sensitive Gram-negative strains, achieving 36.09% inhibition at 500 μL/L but only 7.58% at the lowest concentration. Among Gram-positive bacteria, β-pinene affected *E. faecalis* the most, reaching 37.43% inhibition at 500 μL/L and decreasing to 7.88% at 62.5 μL/L. *S. aureus* reached 33.23% at 500 μL/L and only 5.58% at 62.5 μL/L. *L. monocytogenes* was among the less sensitive species, with 33.04% inhibition at the highest concentration and 4.98% at the lowest. Within the yeast group, inhibition levels remained low. *C. albicans* reached 32.23% at 500 μL/L and 6.15% at 62.5 μL/L. *C. glabrata* reached 33.07% at 500 μL/L and 5.58% at 62.5 μL/L. *C. parapsilosis* showed 32.25% inhibition at 500 μL/L and 6.14% at 62.5 μL/L, while *C. tropicalis* showed 32.43% and 5.59%, respectively. The biofilm-forming *S. enterica* strain was inhibited only moderately β-pinene achieved 35.75% inhibition at 500 μL/L, decreasing to 5.32% at the lowest concentration. Overall, β-pinene demonstrated only mild, concentration-dependent activity on parsley, and for all tested microorganisms, it remained markedly weaker than CMEO, confirming that β-pinene alone cannot account for the antimicrobial strength exhibited by the full EO.

Borneol showed weaker inhibitory activity than α-terpineol on parsley (Table S3). Among Gram-negative bacteria, *E. coli* showed inhibition of 37.87% at 500 μL/L and 4.34% at 62.5 μL/L, *S. enterica* reached 39.19% at 500 μL/L and 7.22% at 62.5 μL/L, and *Y. enterocolitica* showed 41.65% at 500 μL/L and 10.10% at 62.5 μL/L. Among Gram-positive bacteria, *E. faecalis* showed inhibition of 38.72% at 500 μL/L and 7.25% at 62.5 μL/L, *L. monocytogenes* reached 34.44% at 500 μL/L and 6.77% at 62.5 μL/L, and *S. aureus* showed 30.45% at 500 μL/L and 9.81% at 62.5 μL/L. Within the yeast group, *C. albicans* showed inhibition of 32.86% at 500 μL/L and 3.41% at 62.5 μL/L, *C. glabrata* reached 31.85% at 500 μL/L and 5.37% at 62.5 μL/L, *C. krusei* showed 33.50% at 500 μL/L and 3.96% at 62.5 μL/L, *C. parapsilosis* reached 32.78% at 500 μL/L and 7.49% at 62.5 μL/L, and *C. tropicalis* showed 30.74% at 500 μL/L and 4.13% at 62.5 μL/L. The biofilm-forming *S. enterica* strain showed inhibition of 31.70% at 500 μL/L and 3.86% at 62.5 μL/L.

Camphor showed the weakest inhibitory activity among the tested constituents on parsley. Among Gram-negative bacteria, *E. coli* showed

inhibition of 37.69% at 500 μL/L and 8.40% at 62.5 μL/L, *S. enterica* reached 35.88% at 500 μL/L and 9.56% at 62.5 μL/L, and *Y. enterocolitica* showed 34.60% at 500 μL/L and 5.84% at 62.5 μL/L. Among Gram-positive bacteria, *E. faecalis* showed inhibition of 37.47% at 500 μL/L and 8.84% at 62.5 μL/L, *L. monocytogenes* reached 31.70% at 500 μL/L and 4.16% at 62.5 μL/L, and *S. aureus* showed 31.85% at 500 μL/L and 4.18% at 62.5 μL/L. Within the yeast group, *C. albicans* showed inhibition of 30.23% at 500 μL/L and 7.52% at 62.5 μL/L, *C. glabrata* reached 31.70% at 500 μL/L and 4.10% at 62.5 μL/L, *C. krusei* showed 33.34% at 500 μL/L and 3.94% at 62.5 μL/L, *C. parapsilosis* reached 30.29% at 500 μL/L and 7.46% at 62.5 μL/L, and *C. tropicalis* showed 30.74% at 500 μL/L and 4.13% at 62.5 μL/L. The biofilm-forming *S. enterica* strain showed inhibition of 31.77% at 500 μL/L and 3.56% at 62.5 μL/L.

On parsley samples, CMEO again displayed a clearly stronger antimicrobial effect than all tested constituents across all tested microorganisms. CMEO maintained inhibitory activity even at lower concentrations, whereas the individual constituents produced only limited suppression and their effect declined rapidly as the concentration decreased. Gram-negative bacteria showed markedly higher sensitivity to CMEO, while the individual constituents resulted in only modest inhibition. A similar pattern was observed among Gram-positive bacteria, where CMEO consistently outperformed all tested constituents across the entire concentration range. In yeasts, the difference became even more pronounced: CMEO reduced growth steadily at all doses, while several *Candida* species exhibited minimal inhibition in the presence of the individual constituents. The biofilm-forming *S. enterica* strain also responded substantially better to CMEO, confirming that the EO retains strong antimicrobial activity within the parsley matrix, whereas no single constituent alone is sufficient to achieve comparable effects.

The heatmap analysis of parsley samples (Fig. 3) showed a clear concentration-dependent increase in antimicrobial activity for CMEO and its individual components across all tested microorganisms. CMEO consistently exhibited the highest inhibitory effect, with values exceeding 70–80% at the highest concentration (500 μL/L) for most strains, confirming its strong antimicrobial potential.

Among the tested microorganisms, *L. monocytogenes*, *S. aureus*, and several *Candida* species (*C. albicans, C. glabrata, and C. parapsilosis*) demonstrated particularly high susceptibility to CMEO, reaching inhibition values close to or above 85%. In contrast, biofilm-forming *S. enterica* and *C. krusei* showed lower sensitivity at lower concentrations but exhibited a marked increase in inhibition at higher doses, indicating a pronounced dose-response effect.

Regarding individual components, α-terpineol again displayed the highest antimicrobial activity among the tested compounds, reaching values above 40% inhibition at the highest concentration for several microorganisms. β-pinene, borneol, and camphor showed comparable trends, with moderate inhibitory effects that increased gradually with concentration but remained significantly lower than those observed for CMEO.

Unlike the pear dataset, no negative inhibition values were observed, suggesting a more consistent antimicrobial response in parsley across all tested conditions. This indicates a more stable interaction between the tested compounds and the microbial strains in this matrix.

Overall, the results confirm that CMEO exhibits superior antimicrobial activity compared to its individual constituents, likely due to synergistic interactions among its components. Additionally, the parsley matrix appears to enhance or stabilize the antimicrobial effectiveness, resulting in more uniform and pronounced inhibition patterns across microorganisms.

3.4.4. *In situ vapor phase antimicrobial effects on Hokkaido pumpkin slices*

The three-way ANOVA (Table 8) revealed significant main effects of microorganism, oil, and concentration on antimicrobial activity ($p < 0.001$ for all factors). Among these, oil ($F = 170.07$, $\eta p^2 = 0.586$) and concentration ($F = 172.79$, $\eta p^2 = 0.519$) showed the strongest effects, indicating that antimicrobial efficacy in the Hokkaido pumpkin matrix is primarily driven by treatment-related factors.

Microorganism identity also had a significant but comparatively smaller effect ($F = 28.03$, $\eta p^2 = 0.391$), suggesting moderate variability

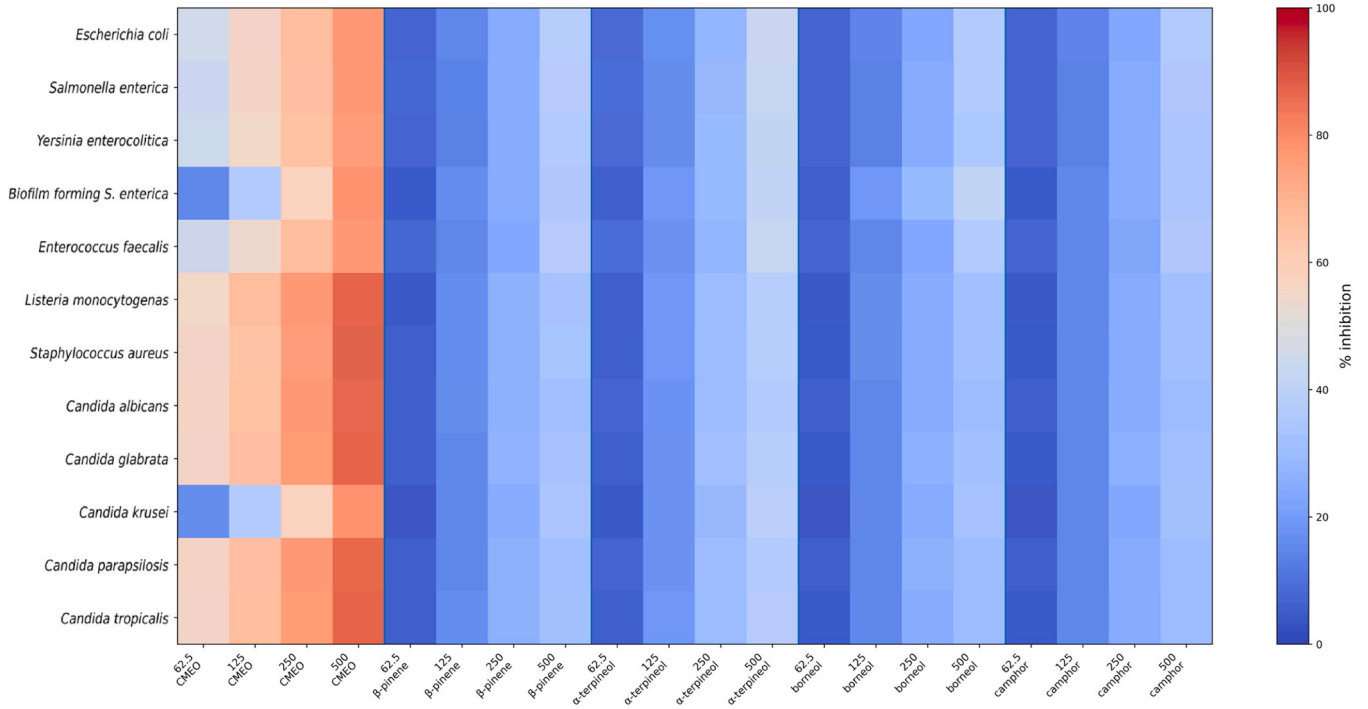

Fig. 3. Heatmap representing in situ analysis of the inhibition of microbial growth (%) by the vapor phase of CMEO and its main components (β-pinene, α-terpineol, borneol, and camphor) against selected microorganisms in parsley samples at increasing concentrations (62.5–500 μL/L). Values are expressed as mean percentages of inhibition obtained from three independent replicates. Color gradient ranges from blue (low inhibition) to red (high inhibition).

Table 8
Three-way ANOVA evaluating the effects of microorganism, essential oil, and concentration on antimicrobial response in Hokkaido pumpkin matrix.

Variable	df	Sum of Squares	F	*p*-value	η^2	ηp^2
Microorganism	11	981.52	28.03	< 0.001	0.047	0.391
Essential Oil	4	2165.29	170.07	< 0.001	0.104	0.586
Concentration	3	1649.92	172.79	< 0.001	0.079	0.519
Microorganism × Essential Oil	44	806.99	5.76	< 0.001	0.039	0.346
Microorganism × Concentration	33	48.21	0.46	0.996	0.002	0.031
Essential Oil × Concentration	12	44.40	1.16	0.308	0.002	0.028
Microorganism × Essential Oil × Concentration	132	115.66	0.28	1.000	0.006	0.070
Residual	480	1527.77			0.073	

Effect sizes are reported as eta squared (η^2) and partial eta squared (ηp^2).

in susceptibility among the tested species.

Among interaction terms, only the microorganism × oil interaction was statistically significant ($F = 5.76$, $\eta p^2 = 0.346$), indicating that the relative effectiveness of oils varies depending on the microbial species. In contrast, the microorganism × concentration ($p = 0.996$), oil × concentration ($p = 0.308$), and the three-way interaction ($p = 1.000$) were not significant, all showing very small effect sizes (Table 8).

The results indicate that antimicrobial activity in the Hokkaido pumpkin matrix is predominantly governed by the independent effects of oil type and concentration, with minimal contribution from interaction effects. This suggests a largely additive behavior of the tested factors. The strong effect of oil type highlights the importance of chemical composition in determining antimicrobial efficacy, while the similarly strong effect of concentration confirms a clear dose-dependent response. Together, these findings suggest that treatment optimization in this matrix can be effectively achieved by independently selecting the appropriate oil and concentration. In contrast to other matrices, the relatively smaller effect of microorganism identity indicates reduced variability in microbial susceptibility. This may reflect a more homogeneous interaction between the matrix and microbial cells, potentially due to the physicochemical properties of the pumpkin matrix.

The lack of significant interactions, particularly the absence of a three-way interaction, suggests that the antimicrobial response is predictable and not strongly influenced by complex factor interdependencies. This contrasts with more complex matrices where interactions play a major role. Overall, these findings indicate that the Hokkaido pumpkin matrix represents a simpler system in which antimicrobial efficacy is driven mainly by direct treatment effects rather than by intricate biological interactions.

In the Hokkaido pumpkin model (Table S4), among Gram-negative bacteria, *E. coli* exhibited a clear concentration-dependent response, with 35.93% inhibition at 500 μL/L and increasing to 66.27% at 62.5 μL/L. *S. enterica* showed a similar trend, reaching 35.03% at 500 μL/L and 65.90% at 62.5 μL/L, while *Y. enterocolitica* responded comparably, with inhibition values of 36.27% at 500 μL/L and 67.56% at 62.5 μL/L. Among Gram-positive bacteria, *E. faecalis* was moderately inhibited, with 35.60% inhibition at 500 μL/L and 65.90% at 62.5 μL/L. *L. monocytogenes* showed stronger sensitivity, with inhibition increasing from 46.23% at 500 μL/L to 77.23% at 62.5 μL/L, while *S. aureus* displayed a very similar pattern, reaching 45.23% and 77.27% at the same respective concentrations.

Within the yeast panel (Table S4), *C. albicans* exhibited substantial suppression, with inhibition rising from 45.97% at 500 μL/L to 77.64% at 62.5 μL/L. *C. glabrata* showed consistently high values, ranging from 45.01% at 500 μL/L to 76.01% at 62.5 μL/L. *C. parapsilosis* demonstrated strong responsiveness, with inhibition of 45.93% and 77.38%, while *C. tropicalis* exhibited similarly elevated values, between 44.93% and 76.15% across the tested range. *C. krusei* showed lower inhibition at 500 μL/L (35.93%) but increased notably to 66.82% at 62.5 μL/L. The biofilm-forming *S. enterica* strain reacted strongly to CMEO, with inhibition of 35.93% at 500 μL/L, increasing to 67.01% at 62.5 μL/L. These results show that CMEO retains high antimicrobial potential on the Hokkaido matrix, affecting not only planktonic but also biofilm-associated populations.

α-Terpineol showed the strongest inhibitory activity among the tested constituents on Hokkaido pumpkin slices (Table S4). Among Gram-negative bacteria, *E. coli* showed inhibition of 10.88% at 500 μL/L and 42.62% at 62.5 μL/L, *S. enterica* reached 10.26% at 500 μL/L and 41.76% at 62.5 μL/L, and *Y. enterocolitica* showed 10.67% at 500 μL/L and 41.94% at 62.5 μL/L. Among Gram-positive bacteria, *E. faecalis* showed inhibition of 10.23% at 500 μL/L and 41.50% at 62.5 μL/L, *L. monocytogenes* reached 9.46% at 500 μL/L and 43.29% at 62.5 μL/L, and *S. aureus* showed 8.40% at 500 μL/L and 37.55% at 62.5 μL/L. Within the yeast group, *C. albicans* showed inhibition of 8.23% at 500 μL/L and 40.33% at 62.5 μL/L, *C. glabrata* reached 9.88% at 500 μL/L and 41.40% at 62.5 μL/L, *C. krusei* showed 9.24% at 500 μL/L and 41.03% at 62.5 μL/L, *C. parapsilosis* reached 9.11% at 500 μL/L and 40.33% at 62.5 μL/L, and *C. tropicalis* showed 9.88% at 500 μL/L and 41.02% at 62.5 μL/L. The biofilm-forming *S. enterica* strain showed inhibition of 8.72% at 500 μL/L and 41.03% at 62.5 μL/L.

Among Gram-negative bacteria (Table S4), *E. coli* showed only weak inhibition, reaching 8.98% at 500 μL/L and increasing to 34.23% at 62.5 μL/L, indicating that β-pinene did not suppress but rather allowed progressive microbial growth with decreasing concentration. *S. enterica* exhibited a similar pattern, with 8.76% inhibition at 500 μL/L and 36.48% at 62.5 μL/L. *Y. enterocolitica* showed slightly higher inhibition at the highest concentration (9.07% at 500 μL/L), but the inhibitory effect again diminished at lower doses, reaching 35.56% at 62.5 μL/L, demonstrating insufficient antimicrobial pressure. Among Gram-positive bacteria, *E. faecalis* showed modest inhibition at the highest dose (8.90% at 500 μL/L), followed by a substantial loss of activity, with inhibition increasing to 35.48% at 62.5 μL/L, again indicating minimal antimicrobial impact. *L. monocytogenes* responded slightly better at higher concentrations (8.23% at 500 μL/L) but showed increasing growth at lower concentrations (37.64% at 62.5 μL/L). *S. aureus* exhibited only mild inhibition (7.31% at 500 μL/L) and again showed increased growth at 32.65% when exposed to the lowest concentration. Within the yeast group, β-pinene demonstrated low and inconsistent activity. *C. albicans* reached 7.16% inhibition at 500 μL/L, yet inhibition rapidly decreased and values rose to 36.74% at 62.5 μL/L. *C. glabrata* showed similarly weak suppression (7.92% at 500 μL/L; 36.00% at 62.5 μL/L). *C. krusei* displayed slightly higher inhibition at 500 μL/L (9.25%), but its effect again diminished toward 36.00% at the lowest concentration. *C. parapsilosis* and C. tropicalis exhibited nearly identical patterns, with inhibition at 7.92–8.92% (500 μL/L) and increased growth at 37.34–35.67% (62.5 μL/L). The biofilm-forming *S. enterica* strain showed only minimal responsiveness to β-pinene, with 7.59% inhibition at 500 μL/L and 37.00% at 62.5 μL/L, confirming that β-pinene is largely ineffective against biofilm-associated cells in the Hokkaido pumpkin matrix.

Borneol showed weaker inhibitory activity than α-terpineol on Hokkaido pumpkin slices (Table S4). Among Gram-negative bacteria, *E. coli* showed inhibition of 8.66% at 500 μL/L and 35.53% at 62.5 μL/L, *S. enterica* reached 8.73% at 500 μL/L and 34.54% at 62.5 μL/L, and *Y. enterocolitica* showed 8.66% at 500 μL/L and 31.67% at 62.5 μL/L. Among Gram-positive bacteria, *E. faecalis* showed inhibition of 7.98% at 500 μL/L and 31.91% at 62.5 μL/L, *L. monocytogenes* reached 7.89% at 500 μL/L and 36.09% at 62.5 μL/L, and *S. aureus* showed 7.76% at 500 μL/L and 33.50% at 62.5 μL/L. Within the yeast group, *C. albicans* showed inhibition of 6.05% at 500 μL/L and 33.02% at 62.5 μL/L, *C. glabrata* reached 6.02% at 500 μL/L and 17.31% at 62.5 μL/L, *C. krusei* showed 7.01% at 500 μL/L and 19.05% at 62.5 μL/L, *C. parapsilosis* reached 8.24% at 500 μL/L and 14.17% at 62.5 μL/L, and

C. tropicalis showed 8.27% at 500 µL/L and 14.24% at 62.5 µL/L. The biofilm-forming *S. enterica* strain showed inhibition of 7.31% at 500 µL/L and 13.62% at 62.5 µL/L.

Camphor showed the weakest inhibitory activity among the tested constituents on Hokkaido pumpkin slices (Table S4). Among Gram-negative bacteria, *E. coli* showed inhibition of 8.66% at 500 µL/L and 33.53% at 62.5 µL/L, *S. enterica* reached 8.40% at 500 µL/L and 32.82% at 62.5 µL/L, and *Y. enterocolitica* showed 8.66% at 500 µL/L and 31.67% at 62.5 µL/L. Among Gram-positive bacteria, *E. faecalis* showed inhibition of 7.94% at 500 µL/L and 31.91% at 62.5 µL/L, *L. monocytogenes* reached 7.25% at 500 µL/L and 34.19% at 62.5 µL/L, and *S. aureus* showed 5.11% at 500 µL/L and 31.98% at 62.5 µL/L. Within the yeast group, *C. albicans* showed inhibition of 5.78% at 500 µL/L and 33.34% at 62.5 µL/L, *C. glabrata* reached 8.24% at 500 µL/L and 22.35% at 62.5 µL/L, *C. krusei* showed 9.19% at 500 µL/L and 24.51% at 62.5 µL/L, *C. parapsilosis* reached 8.24% at 500 µL/L and 14.17% at 62.5 µL/L, and *C. tropicalis* showed 8.25% at 500 µL/L and 12.62% at 62.5 µL/L. The biofilm-forming *S. enterica* strain showed inhibition of 6.30% at 500 µL/L and 12.58% at 62.5 µL/L (Table S4).

Overall, β-pinene and the other individual constituents exhibited very weak and inconsistent *in situ* antimicrobial activity on Hokkaido slices. In most cases, inhibition at high concentrations was low, and at lower concentrations, microorganisms often exhibited increased growth, demonstrating that no single constituent alone provides meaningful antimicrobial protection in this food system. On pumpkin squash slices, CMEO again displayed a markedly stronger antimicrobial effect than all tested constituents. CMEO maintained inhibitory activity across the entire concentration range, whereas the individual constituents showed only limited suppression that declined rapidly as the dose decreased. Gram-negative bacteria exhibited substantially higher sensitivity to CMEO, while the individual constituents produced only weak to moderate inhibition. A similar trend was observed among Gram-positive species, where CMEO consistently outperformed all tested constituents under all tested conditions. In yeasts, the difference became even more pronounced: CMEO produced stable inhibition, whereas several *Candida* species exhibited minimal inhibition or even signs of growth stimulation in the presence of the individual constituents. The biofilm-forming *S. enterica* strain was also inhibited much more effectively by CMEO, confirming that the EO retains strong antimicrobial activity within the pumpkin matrix, whereas no single constituent alone can achieve comparable effects.

The heatmap analysis of Hokkaido pumpkin samples (Fig. 4) revealed a markedly different antimicrobial pattern compared to the other matrices. In contrast to apple, pear, and parsley, CMEO exhibited a decreasing inhibitory effect with increasing concentration, indicating an inverse dose–response relationship.

Specifically, higher inhibition values were observed at the lowest concentration (62.5 µL/L), with percentages frequently exceeding 65–75% for several microorganisms, including *L. monocytogenes*, *S. aureus*, and various *Candida* species. However, as the concentration increased, the inhibitory activity progressively declined, reaching values around 35–45% at the highest concentration (500 µL/L).

A similar decreasing trend was observed for all individual components (β-pinene, α-terpineol, borneol, and camphor), which showed relatively higher activity at lower concentrations followed by a consistent reduction at higher doses. Among them, α-terpineol remained the most active compound, although its efficacy also declined with increasing concentration.

Interestingly, both Gram-positive and Gram-negative bacteria followed this inverse pattern, suggesting that the effect is not microorganism-specific but rather related to the interaction between the compounds and the pumpkin matrix. Fungal strains, including *C. albicans* and *C. glabrata*, also exhibited high sensitivity at low concentrations, further confirming this trend.

This atypical behavior may be attributed to matrix-related factors, such as compound instability, interactions with pumpkin components, or reduced bioavailability at higher concentrations. These findings highlight the importance of the food matrix in modulating antimicrobial efficacy and suggest that optimal concentrations may vary significantly depending on the substrate.

3.4.5. *Comparison of in situ vapor phase antimicrobial effects on fruits and vegetables*

A comparative analysis of the four tested matrices (apple, pear,

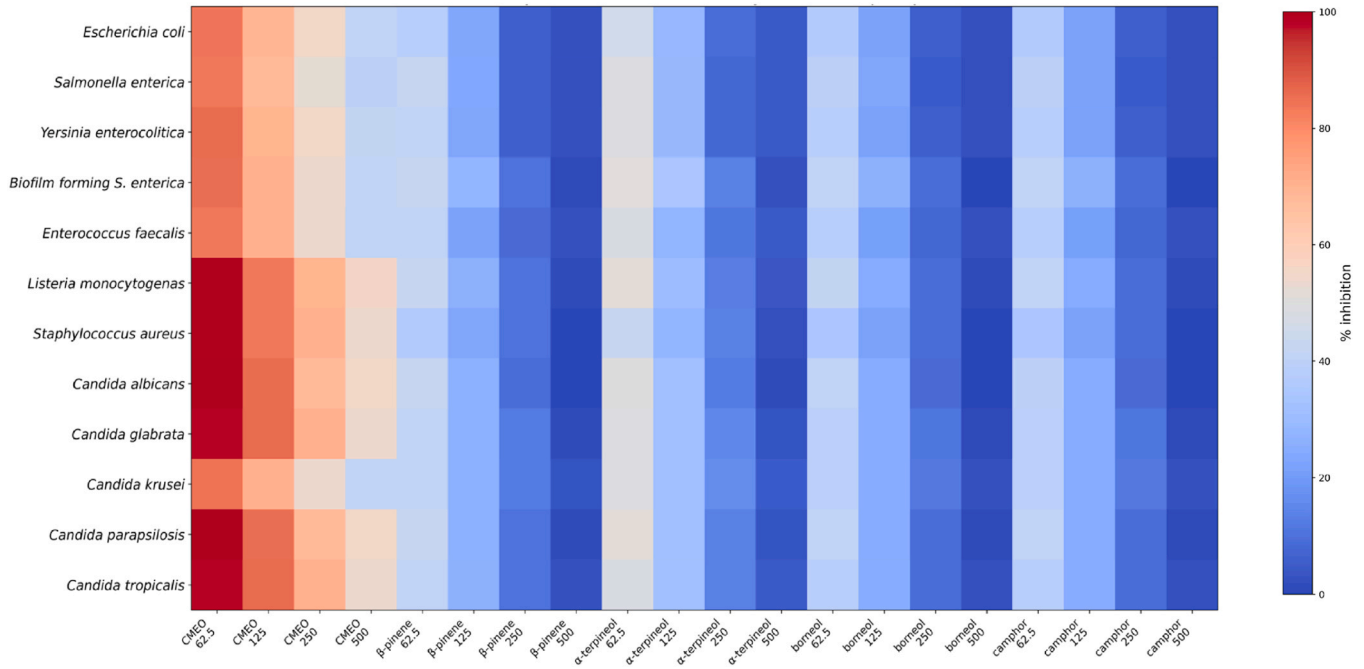

Fig. 4. Heatmap representing in situ analysis of the inhibition of microbial growth (%) by the vapor phase of CMEO and its main components (β-pinene, α-terpineol, borneol, and camphor) against selected microorganisms in Hokkaido pumpkin samples at increasing concentrations (62.5–500 µL/L). Values are expressed as mean percentages of inhibition obtained from three independent replicates. Color gradient ranges from blue (low inhibition) to red (high inhibition).

parsley, and Hokkaido pumpkin) revealed a strong matrix-dependent modulation of the antimicrobial activity of CMEO and its individual components. In apple, pear, and parsley samples, a consistent concentration-dependent increase in inhibition was observed, with CMEO showing the highest efficacy at 250–500 μL/L across most microorganisms. Among these matrices, parsley exhibited the most pronounced antimicrobial effect, reaching inhibition values above 85% for several bacterial and fungal strains, followed by pear and apple, which displayed slightly lower but still significant activity.

In contrast, Hokkaido pumpkin demonstrated a markedly different behavior, characterized by an inverse dose–response relationship, where higher antimicrobial activity was observed at lower concentrations (62.5 μL/L), followed by a progressive decrease at increasing doses. This atypical trend was consistently observed across both bacterial and fungal strains and for all tested compounds, suggesting a strong influence of the food matrix on compound efficacy.

Across all matrices, CMEO consistently outperformed its individual constituents, confirming the importance of synergistic interactions among its components. Among the isolated compounds, α-terpineol showed the highest antimicrobial activity, whereas β-pinene, borneol, and camphor displayed comparable but generally lower effects.

Microorganism susceptibility patterns were relatively consistent across matrices, with Gram-positive bacteria (e.g., *S. aureus* and *L. monocytogenes*) generally more sensitive than Gram-negative species, while *Candida* spp. exhibited variable responses depending on both the matrix and concentration. Notably, the absence of negative inhibition values in parsley and pumpkin, compared to their presence in pear at low concentrations of individual compounds, further highlights the role of matrix-specific interactions. Overall, these findings demonstrate that the antimicrobial efficacy of CMEO is not only compound-dependent but also strongly influenced by the surrounding matrix, which can enhance, stabilize, or even invert the dose–response relationship. This highlights the importance of considering food-specific factors when evaluating the practical application of essential oils as antimicrobial agents.

The fruit-based matrices (pear and apple) exhibited complex and highly interactive patterns of antimicrobial activity, highlighting the strong influence of matrix composition on treatment efficacy.

In the pear matrix, antimicrobial activity was predominantly driven by interaction effects, particularly the microorganism × oil interaction, which showed the highest effect size among all factors. This indicates that the effectiveness of essential oils is strongly dependent on the microbial target, suggesting a highly selective antimicrobial behavior. Notably, the lack of a significant oil × concentration interaction suggests that, although oils differ in efficacy, their relative performance remains consistent across concentrations.

Similarly, the apple matrix displayed a highly complex system, with all main effects and interaction terms being statistically significant. However, unlike pear, the effects in apple were more balanced across factors, with both microorganism identity and concentration contributing substantially to antimicrobial variability. The significant three-way interaction further indicates that antimicrobial efficacy in apple depends on the combined influence of oil type, concentration, and microbial species.

Overall, fruit matrices are characterized by strong interaction effects, indicating that antimicrobial activity cannot be predicted based on individual factors alone. Instead, these systems require a multifactorial approach, as the interplay between chemical composition, dosage, and microbial susceptibility plays a central role.

In contrast, vegetable-based matrices exhibited more variable and, in some cases, simpler patterns of antimicrobial behavior.

The parsley matrix was primarily driven by concentration, which showed one of the strongest effects across all datasets. This indicates a pronounced dose-dependent antimicrobial response, where increasing concentration significantly enhances efficacy. Although oil type was statistically significant, its effect size was comparatively small, suggesting that dosage plays a more critical role than chemical composition in this matrix. Importantly, the significant oil × concentration interaction indicates that the effectiveness of individual oils varies across concentrations, highlighting a dynamic response to dosage.

Conversely, the Hokkaido pumpkin matrix displayed a markedly different pattern, characterized by strong main effects but minimal interaction effects. In this system, oil type and concentration independently influenced antimicrobial activity, while most interaction terms were not significant. This suggests a largely additive behavior, where the effects of individual factors can be considered independently. The reduced importance of microorganism-related variability further indicates a more homogeneous response across species.

The comparative analysis clearly demonstrates that antimicrobial activity is strongly matrix-dependent, with distinct patterns emerging between fruit and vegetable systems.

Fruit matrices (pear and apple) are characterized by complex interaction-driven behavior, where antimicrobial efficacy depends on the combined effects of oil type, concentration, and microbial species. This suggests that the physicochemical properties of fruit matrices, such as higher sugar content, acidity, and water activity, may influence both microbial physiology and the diffusion or stability of essential oil components, leading to intricate interaction patterns.

In contrast, vegetable matrices exhibit more variable responses. Parsley represents a dose-driven system, where concentration is the dominant factor, while Hokkaido pumpkin represents an additive system with minimal interactions. These differences may be attributed to variations in matrix composition, including fiber content, structural complexity, and the presence of bioactive compounds that can modulate antimicrobial activity.

Overall, these findings highlight that the antimicrobial efficacy of essential oils cannot be generalized across food systems. Instead, the food matrix plays a critical role in modulating both the magnitude and the nature of antimicrobial effects. This underscores the importance of evaluating antimicrobial agents within the specific context of their intended application.

3.5. Antibiofilm activity of CMEO and major constituents against biofilm-forming S. enterica

3.5.1. Antibiofilm activity of CMEO

The antibiofilm effect of CMEO on the strong biofilm-forming strain of *S. enterica* was first evaluated by the crystal violet assay. The EO reduced biofilm biomass with MIC_{50} = 2.46 mg/mL and MIC_{90} = 2.64 mg/mL, indicating that relatively high concentrations are required to inhibit established biofilms of this strain (Table 3 and Table 4). MALDI-TOF MS spectra confirmed clear structural and compositional differences between planktonic cells and biofilms formed on wood and stainless-steel surfaces (Fig. 5A-C). After 3 days of incubation (Fig. 5A), planktonic cells (SEPC 3) displayed dominant signals at 2980.3, 3579.4, 4761.7, 5235.3, 6662.4, 7164.9, 7707.8 and 9244.1 *m/z*, together with high-mass peaks above 15,000 *m/z* (15,721.4, 16,996.1 and 17,778.9 *m/z*). The biofilm on wood (SEW 3) showed a more diversified mid-mass region, characterized by peaks at 2629.0, 3579.4, 4351.9, 5357.5, 6512.1, 7165.8, 8035.9 and 9557.9 *m/z*, while high-mass signals at 17,226.3 and 19,472.2 *m/z* were less intense than in planktonic cells, indicating altered protein expression associated with surface attachment. The biofilm on stainless steel (SESS 3) retained several planktonic peaks (3580.3, 4016.6, 4778.8, 6665.6, 7168.0, 7664.4, 8038.3 and 9560.8 *m/z*) but also exhibited additional signals at 2629.9 and 5919.4 *m/z*, suggesting specific adjustments linked to colonization of the stainless-steel surface.

After 7 days (Fig. 5B), spectra of planktonic cells (SEPC 7) became markedly more complex, with numerous dominant peaks between 2600 and 11,000 *m/z*, including 2671.3, 3021.9, 3649.3, 4364.3, 4761.2, 5355.2, 6257.5, 7306.2, 7686.6, 8371.8, 8901.1, 9062.8, 10,289.3 and 10,942.8 *m/z*, as well as extended high-mass signals above 10,000 *m/z*. Wood biofilms (SEW 7) preserved several of these features (e.g. 3630.3,

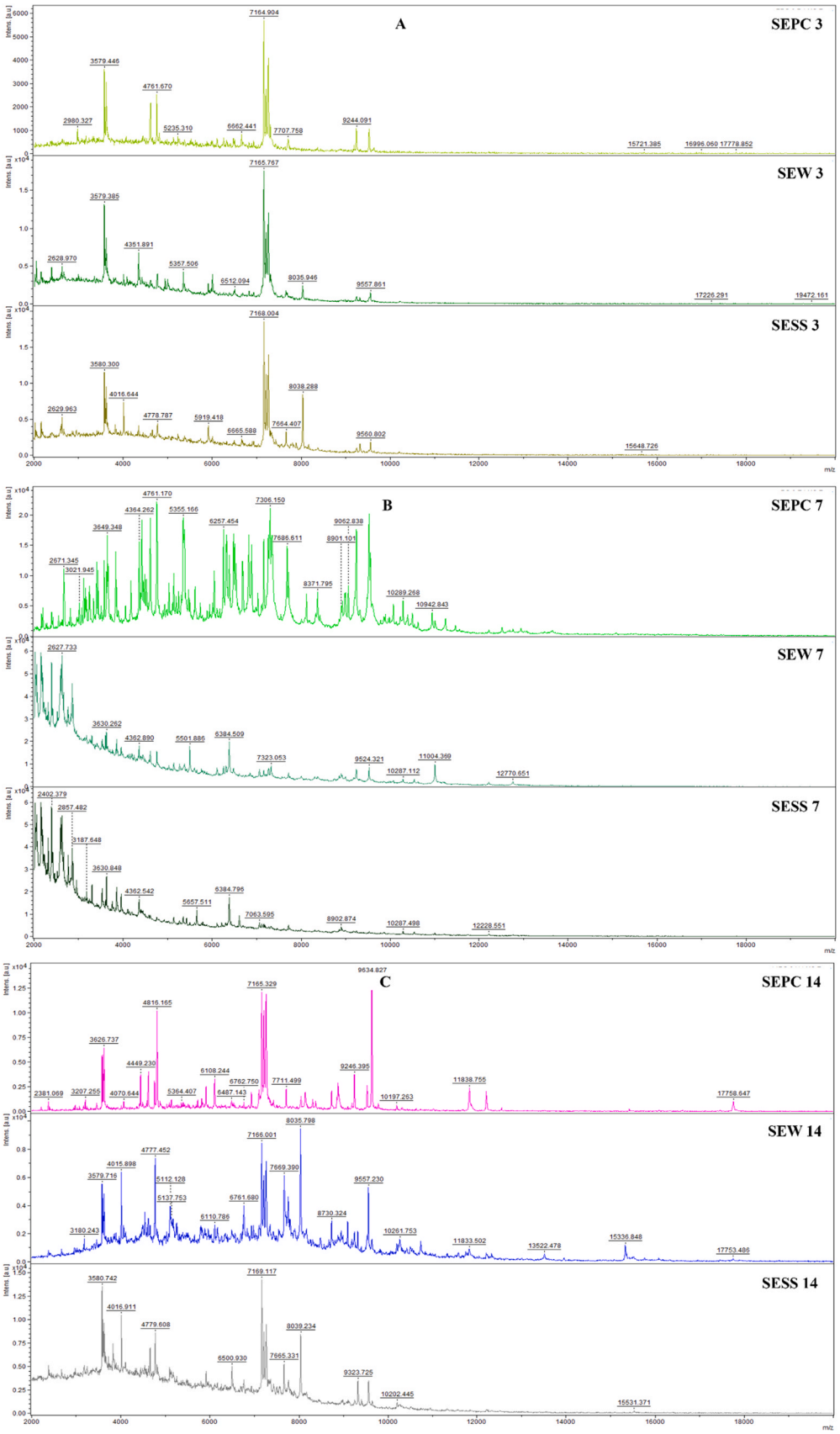

Fig. 5. MALDI-TOF MS spectral profiles of *S. enterica* planktonic culture and biofilms developed on wood and stainless-steel surfaces in the presence of CMEO after 3 (**A**), 7 (**B**), and 14 (**C**) days of incubation. SEPC 3/7/14 - planktonic culture; SEW 3/7/14 - biofilm on wood; SESS 3/7/14 - biofilm on stainless steel.

4362.9, 5501.9, 6384.5, 7323.1, 9524.3 and 11,004.4 *m/z*), but the overall intensity was lower and new peaks appeared, reflecting biofilm maturation on wood. Stainless-steel biofilms (SESS 7) also shared some planktonic signals (3630.8, 4362.5, 5657.5, 6384.8, 8902.9 and 10,287.5 *m/z*), yet showed prominent additional peaks at 2402.4, 2857.5 and 7063.6 *m/z*, pointing to distinct protein patterns linked to long-term colonization of stainless steel.

On day 14 (Fig. 5C), planktonic cells (SEPC 14) exhibited highly complex spectra with dominant peaks at 7165.3 and 9634.8 *m/z*, accompanied by intense signals at 2381.1, 3207.3, 3626.7, 4449.2, 4816.2, 5364.4, 6108.2, 6487.1, 6762.8, 7711.5, 9246.4 and 10,197.3 *m/z* and high-mass peaks at 11,838.8 and 17,758.6 *m/z*. The biofilm on wood (SEW 14) maintained the dominant 7166.0 *m/z* peak but displayed a broadened pattern of mid- and high-mass signals (e.g. 3579.7, 4015.9, 4777.5, 8035.8, 9557.2, 10,261.8, 13,522.5 and 15,336.8 *m/z*), indicative of increased spectral heterogeneity at late maturation. Biofilms on stainless steel (SESS 14) showed a less intense yet stable profile, retaining peaks at 3580.7, 4016.9, 4779.6, 6500.9, 7665.3, 8039.2, 9233.7 and 10,202.4 *m/z*, with additional signals at 15,531.4 *m/z*. Compared with wood biofilms, stainless-steel biofilms were characterized by lower overall intensity but a more conserved set of dominant signals. Across all time points, planktonic cultures consistently exhibited the most complex and intense spectral profiles, whereas biofilms formed on wood and stainless steel showed surface-dependent shifts in peak composition and intensity. Wood supported progressive spectral diversification and increasing heterogeneity during maturation, while stainless steel favoured more stable, less heterogeneous but compositionally distinct biofilm structures.

The MSP dendrogram derived from MALDI-TOF MS spectra shows clear separation between planktonic cells and biofilm-associated *S. enterica* across all incubation periods (Fig. 6). Planktonic controls (PC) cluster tightly together, indicating that their spectral profiles remain stable over time. Biofilm-associated cells form distinct branches separate from planktonic cultures. After 3 days, biofilms developing on wood and stainless steel (SECMW, SEC MSS) already group together and remain distant from planktonic cells, showing early biofilm-related changes in spectral patterns. The similarity between wood and stainless-steel clusters suggests that initial biofilm formation produces comparable spectral shifts regardless of surface type. By day 7, wood- and stainless-steel biofilms continue to cluster together and remain separated from planktonic cells. Their grouping indicates that the spectral characteristics of maturing biofilms become more uniform between the two surfaces. After 14 days, biofilms on both materials form a distinct, highly separated cluster, clearly different from both planktonic controls and earlier biofilm stages. This demonstrates progressive, time-dependent changes in the spectral patterns of maturing biofilms. Overall, the dendrogram shows that planktonic cells retain stable mass spectral profiles, while biofilms undergo gradual and surface-modulated changes, becoming increasingly distinct with longer incubation.

3.5.2. *Antibiofilm activity of α-terpineol*

The antibiofilm effect of α-terpineol on the strong biofilm-forming strain of *S. enterica* was evaluated using the crystal violet assay. The compound reduced biofilm biomass with $MBIC_{50}$ = 2.64 mg/mL and $MBIC_{90}$ = 2.89 mg/mL (Table 3 and Table 4), indicating a moderate antibiofilm activity. MALDI-TOF MS spectra confirmed clear structural and compositional differences between planktonic cells and biofilms formed on wood and stainless-steel surfaces (Fig. 7A-C).

After 3 days of incubation (Fig. 7A), planktonic cells (SEPC 3) displayed dominant signals at 2671.3, 3409.9, 4068.0, 4182.7, 4363.4, 4760.1, 5141.1, 6255.8, 6827.8, 7705.9, 8369.6, 8896.9, 9182.2 and 9521.9 *m/z*, together with a higher-mass peak at 15,409.1 *m/z*. The biofilm on wood (SEW 3) showed a modified mid-mass region characterized by peaks at 2403.3, 2821.8, 3124.9, 3608.5, 4211.8, 4761.8, 5380.9, 6256.3, 7159.6, 7686.0, 8368.8 and 9522.0 *m/z*, indicating early changes associated with surface attachment. The biofilm on stainless steel (SESS 3) retained several planktonic peaks (3575.8, 4363.8, 5381.5, 6256.4 and 7159.9 *m/z*) but also exhibited additional signals at 2401.9, 4618.5, 5739.2, 7720.5, 8900.1, 9187.2 and 9524.3 *m/z*, suggesting surface-specific adaptation.

After 7 days (Fig. 7B), spectra of planktonic cells (SEPC 7) became more complex, with numerous dominant peaks between approximately 2600 and 10,000 *m/z*, including 2671.0, 3153.7, 3250.7, 3648.8, 4055.7, 4182.4, 4363.1, 4759.8, 5353.7, 6255.5, 6827.0, 7303.9, 7683.9, 8118.7, 8898.2, 9058.8 and 9521.4 *m/z*. Wood biofilms (SEW 7) preserved several of these signals (e.g. 2402.6, 2857.9, 3608.3,

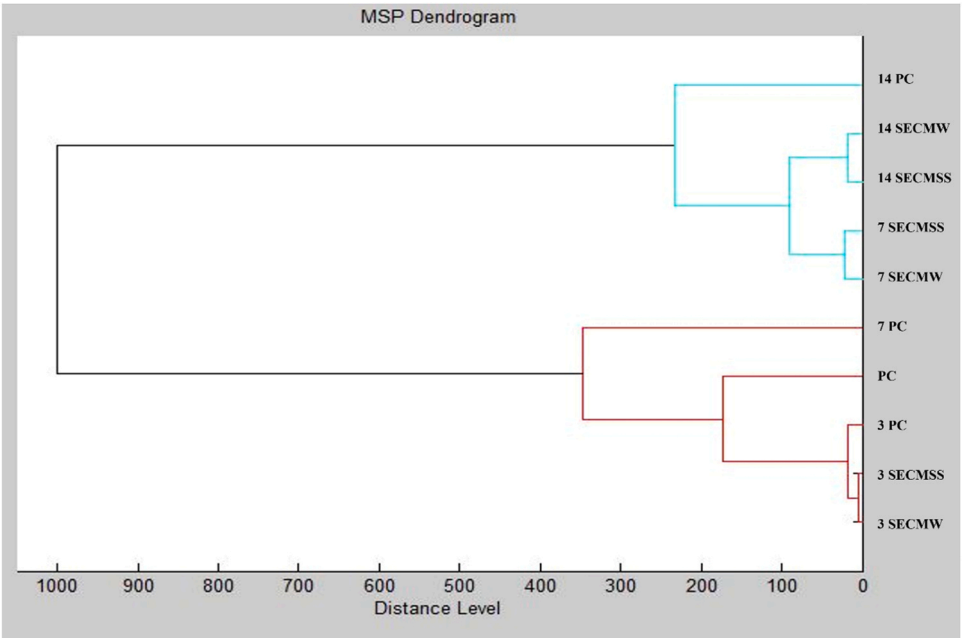

Fig. 6. MALDI-TOF MS MSP dendrogram illustrating the clustering of *S. enterica* planktonic cultures and biofilms formed on wood and stainless-steel surfaces after 3, 7, and 14 days of incubation in the presence of CMEO. SEPC 3, SEPC 7, SEPC 14 - planktonic cultures; SEW 3, SEW 7, SEW 14 - biofilms on wood; SESS 3, SESS 7, SESS 14 - biofilms on stainless steel.

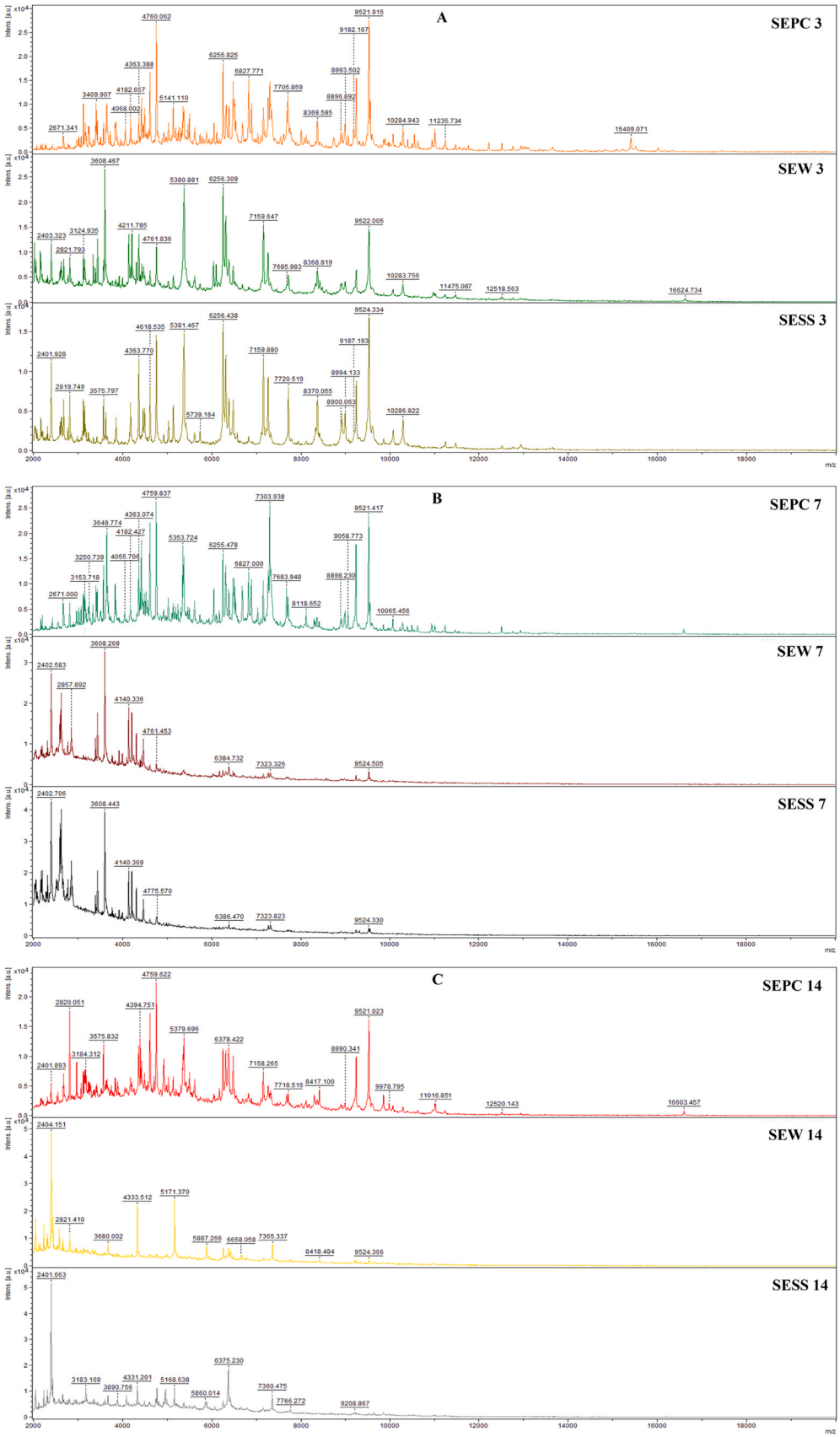

Fig. 7. MALDI-TOF MS spectral profiles of *S. enterica* planktonic culture and biofilms developed on wood and stainless-steel surfaces after 3 (A), 7 (B), and 14 (C) days of incubation in the presence of α-terpineol. SEPC 3/7/14 - planktonic culture; SEW 3/7/14 - biofilm on wood; SESS 3/7/14 - biofilm on stainless steel.

4140.3, 4761.5, 6384.7, 7323.3 and 9524.5 *m/z*), but the overall intensity was lower, reflecting biofilm maturation on wood. Stainless-steel biofilms (SESS 7) also shared some planktonic peaks (3608.4, 4140.4, 4775.6, 6386.5 and 7323.8 *m/z*), yet exhibited additional signals at 2402.7 and 9524.3 *m/z*, indicating distinct protein profiles linked to longer-term colonization of stainless steel.

On day 14 (Fig. 7C), planktonic cells (SEPC 14) exhibited highly complex spectra with dominant peaks at 2820.1, 3184.3, 3575.8, 4394.8, 4759.6, 5379.7, 6378.4, 7158.3, 7718.5, 8417.1, 8990.3, 9521.0 and 9978.8 *m/z*, accompanied by higher-mass signals at 11,016.9, 12,520.1 and 16,603.5 *m/z*. The biofilm on wood (SEW 14) displayed a reduced and more stable spectral pattern, with peaks at 2404.2, 2821.4, 3680.0, 4333.5, 5171.4, 5887.3, 6658.1, 7365.3, 8418.5 and 9524.4 *m/z*, indicating increased stabilization during late biofilm maturation. Biofilms on stainless steel (SESS 14) retained peaks at 3183.2, 3890.8, 4331.2, 5168.6, 5860.0, 6375.2, 7360.5 and 7766.3 *m/z*, with additional signals at 9208.9 *m/z*, confirming a more conserved but distinct spectral profile compared with planktonic cells.

Across all time points, planktonic cultures consistently exhibited more complex and intense spectra, whereas biofilms formed on wood and stainless steel showed surface-dependent shifts in peak composition and intensity. Wood-supported biofilms displayed gradual diversification and increasing heterogeneity, while stainless steel promoted more stable but compositionally distinct biofilm structures.

The MSP dendrogram constructed from MALDI-TOF MS spectra shows clear separation between planktonic cells and biofilm-associated *S. enterica* across all incubation periods (Fig. 8). Planktonic controls (PC) cluster tightly together, indicating that their spectral profiles remain stable over time. Biofilm-associated cells form distinct branches separate from planktonic cultures. After 3 days, biofilms developing on wood and stainless steel (SEW 3, SESS 3) group together and remain distant from planktonic cells, showing early biofilm-related changes in spectral patterns. The similarity between wood and stainless-steel clusters suggests that initial biofilm formation produces comparable spectral shifts regardless of surface type. By day 7, wood- and stainless-steel biofilms (SEW 7, SESS 7) continue to cluster together and remain separated from planktonic cells. Their grouping indicates that the spectral characteristics of maturing biofilms become more uniform between the two surfaces. After 14 days, biofilms on both materials (SEW 14, SESS 14) form a distinct, highly separated cluster, clearly different from both planktonic controls and earlier biofilm stages. This demonstrates progressive, time-dependent changes in the spectral patterns of maturing biofilms. Overall, the dendrogram shows that planktonic cells retain stable mass spectral profiles, while biofilms undergo gradual and surface-modulated changes, becoming increasingly distinct with longer incubation.

3.5.3. *Antibiofilm activity of β-pinene*

The antibiofilm effect of β-pinene on the strong biofilm-forming strain of *S. enterica* was first evaluated by the crystal violet assay. β-Pinene reduced biofilm biomass with MIC_{50} = 4.39 mg/mL and MIC_{90} = 4.70 mg/mL, showing that considerably higher concentrations are needed to inhibit established biofilms of this strain than in the case of CMEO (Table 3). MALDI-TOF MS spectra confirmed clear differences between planktonic cells and biofilms formed on wood and stainless-steel surfaces in the presence of β-pinene (Fig. 9A-C). After 3 days of incubation (Fig. 9A), planktonic cells (SEPC 3) showed dominant peaks at 2983.2, 3403.0, 4075.8, 4763.6, 5144.9, 6487.0, 7264.1, 8851.1, 9524.6 and 10 190.8 *m/z*, together with high-mass signals at 12 229.2, 15 417.2 and 17 751.5 *m/z*. The biofilm on wood (SEW 3) displayed a richer pattern in the mid-mass region, with characteristic peaks at 2685.3, 3124.0, 3650.2, 4364.6, 4762.1, 5355.5, 6257.2, 6829.4, 7305.4, 7686.7, 8371.2, 8901.2, 8988.2, 9526.1, 10 288.9 and 10 941.7 *m/z*, whereas high-mass signals at 17 226.3 and 19 472.2 *m/z* were less intense than in planktonic cells, indicating changes in the mass spectral pattern associated with surface attachment. The biofilm on stainless steel (SESS 3) retained several of the planktonic peaks (2983.3, 3402.3, 4075.8, 4760.6, 5381.4, 5738.3, 6256.3, 7304.3, 7685.0, 8370.2, 8993.2, 9523.1 and 10 285.5 *m/z*), but additional signals at 2629.3 and 5919.4 *m/z* suggested further adjustments specific to colonization of the stainless-steel surface.

After 7 days (Fig. 9B), spectra of planktonic cells (SEPC 7) became more complex, with numerous dominant peaks between approximately 3000 and 12 000 *m/z*, including 2996.5, 3402.0, 4090.1, 4762.1, 5504.9, 6484.0, 7297.1, 7744.5, 8193.3, 8739.9, 9688.3, 10 469.6 and 11 317.9 *m/z*, and extended high-mass peaks at 11 890.3, 12 288.7, 15 495.3, 17 844.7 and 18 697.3 *m/z*. Wood biofilms (SEW 7) preserved several of these signals (e.g. 2627.7, 3402.7, 4186.3, 4763.3, 5505.0, 6487.4, 7265.0, 7941.5, 8330.9, 8995.7, 9525.4, 10 069.3 and 11

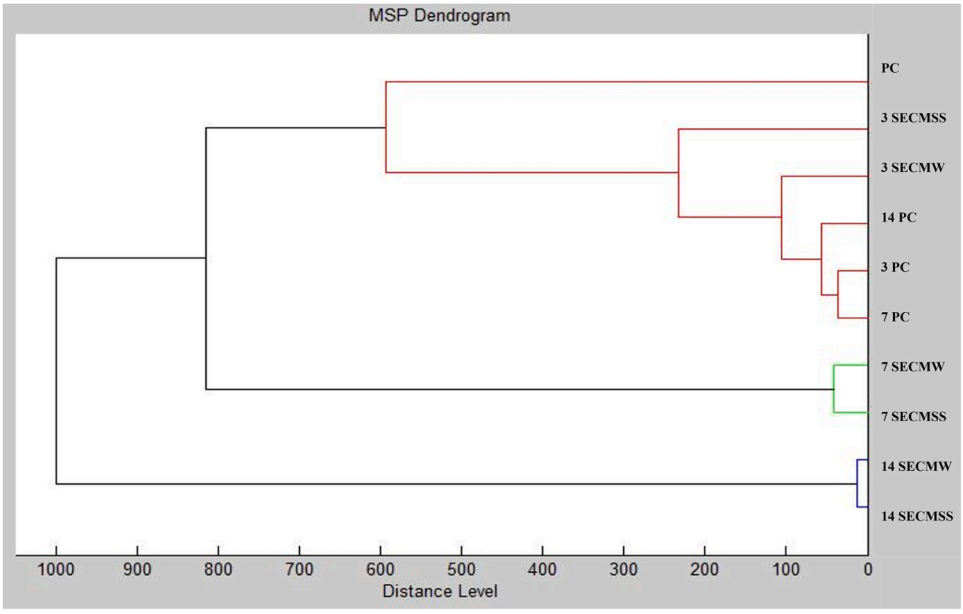

Fig. 8. MALDI-TOF MS MSP dendrogram illustrating the clustering of *S. enterica* planktonic cultures and biofilms formed on wood and stainless-steel surfaces after 3, 7, and 14 days of incubation in the presence of α-terpineol. SEPC 3, SEPC 7, SEPC 14 - planktonic cultures; SEW 3, SEW 7, SEW 14 - biofilms on wood; SESS 3, SESS 7, SESS 14 - biofilms on stainless steel.

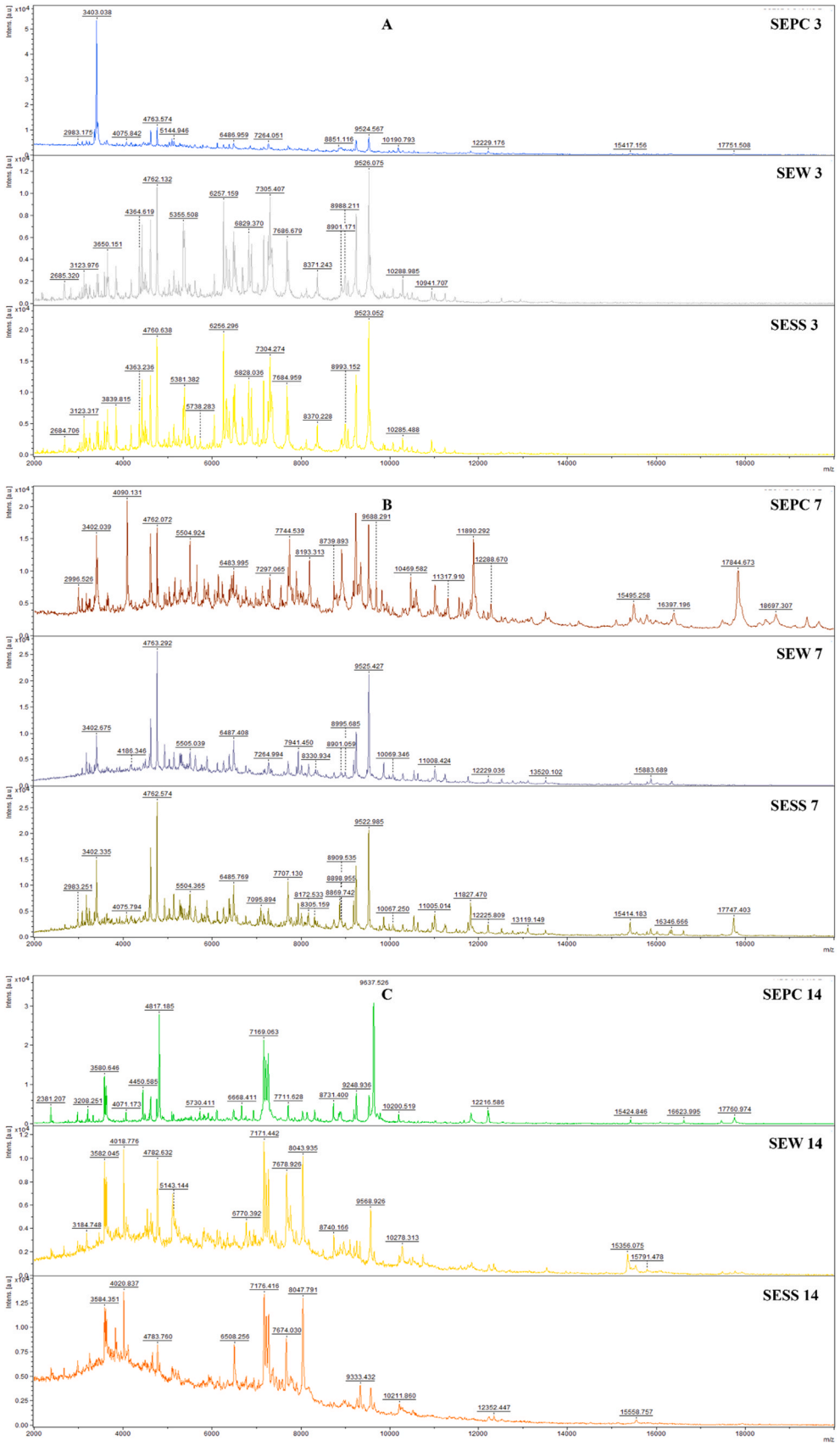

Fig. 9. MALDI-TOF MS spectral profiles of *S. enterica* planktonic culture and biofilms developed on wood and stainless-steel surfaces after 3 (**A**), 7 (**B**), and 14 (**C**) days of incubation in the presence of β-pinene. SEPC 3/7/14 - planktonic culture; SEW 3/7/14 - biofilm on wood; SESS 3/7/14 - biofilm on stainless steel.

008.4 *m/z*), but peak intensities were generally lower and new signals appeared, reflecting biofilm maturation on wood. Stainless-steel biofilms (SESS 7) also shared some planktonic peaks (2983.3, 3402.3, 4075.8, 4762.6, 5504.4, 6485.8, 7707.1, 8899.5, 9523.0, 10 067.3 and 11 005.0 *m/z*), yet showed additional signals such as 8172.5, 8305.2, 11 827.5, 12 225.8, 13 119.1, 15 414.2 and 17 747.4 *m/z*, indicating distinct spectral profiles linked to longer-term colonization of stainless steel.

On day 14 (Fig. 9C), planktonic cells (SEPC 14) exhibited highly complex spectra with dominant peaks at 7169.1 and 9637.5 *m/z*, accompanied by intense signals at 2381.2, 3208.3, 3580.6, 4071.2, 4450.6, 4817.2, 5730.4, 6668.4, 7711.6, 8731.4, 9248.9 and 10 200.5 *m/z*, and high-mass signals at 12 216.6, 15 424.8, 16 623.9 and 17 760.9 *m/z*. The biofilm on wood (SEW 14) maintained a strong peak around 7171.4 *m/z* but showed a broadened pattern of mid- and high-mass signals (3184.7, 3582.0, 4018.8, 4782.6, 5143.1, 6770.4, 7678.9, 8043.9, 8740.2, 9568.9, 10 278.3, 15 356.1 and 15 791.5 *m/z*), indicating increased spectral heterogeneity at late maturation. Biofilms on stainless steel (SESS 14) presented a less intense yet stable profile, retaining peaks at 3584.4, 4020.8, 4783.8, 6508.3, 7176.4, 7674.0, 8047.8, 9333.4 and 10 211.9 *m/z*, with additional high-mass signals at 12 352.4 and 15 558.8 *m/z*. Compared with wood biofilms, stainless-steel biofilms were characterized by lower overall intensity but a more conserved set of dominant peaks.

Taken together, the crystal violet assay and MALDI-TOF MS analyses show that β-pinene alone has a measurable but weaker antibiofilm effect on *S. enterica* than CMEO. Biofilms on wood and stainless steel both undergo time-dependent spectral shifts in the presence of β-pinene, but these changes are less pronounced than those observed with the complete EO, supporting the view that the full CMEO mixture is required for maximal disruption of biofilm development.

The MSP dendrogram constructed from MALDI-TOF MS spectra shows a clear separation between planktonic cells and biofilm-associated *S. enterica* exposed to β-pinene across all incubation periods (Fig. 10).

Planktonic controls (PC) form a tight cluster with minimal distance between samples, indicating highly stable spectral profiles over time. Biofilm-associated cells, however, cluster separately from the planktonic group. After 3 days, wood- and stainless-steel biofilms (3 SEBW and 3 SEBSS) group together and remain distinct from planktonic cells, demonstrating early β-pinene-induced changes in the spectral patterns of attached cells. Their close clustering suggests that initial biofilm formation on both materials results in similar spectral shifts. By day 7, the biofilms on wood and stainless steel (7 SEBW, 7 SEBSS) continue to cluster together and remain clearly separated from the planktonic controls. This indicates that as biofilms mature under β-pinene exposure, their spectral profiles become more uniform across surface types while remaining distinct from planktonic populations. After 14 days, wood- and stainless-steel biofilms (14 SEBW, 14 SEBSS) form a strongly separated branch, clearly distant from both earlier biofilm stages and planktonic cells. This demonstrates pronounced, time-dependent alterations in biofilm spectral characteristics during long-term exposure to β-pinene. Overall, the dendrogram shows that planktonic cultures maintain stable mass-spectral profiles, whereas biofilms undergo progressive, surface-associated and time-dependent changes. β-pinene does not prevent these modifications; instead, mature biofilms become increasingly distinct from planktonic cells and from early biofilm stages.

3.5.4. *Antibiofilm activity of borneol against biofilm-forming S. enterica*

The antibiofilm effect of borneol on the strong biofilm-forming strain of *S. enterica* was evaluated using the crystal violet assay. The compound reduced biofilm biomass with $MBIC_{50}$ = 4.66 mg/mL and $MBIC_{90}$ = 4.96 mg/mL (Table 3 and Table 4). The antibiofilm effect of borneol on the strong biofilm-forming strain of *S. enterica* was evaluated using MALDI-TOF MS analysis. The spectra revealed clear differences between planktonic cells and biofilms formed on wood and stainless-steel surfaces (Fig. 11A-C).

After 3 days of incubation (Fig. 11A), planktonic cells (SEPC 3) showed dominant peaks at 2401.9, 2820.1, 3184.3, 3575.8, 4394.8, 4759.6, 5379.7, 6378.4, 7158.3, 8990.3 and 9521.0 *m/z*, together with a high-mass signal at 16603.5 *m/z*. The biofilm on wood (SEW 3) was characterized by peaks at 2404.2, 2821.4, 3680.0, 4333.5, 5171.4, 5887.3, 6658.1, 7365.3, 8418.5 and 9524.4 *m/z*, indicating a modified mid-mass profile. The biofilm on stainless steel (SESS 3) retained several signals (2401.7, 3183.2, 3890.8, 4331.2, 5168.6, 5860.0, 6375.2, 7360.5 and 9208.9 *m/z*), but with lower overall intensity, suggesting early adaptation to the surface.

After 7 days (Fig. 11B), planktonic cells (SEPC 7) exhibited a more complex spectrum with dominant peaks at 2671.0, 3153.7, 3250.7, 3648.8, 4182.4, 4363.1, 4759.8, 5353.7, 6255.5, 6827.0, 7303.9, 7683.9, 8898.2 and 9521.4 *m/z*, along with additional signals above 10,000 *m/z*. Wood biofilms (SEW 7) displayed peaks at 2402.6, 2857.9,

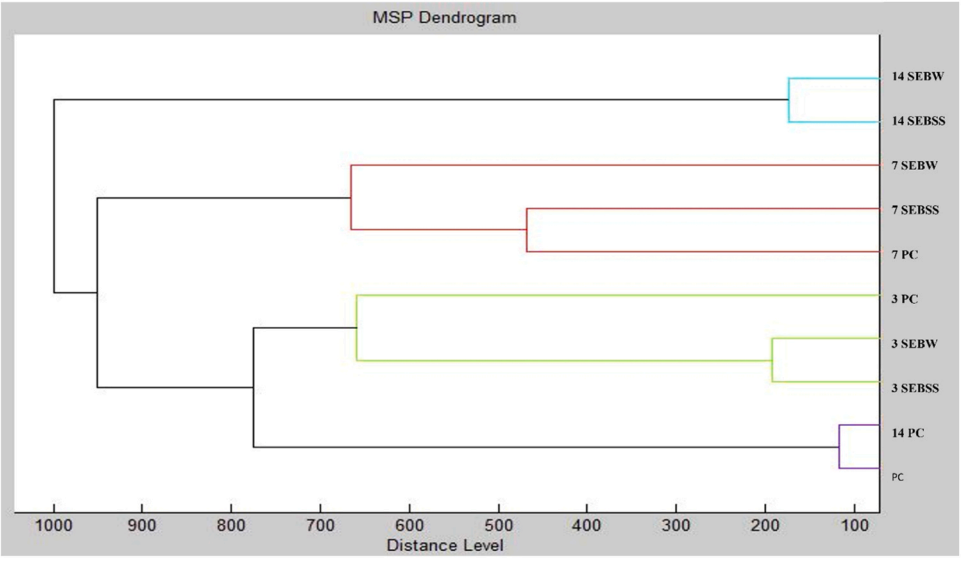

Fig. 10. MALDI-TOF MS MSP dendrogram illustrating the clustering of *S. enterica* planktonic cultures and biofilms formed on wood and stainless-steel surfaces after 3, 7, and 14 days of incubation in the presence of β-pinene. SEPC 3, SEPC 7, SEPC 14 - planktonic cultures; SEW 3, SEW 7, SEW 14 - biofilms on wood; SESS 3, SESS 7, SESS 14 - biofilms on stainless steel.

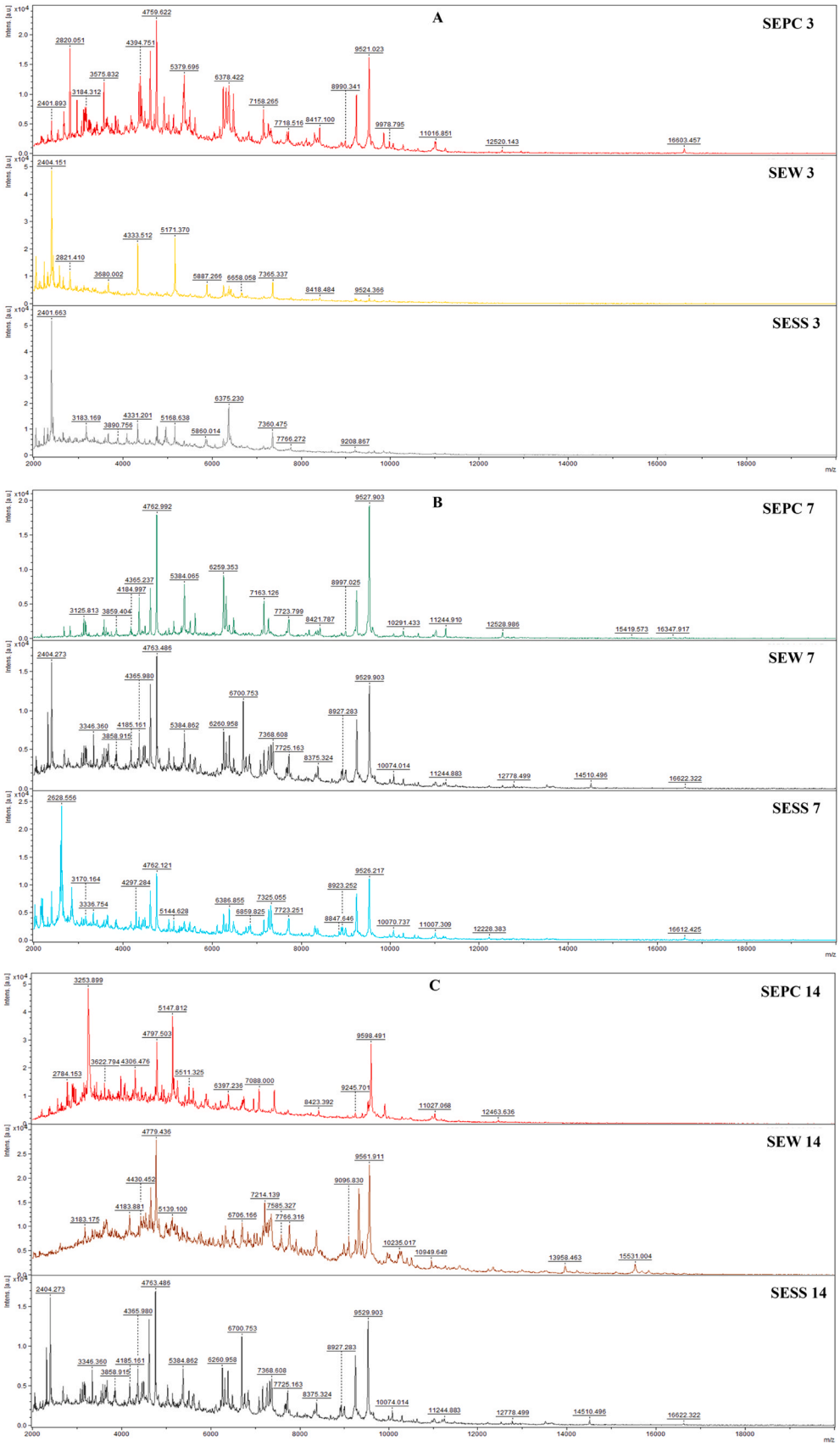

Fig. 11. MALDI-TOF MS spectral profiles of *S. enterica* planktonic culture and biofilms developed on wood and stainless-steel surfaces after 3 (A), 7 (B), and 14 (**C**) days of incubation in the presence of borneol. SEPC 3/7/14 - planktonic culture; SEW 3/7/14 - biofilm on wood; SESS 3/7/14 - biofilm on stainless steel.

3608.3, 4140.3, 4761.5, 6384.7, 7323.3 and 9524.5 *m/z*, with reduced intensity but preserved key features. Stainless-steel biofilms (SESS 7) showed signals at 2402.7, 3170.2, 3336.8, 4297.3, 5144.6, 6386.9, 7325.1, 8847.6 and 9526.2 *m/z*, indicating further divergence in spectral composition.

On day 14 (Fig. 11C), planktonic cells (SEPC 14) were dominated by peaks at 3253.9, 4797.5, 5147.8 and 9598.5 *m/z*, with additional signals at 2784.2, 3622.8, 4306.5, 5511.3, 6397.2, 7088.0, 8423.4 and 9245.7 *m/z*, as well as high-mass peaks up to 12463.6 *m/z*. The biofilm on wood (SEW 14) showed a broadened spectrum with peaks at 3183.2, 4183.9, 4430.5, 4779.4, 5139.1, 6706.2, 7214.1, 7766.3, 9096.8, 9561.9 and 10,235.0 *m/z*, indicating increased heterogeneity. Stainless-steel biofilms (SESS 14) retained a simpler profile with peaks at 2401.7, 3346.4, 4185.2, 5384.9, 6700.8, 7368.6, 8927.3 and 9529.9 *m/z*, together with weaker high-mass signals (Fig. 12).

3.5.5. *Antibiofilm activity of camphor against biofilm-forming S. enterica*

The antibiofilm effect of camphor on the strong biofilm-forming strain of *S. enterica* was evaluated using the crystal violet assay. The compound reduced biofilm biomass with $MBIC_{50}$ = 4.83 mg/mL and $MBIC_{90}$ = 5.19 mg/mL (Table 3 and Table 4). The antibiofilm activity of camphor against the strong biofilm-forming strain of *S. enterica* was evaluated using MALDI-TOF MS analysis. The obtained spectra revealed distinct differences between planktonic cells and biofilms formed on wood and stainless-steel surfaces (Fig. 13A-C).

After 3 days of incubation (Fig. 13A), planktonic cells (SEPC 3) showed dominant peaks at 2703.2, 3099.0, 3580.7, 4430.5, 5504.5, 6208.3, 7169.5, 7692.7 and 9533.1 *m/z*, with additional signals at 7728.4 and 10298.2 *m/z*. The biofilm on wood (SEW 3) exhibited peaks at 3208.4, 3580.1, 4450.9, 4817.9, 5730.2, 6667.7, 7166.7, 7549.8, 7712.6, 9096.1, 9248.1 and 9637.9 *m/z*, indicating modification of the mid-mass region. The stainless-steel biofilm (SESS 3) retained several signals (3183.2, 4183.9, 4430.5, 4779.4, 5139.1, 6706.2, 7214.1 and 7585.3 *m/z*) but also showed peaks at 9561.9 and 10,235.0 *m/z*, suggesting early surface-related adaptation.

After 7 days (Fig. 13B), planktonic cells (SEPC 7) displayed a more complex spectral pattern with dominant peaks at 2822.2, 3577.7, 4365.6, 4762.8, 5384.0, 6259.3, 7162.1, 7722.5, 8422.0, 9187.5 and 9527.2 *m/z*, along with additional signals above 10,000 *m/z*. Wood biofilms (SEW 7) showed peaks at 3172.7, 4186.7, 4366.9, 4764.3, 5623.4, 6261.7, 6831.2, 7713.5, 8377.5, 9002.2 and 9530.1 *m/z*, reflecting reduced intensity but preservation of key spectral features. Stainless-steel biofilms (SESS 7) retained signals at 2404.3, 3346.4, 4185.2, 5384.9, 6700.8, 7368.6, 8927.3 and 9529.9 *m/z*, together with weaker high-mass peaks.

On day 14 (Fig. 13C), planktonic cells (SEPC 14) were characterized by dominant peaks at 3253.4, 4763.0, 6259.4, 7163.1 and 9527.9 *m/z*, accompanied by signals at 4185.0, 5384.1, 7723.8, 8421.8 and 8997.0 *m/z*, as well as peaks above 11,000 *m/z*. The biofilm on wood (SEW 14) showed a simplified profile with dominant peaks at 3253.4, 4798.0, 5148.0 and 9598.7 *m/z*, indicating reduced spectral complexity. Stainless-steel biofilms (SESS 14) exhibited a similar but slightly less intense pattern with peaks at 2896.6, 4078.6, 4797.9, 5148.4, 6964.8 and 9597.8 *m/z*, suggesting stabilization of biofilm-associated protein profiles at later stages.

The MSP dendrogram constructed from MALDI-TOF MS spectra demonstrates a clear separation between planktonic cells and biofilm-associated *S. enterica* exposed to camphor (Fig. 14). Planktonic controls (PC) cluster closely together, indicating stable spectral profiles over time. In contrast, biofilm-associated samples form distinct branches.

After 3 days, biofilms on wood and stainless steel (SEW 3, SESS 3) group together and remain separated from planktonic cells, reflecting early structural changes during surface attachment. By day 7, biofilms (SEW 7, SESS 7) cluster together with reduced distance, indicating increasing similarity between surfaces during maturation. After 14 days, biofilms (SEW 14, SESS 14) form a distinct and clearly separated cluster, distant from both planktonic controls and earlier biofilm stages, demonstrating pronounced time-dependent changes.

Overall, the dendrogram confirms that planktonic cells maintain relatively stable mass spectral profiles, whereas biofilms undergo progressive and surface-associated modifications, becoming increasingly distinct with prolonged incubation in the presence of camphor.

CMEO showed a clearly stronger antibiofilm effect against the strong biofilm-forming *S. enterica* strain than all tested constituents. In the crystal violet assay, CMEO reduced established biofilm biomass with MIC_{50} = 2.46 mg/mL and MIC_{90} = 2.64 mg/mL, whereas α-terpineol required moderately higher concentrations ($MBIC_{50}$ = 2.64 mg/mL; $MBIC_{90}$ = 2.89 mg/mL), and β-pinene, borneol, and camphor required

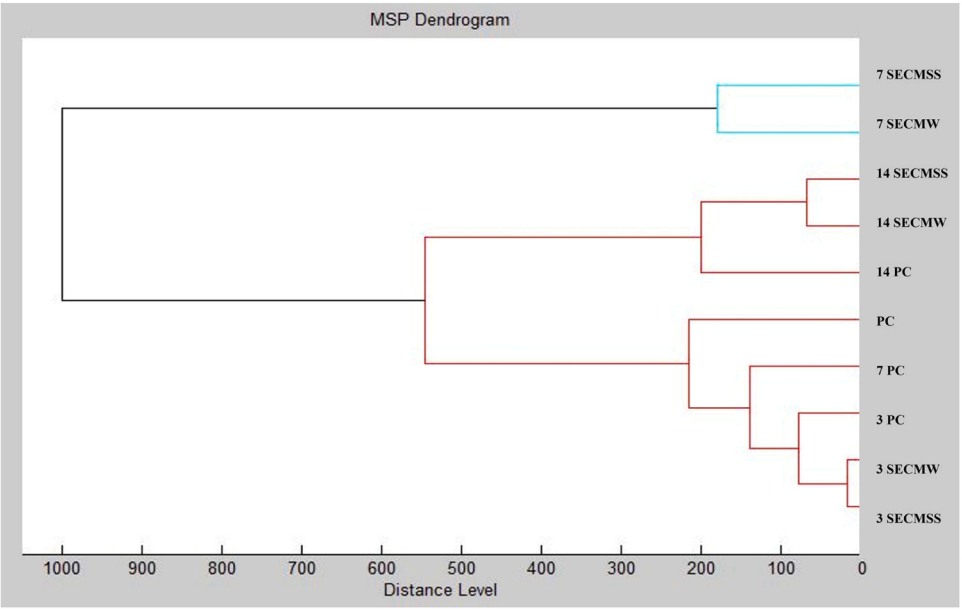

Fig. 12. MALDI-TOF MS MSP dendrogram illustrating the clustering of *S. enterica* planktonic cultures and biofilms formed on wood and stainless-steel surfaces after 3, 7, and 14 days of incubation in the presence of borneol. SEPC 3, SEPC 7, SEPC 14 - planktonic cultures; SEW 3, SEW 7, SEW 14 - biofilms on wood; SESS 3, SESS 7, SESS 14 - biofilms on stainless steel.

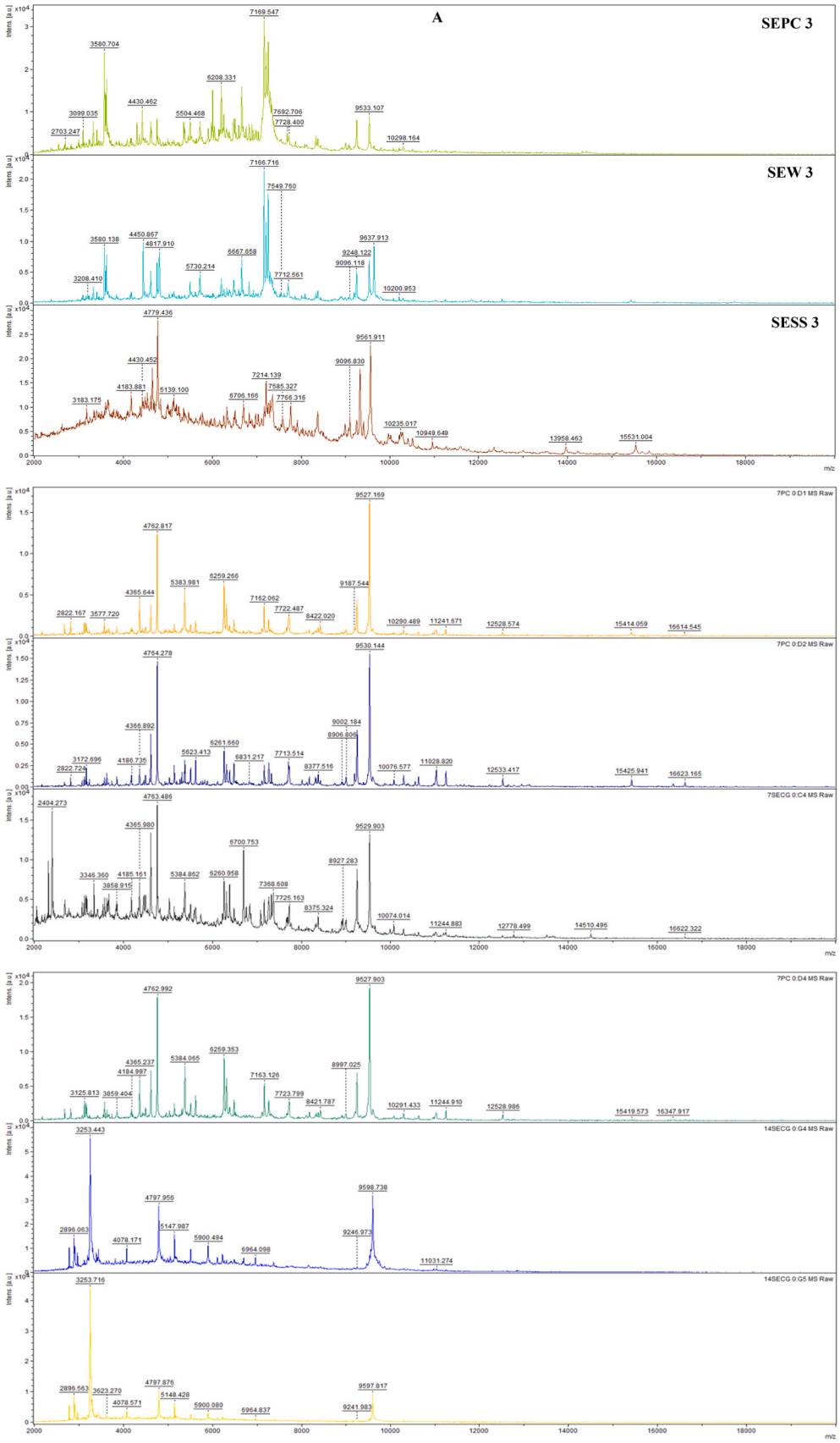

Fig. 13. MALDI-TOF MS spectral profiles of *S. enterica* planktonic culture and biofilms developed on wood and stainless-steel surfaces after 3 (A), 7 (B), and 14 (**C**) days of incubation in the presence of camphor. SEPC 3/7/14 - planktonic culture; SEW 3/7/14 - biofilm on wood; SESS 3/7/14 - biofilm on stainless steel.

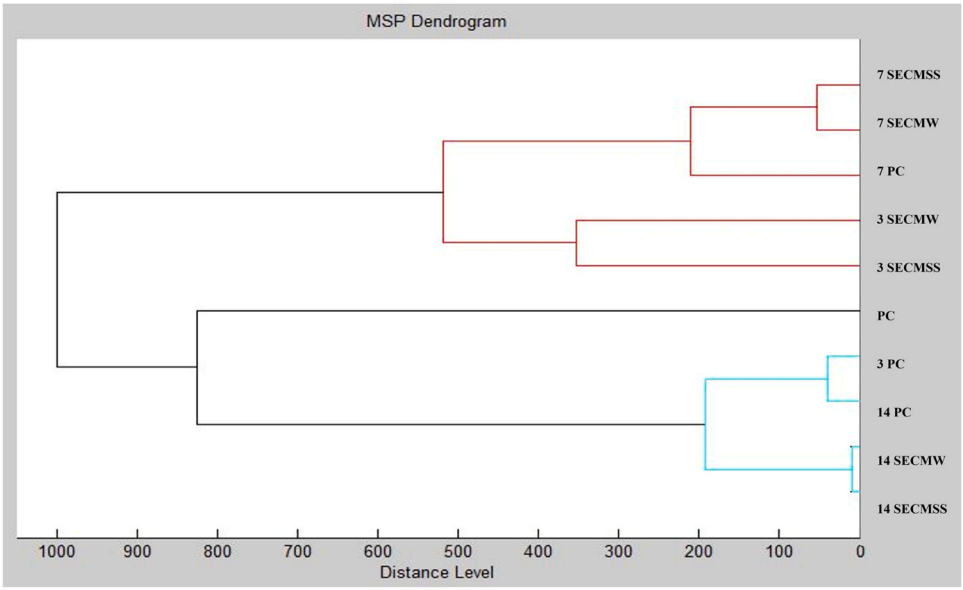

Fig. 14. MALDI-TOF MS MSP dendrogram illustrating the clustering of *S. enterica* planktonic cultures and biofilms formed on wood and stainless-steel surfaces after 3, 7, and 14 days of incubation in the presence of camphor. SEPC 3, SEPC 7, SEPC 14 - planktonic cultures; SEW 3, SEW 7, SEW 14 - biofilms on wood; SESS 3, SESS 7, SESS 14 - biofilms on stainless steel.

substantially higher concentrations (MIC_{50} = 4.39, 4.66, and 4.83 mg/mL; MIC_{90} = 4.70, 4.96, and 5.19 mg/mL, respectively). MALDI-TOF MS spectral profiles and MSP dendrograms revealed pronounced, time-dependent differences between planktonic and surface-attached cells on wood and stainless steel, with more extensive shifts in peak patterns in cultures exposed to CMEO than to any of the individual constituents. In all treatments, biofilms on wood and stainless steel diverged progressively from planktonic controls over 3, 7 and 14 days, but the changes were deeper and more complex in the presence of the whole EO. Together, these results indicate that CMEO more effectively disrupts and remodels *S. enterica* biofilms than any individual constituent alone, supporting the conclusion that the antibiofilm activity of CMEO reflects the combined contribution of multiple EO constituents.

3.6. Insecticidal activity against C. maculatus and M. dorsalis

CMEO exhibited markedly stronger insecticidal activity than β-pinene across all tested concentrations (Table 9 and Table 10).

At 100%, CMEO achieved 96.67% mortality, whereas β-pinene reached only 90.33%. α-Terpineol reached 90.33%, borneol 90.67%, and camphor 91.67%. Similarly, at 50%, CMEO maintained high mortality (78.33%), while β-pinene performed substantially weaker (64.67%) (Table 9). α-Terpineol achieved 72.33%, borneol 66.67%, and camphor 61.67%. At 25%, the effect of CMEO remained pronounced (57.33%), whereas β-pinene achieved only 45% mortality. α-Terpineol reached 48%, borneol 42.67%, and camphor 40.33%. Even at 12.5%, the difference remained distinct CMEO reached 32.67% mortality, compared to 19.33% for β-pinene. α-Terpineol achieved 24.67%, borneol 16.67%, and camphor 13.67%. The lowest tested concentration, 3.125%, highlighted the contrast between the substances most clearly: CMEO still showed measurable activity (8.33%), while β-pinene produced no mortality (0%). α-Terpineol achieved 2.33%, while borneol and camphor produced no mortality (0%). Overall, CMEO demonstrates strong, consistent, and concentration-dependent insecticidal activity, whereas the effectiveness of the individual constituents is weaker and declines rapidly, becoming completely or nearly inactive at the lowest concentration. These results align with previous observations indicating that the insecticidal effect of CMEO is substantially stronger than that of any individual constituent and cannot be reproduced by any single component alone.

Table 9
Mortality (%) at different concentrations of CMEO, β-pinene, α-terpineol, borneol, and camphor against *C. maculatus*.

Concentration of EO (%)	*C. maculatus*				
	CMEO	**β-Pinene**	**α-Terpineol**	**Borneol**	**Camphor**
3.125	8.33 ± 1.15^{f,A}	0.00 ± 0.00^{e,C}	2.33 ± 1.52^{f,B}	0.00 ± 0.00^{e,C}	0.00 ± 0.00^{e,C}
6.25	23.00 ± 2.00^{e,A}	15.67 ± 2.08^{d,BC}	16.33 ± 3.79^{e,B}	14.33 ± 2.52^{d,BC}	12.33 ± 1.53^{d,C}
12.5	32.67 ± 1.53^{d,A}	19.33 ± 3.06^{d,BC}	24.67 ± 2.08^{d,B}	16.67 ± 2.52^{d,C}	13.67 ± 3.21^{d,C}
25	57.33 ± 1.16^{c,A}	45.00 ± 2.65^{c,BC}	48.00 ± 1.00^{c,B}	42.67 ± 3.51^{c,CD}	40.33 ± 1.53^{c,D}
50	78.33 ± 1.52^{b,A}	64.67 ± 2.08^{b,C}	72.33 ± 2.08^{b,B}	66.67 ± 3.06^{b,C}	61.67 ± 8.08^{b,C}
100	96.67 ± 2.52^{a,A}	90.33 ± 3.21^{a,B}	90.33 ± 1.53^{a,B}	90.67 ± 4.04^{a,AB}	91.67 ± 6.81^{a,AB}

Data represents the mean (± standard deviation) of 3 replicates. $^{a–f}$ Different superscript lowercase letters indicate statistically different values within the column ($p \leq 0.05$). $^{A–D}$ Different superscript uppercase letters indicate statistically different values within the row ($p \leq 0.05$). CMEO= *C.* × *morifolium* essential oil.

CMEO exhibited markedly higher mortality in *M. dorsalis* than all tested constituents at all tested concentrations (Table 10). At 100% concentration, CMEO reached a mortality of 96.33%, whereas β-pinene achieved only 91.67%, α-terpineol 91.33%, borneol 90.33%, and camphor 90.33%, confirming the higher acute efficacy of the whole EO. At 50% concentration, CMEO maintained a high mortality (74.67%), while β-pinene dropped to 55.67%, α-terpineol reached 61.33%, borneol 53.67%, and camphor 54%, indicating that the individual constituents lose activity much more rapidly upon dilution. At 25% concentration, CMEO still caused substantial mortality (52%), while β-pinene achieved only 35.67%, α-terpineol 39.67%, borneol 36.33%, and camphor 32.33%. At 12.5% concentration, the difference increased further:

Table 10
Mortality (%) at different concentrations of CMEO, β-pinene, α-terpineol, borneol, and camphor against *M. dorsalis*.

Concentration of EO (%)	*M. dorsalis*				
	CMEO	β-Pinene	α-Terpineol	Borneol	Camphor
3.125	0.00 ± 0.00 ^{f,A}	0.00 ± 0.00 ^{f,A}	0.00 ± 0.00^{e,A}	0.00 ± 0.00^{e,A}	0.00 ± 0.00^{e,A}
6.25	21.67 ± 2.52^{e,A}	9.00 ± 2.00^{e,BC}	11.67 ± 1.53^{d,B}	8.67 ± 1.53^{d,C}	7.67 ± 0.58^{d,C}
12.5	31.67 ± 3.21^{d,A}	16.33 ± 1.53^{d,B}	13.67 ± 1.53^{d,BC}	11.67 ± 2.08^{d,C}	9.67 ± 2.09^{d,C}
25	52.00 ± 3.46^{c,A}	35.67 ± 2.08^{c,B}	39.67 ± 3.51^{c,B}	36.33 ± 4.16^{c,B}	32.33 ± 2.89^{c,B}
50	74.67 ± 2.31^{b,A}	55.67 ± 3.21^{b,C}	61.33 ± 1.53^{b,B}	53.67 ± 1.54^{b,C}	54.00 ± 4.58^{b,C}
100	96.33 ± 2.08^{a,A}	91.67 ± 3.21^{a,AB}	91.33 ± 4.16^{a,AB}	90.33 ± 5.31^{a,AB}	90.33 ± 1.53^{a,B}

Data represents the mean (± standard deviation) of 3 replicates. $^{a–f}$ Different superscript lowercase letters indicate statistically different values within the column ($p \leq 0.05$). $^{A–C}$ Different superscript uppercase letters indicate statistically different values within the row ($p \leq 0.05$). CMEO= *C.* × *morifolium* essential oil.

CMEO caused 31.67% mortality, while β-pinene only 16.33%, α-terpineol 13.67%, borneol 11.67%, and camphor 9.67%. At 3.125% concentration, none of the treatments produced mortality, representing the threshold below which insecticidal activity is no longer detectable. CMEO acts on *M. dorsalis* markedly more strongly than all tested constituents across all tested concentrations. These results support the conclusion that the insecticidal effect of CMEO reflects the contribution of several constituents present in the whole EO.

On both tested insect species (Table 9 and Table 10), *C. maculatus* and *M. dorsalis*, CMEO showed clearly stronger insecticidal activity than all tested constituents at all evaluated concentrations. CMEO maintained high mortality even at 50% and 25%, whereas the individual constituents achieved only moderate effects at the highest doses and rapidly lost efficacy upon dilution. At 12.5%, CMEO still caused relevant mortality on both species, while the individual constituents were only weakly active or almost ineffective. Among the tested constituents, α-terpineol consistently showed the strongest insecticidal activity, followed by borneol and camphor. Overall, CMEO consistently outperformed all tested constituents in both insects, confirming that the insecticidal potential of the EO reflects the combined contribution of multiple components rather than any single constituent alone.

The LC_{50} and LC_{90} values calculated by probit analysis (Table 11) confirmed that CMEO exhibited the highest insecticidal potency against both tested species. Against *C. maculatus*, CMEO showed the lowest LC_{50} (16.92% v/v) and LC_{90} (72.88% v/v). Among the individual constituents, α-terpineol was the most active (LC_{50} = 24.74%), followed by β-pinene (LC_{50} = 30.48%), borneol (LC_{50} = 30.80%), and camphor (LC_{50} = 32.12%). Against *M. dorsalis*, CMEO again showed the lowest LC_{50} (24.07%) and LC_{90} (62.81%), while among the constituents α-terpineol was the most active (LC_{50} = 32.62%, LC_{90} = 90.46%), followed by β-pinene (LC_{50} = 34.24%, LC_{90} = 97.02%), borneol (LC_{90} = 35.80%), and camphor (LC_{50} = 36.88%). LC_{90} values for borneol and camphor against *M. dorsalis* exceeded the tested concentration range and could not be determined. These results confirm that CMEO consistently outperforms all individual constituents in insecticidal efficacy against both species.

Table 11
LC_{50} and LC_{90} values (% v/v) of CMEO and its major constituents against *C. maculatus* and *M. dorsalis* determined by probit analysis.

Compound	*C. maculatus*		*M. dorsalis*	
	LC_{50}	LC_{90}	LC_{50}	LC_{90}
CMEO	16.92	72.88	24.07	62.81
α-Terpineol	24.74	> 100	32.62	90.46
β-Pinene	30.48	85.95	34.24	97.02
Borneol	30.80	85.46	35.80	> 100
Camphor	32.12	88.34	36.88	> 100

4. Discussion

This study provides a comprehensive characterization and comparative evaluation of CMEO and its major constituents α-terpineol, β-pinene, endo-borneol, and camphor, addressing whether the antimicrobial activity of the whole EO is driven by a single constituent or by the combined contribution of multiple constituents (Et-tazy et al., 2025; Kuang et al., 2018). Previous studies have described the antimicrobial properties of various *C.* × *morifolium* chemotypes, but none has simultaneously evaluated an α-terpineol-dominant chemotype alongside its major individual constituents. In addition, the unusually high capric acid content (13.4%) identified in this accession has not been reported at comparable levels in *Chrysanthemum* EOs and may contribute to the observed antimicrobial activity. The α-terpineol-dominant chemotype (20.1%) observed in CMEO deviates markedly from the camphor-rich *C.* × *morifolium* profiles described in the literature. A comprehensive screening of 23 genotypes reported (1S)-camphor at 31.80–45.94%, endo-borneol at 25.70–40.38% and α-pinene at 12.10–17.83% (Gajbhiye et al., 2025). Egyptian accessions showed camphor at 14.56%, curcumene at 10.50% and borneol at 7.95% (Youssef et al., 2020), while the 'Fubaiju' cultivar contained camphor at 16.87% and 1,8-cineole at 10.62% (Zhan et al., 2021). In contrast, CMEO contained only 6.3% camphor and was dominated by α-terpineol, indicating a distinct chemotypic variant. The capric acid level (13.4%) is also atypically high; although Nigerian accessions were reported to contain octadecanoic acid at 19.5% (Lawal et al., 2014), capric acid at this magnitude has not been widely documented. Medium-chain fatty acids can disrupt microbial membranes by destabilizing lipopolysaccharide structures (Zentek et al., 2011), while oxygenated monoterpenes further contribute to antimicrobial activity, with α-terpineol showing membrane-disruptive effects and MIC/MBC values of 0.78 μL/mL against *E. coli* (Li et al., 2014). Borneol, a bicyclic oxygenated monoterpene structurally related to camphor, disrupts bacterial and fungal cell membranes by penetrating the phospholipid bilayer through passive diffusion, and has been documented to inhibit *C. albicans* germ tube formation and biofilm activity at sub-inhibitory concentrations (Wang et al., 2022). Oxygenated monoterpenes exert antimicrobial effects primarily through disruption of the microbial cell membrane, leading to increased permeability and leakage of intracellular contents (Kong et al., 2025). Camphor and borneol, both present in CMEO, have been specifically documented to disrupt bacterial membranes and inhibit respiratory chain function (Kong et al., 2025). Overall, the α-terpineol-dominant, capric acid-rich composition differentiates this accession from the camphor-dominated chemotypes previously reported from other geographical origins.

In this study, the antimicrobial activity of the whole CMEO and its individual constituents (α-terpineol, β-pinene, endo-borneol, and camphor) was evaluated using the disc diffusion method against a panel of bacterial and yeast pathogens. CMEO exhibited the strongest inhibition against enteric Gram-negative bacteria (*S. enterica*, *Y. enterocolitica*, *E. coli*), with inhibition zones of approximately 12–14 mm. These values are substantially lower than those reported by Kuang et al. (2018), who observed inhibition zones up to 20.43 mm against *P. aeruginosa* and 12.29 mm against *E. coli* for CMEO. Such discrepancies likely stem from differences in chemical composition, as Kuang et al. (2018) identified α-curcumene (12.55%) as the major component, whereas white cultivars of *C.* × *morifolium* are typically characterized by camphor-dominated

chemotypes. The activity profile observed for CMEO, with stronger inhibition of Gram-negative compared to Gram-positive bacteria, is somewhat atypical. Youssef et al. (2020) reported that EOs of *C. indicum* and *C.* × *morifolium* exhibited moderate activity against Gram-positive bacteria, with MIC values of 62.5 μg/mL for *B. subtilis*, *S. agalactiae*, and *S. pyogenes*, while showing weak activity against Gram-negative bacteria (MIC > 500 μg/mL). The opposite pattern observed in our study suggests that the white cultivar of *C.* × *morifolium* possesses a unique chemical profile that favours activity against Gram-negative microorganisms. CMEO showed moderate activity toward *L. monocytogenes* and *E. faecalis* (8–10 mm) but weak activity against *S. aureus* (7 mm). Youssef et al. (2020) reported significantly higher inhibition zones (19.6–20.4 mm) for various *Staphylococcus* species. The notably lower susceptibility of *S. aureus* in our study may reflect the thicker peptidoglycan layer and enhanced resistance mechanisms that limit penetration of monoterpene-rich EOs. For yeasts, CMEO exhibited moderate inhibition of *C. albicans* and *C. parapsilosis* (8–9 mm), while other *Candida* species were more tolerant (generally < 8 mm). Youssef et al. (2020) also reported weak antifungal activity of CMEO (MIC > 500 μg/mL), consistent with the naturally high resistance of yeasts due to their robust β-glucan- and chitin-rich cell wall. β-Pinene demonstrated consistently weaker activity across all tested organisms, with inhibition zones of approximately 3–7 mm. Silva et al. (2012) reported MIC values for (+)-β-pinene ranging from 117 to 6250 μg/mL against *C. albicans* and methicillin-resistant *S. aureus*, with only the positive enantiomers showing measurable activity; negative enantiomers exhibited no antimicrobial effect even at 20 mg/mL. Our findings align with these results, confirming that β-pinene alone has only weak antimicrobial properties. The consistently higher activity of CMEO compared with the individual constituents indicates that none of the tested compounds represents the principal antimicrobial constituent of the white CMEO. Among the additionally tested constituents, α-terpineol showed the strongest disc diffusion activity, with inhibition zones of 5.33–8.67 mm, preferentially inhibiting Gram-negative bacteria (*S. enterica*, *E. coli*) over *S. aureus*, consistent with the susceptibility ranking reported by Yang et al. (2023). Borneol produced intermediate inhibition zones of 3.67–7.33 mm; this level of activity is consistent with studies on borneol-rich EOs showing antibacterial activity against *S. typhimurium*, *E. coli*, and *S. aureus* through disruption of cell wall integrity and membrane permeability (Xiao et al., 2025; Yu et al., 2022). Camphor showed the weakest disc diffusion activity (3.67–6.67 mm), which is in agreement with Chen et al. (2013), who noted that camphor as a pure compound generally exhibits only weak to moderate direct antimicrobial activity. The activity hierarchy CMEO > α-terpineol > borneol ≈ camphor > β-pinene confirms that oxygenated monoterpenes are more effective antimicrobial agents than hydrocarbon monoterpenes, and that the superior activity of CMEO arises from synergistic interactions among its multiple constituents (Kong et al., 2025). Youssef et al. (2020) identified camphor (14.56%) as the major component of *C.* × *morifolium*, while Kuang et al. (2018) reported α-curcumene (12.55%). The overall antimicrobial effect of CMEO therefore likely results from the combined contribution of multiple constituents rather than from any single compound, particularly oxygenated monoterpenes such as α-terpineol, camphor, and borneol, which generally exhibit stronger antimicrobial properties than hydrocarbon monoterpenes such as β-pinene.

Following the disc diffusion screening, which showed a generally stronger activity of CMEO compared with the individual constituents, the broth microdilution assay provided a more quantitative assessment of their inhibitory potency expressed as MIC_{50} and MIC_{90} values. For CMEO, the MIC data confirmed a pronounced antimicrobial effect particularly against *Y. enterocolitica*, which exhibited very low MIC_{50} and MIC_{90} values (0.49 and 0.71 mg/mL, respectively). High susceptibility was also observed in *C. albicans* (MIC_{50} = 0.48 mg/mL, MIC_{90} = 0.68 mg/mL). At the opposite end of the spectrum, *C. parapsilosis* showed the weakest response, with MIC_{50} exceeding 6.38 mg/mL, indicating substantial tolerance. These results are partly consistent with Jung (2009), who reported MIC values of *C. indicum* EO in the range 0.1–1.6 mg/mL against oral pathogens. However, whereas Jung (2009) observed the strongest activity against obligate anaerobes (*Fusobacterium nucleatum*, *Prevotella intermedia*; MIC 0.1–0.2 mg/mL), the CMEO tested in this study showed its highest potency against *Y. enterocolitica* and *C. albicans*, reflecting chemotype-dependent differences in antimicrobial performance. Shunying et al. (2005) reported that *C. indicum* EO containing 1,8-cineole, camphor, borneol and bornyl acetate displayed moderate to strong antimicrobial activity. Importantly, the authors showed that isolated monoterpenes such as camphor, 1,8-cineole, terpinen-4-ol, borneol and β-caryophyllene exhibited weaker activity (MIC 0.4 to >12.8 mg/mL) than the complete EO. This observation agrees with the present findings, where CMEO consistently outperformed its individual constituents. α-Terpineol showed the strongest inhibitory potency among the individually tested constituents, with the highest susceptibility recorded against *C. albicans* and *Y. enterocolitica*, mirroring the susceptibility ranking documented by Yang et al. (2023), who reported that the antibacterial activity of α-terpineol decreased in the order *E. coli* O157:H7 > *S. typhimurium* > *L. monocytogenes* > *S. aureus*, consistent with the pattern observed here. Borneol showed intermediate inhibitory activity, in agreement with reports on borneol-rich EOs documenting moderate antibacterial potency against *S. typhimurium*, *E. coli*, and *S. aureus* through disruption of cell wall integrity and increased membrane permeability (Yu et al., 2022). Camphor exhibited the weakest inhibitory potency among the oxygenated constituents, in agreement with Chen et al. (2013), who noted that camphor as a pure compound generally exhibits only weak to moderate antimicrobial activity. In contrast, β-pinene displayed substantially weaker antimicrobial activity, reflected in markedly higher MIC values across the tested panel. The strongest inhibitory effect was again observed against *Y. enterocolitica* (MIC_{50} ≈ 3.49 mg/mL), whereas *C. parapsilosis* showed the lowest susceptibility (MIC_{50} = 8.44 mg/mL). These data are consistent with previous reports describing only moderate potency of β-pinene. Silva et al. (2012) reported MIC values of (+)-β-pinene ranging from 0.117 to 6.25 mg/mL against *C. albicans*, *C. neoformans*, *Rhizopus oryzae* and MRSA, and emphasized that only the (+) enantiomer is microbiologically active. Our MIC_{50} value for *C. albicans* (1.74 mg/mL) falls within this range and confirms the limited intrinsic activity of β-pinene. De Macêdo Andrade et al. (2019) also demonstrated that (+)-β-pinene interferes with fungal cell wall integrity and exhibits antibiofilm activity against several *Candida* species, but MIC values generally remained higher than those of complex EOs. Similarly, Kim et al. (2003) reported MIC values > 800 μg/mL for *C. boreale* EO rich in camphor, α-thujone and 1,8-cineole against 14 bacterial strains, still lower than the concentrations required for β-pinene alone in the present study. A direct comparison between CMEO and the individual constituents clearly shows that the whole EO is substantially more potent. For *Y. enterocolitica*, CMEO reached MIC_{50} at 0.49 mg/mL compared with 3.49 mg/mL for β-pinene, corresponding to roughly a seven-fold difference in potency. A similar pattern was observed for *C. albicans*, where CMEO was more effective (MIC_{50} = 0.48 mg/mL) than β-pinene (MIC_{50} = 1.74 mg/mL). These differences mirror the disc diffusion results, where CMEO produced larger inhibition zones than the individual constituents across the same panel of microorganisms. The superiority of CMEO over individual constituents is consistent with previous work on *Chrysanthemum* EO. Jung (2009) showed that individual monoterpenes (camphor, 1,8-cineole, terpinen-4-ol, borneol) had weaker antimicrobial activity than the whole *C. indicum* EO, and that synergistic interactions between the EO and antibiotics (ampicillin, gentamicin) reduced MIC values by 8–16-fold. Feng et al. (2021) further demonstrated that chemical modification of β-pinene leads to derivatives with much higher antimicrobial activity, supporting the notion that the parent molecule is only moderately active. Taken together, the MIC results confirm that the antimicrobial potential of CMEO cannot be explained by any single constituent alone. The complex composition of *Chrysanthemum* EOs,

typically including oxygenated monoterpenes such as camphor, borneol, 1,8-cineole and α-terpineol, appears essential for achieving strong antimicrobial effects, and the present data indicate that the observed activity of CMEO reflects the combined contribution of several constituents, with α-terpineol, β-pinene, borneol, and camphor each contributing to the overall antimicrobial effect, and none of them individually sufficient to reproduce the potency of the whole EO.

The *in situ* vapor phase experiments performed across four food matrices (apple, pear, parsley, and Hokkaido pumpkin) demonstrated clear and consistent differences between the whole CMEO and the individually tested constituents. At 500 μL/L, CMEO achieved approximately 65–95% inhibition across all matrices, whereas all individual constituents produced substantially lower inhibition (31–44%) compared with CMEO. Among the individual constituents, α-terpineol showed the strongest *in situ* antimicrobial activity (approximately 38–44% inhibition at 500 μL/L), followed by β-pinene, borneol, and camphor, all of which produced substantially weaker inhibition than CMEO, consistent with the superior membrane-disrupting capacity of oxygenated monoterpenes over hydrocarbon terpenes and the limited individual efficacy of isolated compounds compared with complex EO mixtures (Jackson-Davis et al., 2023; Karabörklü and Ayvaz, 2023). These results confirm that the antimicrobial efficacy observed for CMEO is substantially higher than that of the individual constituents, indicating that no single compound alone can account for the activity of the complete EO. Comparable observations were reported by Lin et al. (2024), who tested seven citrus EOs in vapor phase against six fish-spoilage bacterial species. All EOs were effective at 294 μL/L against Gram-negative bacteria, with lemon and orange EO showing the strongest inhibition. Notably, several EOs exhibited stronger antibacterial activity in vapor phase than in direct-contact solid-phase assays. For example, lemon EO produced an inhibition zone of 74.00 ± 19.05 mm against *Shewanella putrefaciens* in vapor phase, compared with only 36.33 ± 0.75 mm in solid phase. These findings support our results by showing that volatilized phytochemicals can exert substantially enhanced antimicrobial effects compared with their liquid-phase counterparts. Matrix-dependent variability in CMEO performance was also evident. The parsley model demonstrated the highest overall inhibition (87.60% against *S. aureus* and 86–87% against most other microorganisms), whereas the Hokkaido pumpkin model showed an unusual inverse concentration effect, with lower concentrations performing more effectively. Kačániová et al. (2023a) likewise observed strong matrix-specific differences when testing rosemary EO on apples, pears, cabbage, and potatoes, with the highest inhibition recorded against *E. faecalis* and *C. glabrata* on apples, and *S. enterica* and *C. glabrata* on pears, while the optimal concentration of 500 μL/L remained consistent. Esteve-Redondo et al. (2024) emphasized the importance of humidity-responsive delivery systems for EOs in food packaging. They reported that β-cyclodextrin-MOF carriers released 96.3% of their volatile load at 100% RH but only 12% at 43% RH after seven days. This mechanism may help explain why the parsley matrix, which typically retains high ambient humidity, supported markedly stronger CMEO activity. Across all matrices, the individual constituents showed consistently weaker antimicrobial activity than CMEO. At 500 μL/L, the tested constituents exhibited limited inhibition, consistent with the expected behavior of isolated monoterpenes. Melkina et al. (2021) demonstrated that monoterpene hydrocarbons such as (−)-limonene and (+)-α-pinene induce oxidative stress and membrane damage yet exhibit considerably weaker action than oxygenated monoterpenes. These hydrocarbons cause a gradual accumulation of reactive oxygen species H_2O_2 formation within 20–30 min, followed by superoxide anion production leading to DNA, protein, and membrane damage. However, this mechanism requires high concentrations and extended exposure times, explaining why simple hydrocarbons do not produce potent antimicrobial effects in food matrices. Jackson-Davis et al. (2023) further highlighted the functional distinction between hydrocarbon terpenes (pinene, myrcene, limonene, terpinene, p-cymene) and oxygenated terpenoids. Oxygenated derivatives can disrupt membranes more rapidly and inhibit protein and DNA synthesis, whereas hydrocarbons are considerably less effective. This agrees with our findings that individual constituents provide only limited microbial suppression under in situ conditions. The strong biofilm-forming *S. enterica* strain displayed slightly reduced sensitivity compared with the planktonic culture, yet CMEO maintained 74–78% inhibition across all matrices, while all individual constituents achieved substantially lower inhibition levels. Somrani et al. (2025) showed that EOs inhibit initial adhesion of *Salmonella Enteritidis* more effectively than they disrupt pre-existing biofilms, with mature 24 h biofilms showing $< 40\%$ inhibition even under optimal conditions. Fernandes et al. (2023) found that oregano EO vapor disrupted quorum-sensing signals, downregulated biofilm-associated genes, and penetrated the extracellular polymeric matrix in resistant *Candida* biofilms. Given that CMEO contains camphor (6.3%), 1,8-cineole (2.4%), and borneol (7.0%), similar mechanisms likely contribute to its antibiofilm activity against *S. enterica*. The most important finding is that CMEO consistently exhibits two- to threefold higher *in situ* antimicrobial activity than all tested individual constituents. This demonstrates that the antimicrobial effect of CMEO cannot be attributed to any single constituent alone, and instead reflects the combined contribution of multiple oxygenated monoterpenes present in the EO. Melkina et al. (2021) showed that hydrocarbon monoterpenes act primarily through oxidative stress, whereas oxygenated monoterpenes, because of their polarity, can rapidly destabilize phospholipid bilayers and increase membrane permeability. Their concurrent presence likely enhances antimicrobial activity, as oxygenated compounds facilitate deeper penetration of less polar constituents. From a practical standpoint, these *in situ* results demonstrate that CMEO has strong potential for use in active food-packaging systems designed for fresh fruits and vegetables. Inhibition levels of 65–95% at 500 μL/L suggest suitability for modified atmosphere packaging (MAP). Esteve-Redondo et al. (2024) report that 200–1000 μL/L vapor concentrations are typical for commercial MAP, and EOs may be incorporated into polymeric films (chitosan, alginate, pectin) or into absorbent pads for gradual release. The high efficacy of CMEO in the parsley model (e.g., 87.60% inhibition of *S. aureus*) suggests that leafy vegetables and herbs may be ideal application targets. Jackson-Davis et al. (2023) noted that EOs at vapor phase concentrations below 1000 μL/L generally do not negatively influence sensory attributes, supporting the viability of CMEO in minimally processed foods. In summary, the *in situ* vapor phase experiments clearly showed that CMEO is substantially more effective than all tested individual constituents across all food matrices, demonstrating matrix-dependent behaviour, sustained antibiofilm activity, and the combined contribution of multiple monoterpenes to overall antimicrobial performance. These results highlight CMEO's potential as a natural antimicrobial agent suitable for integration into active packaging technologies for fresh produce and minimally processed foods.

The antibiofilm assessment confirmed that CMEO has a markedly stronger inhibitory effect on mature *S. enterica* biofilms than all tested individual constituents. The MIC_{50} and MIC_{90} values obtained for CMEO (2.46 and 2.64 mg/mL) indicate that relatively high concentrations are needed to reduce biomass once the biofilm is already formed, which reflects the increased tolerance of sessile communities compared with planktonic cells. Comparable findings were reported for other EOs; for example, *Litsea cubeba* (Lour.) Pers. EO exhibited lower MBIC values (0.33–0.35 mg/mL), but only during inhibition of early biofilm stages rather than disruption of stabilized structures. Similarly, it has been demonstrated that cinnamon EO showed substantially stronger effects on adhesion inhibition than on the removal of pre-formed *S.* Enteritidis biofilms. The antibiofilm performance of CMEO falls within the range reported for EOs with confirmed anti-biofilm potential. MALDI-TOF MS analysis further supported the crystal violet results: spectra of *S. enterica* biofilms differed from planktonic cultures already after three days of incubation in the presence of CMEO. These differences initially appeared as signal broadening in the mid-*m/z* region and a reduction in high-mass

peak intensity, indicating reorganization of the protein composition associated with the transition to a surface-attached phenotype under EO stress rather than a simple quantitative reduction in biomass. Similar patterns were observed in studies employing *Santalum album* L. EO, where long-term incubation induced diversification of mass spectra and separation of biofilm and planktonic profiles (Verešová et al., 2024). In our study, wood supported greater spectral heterogeneity and the emergence of new peaks, whereas stainless steel generated a more stable but compositionally distinct profile. This substrate-dependent behaviour aligns with Paz-Méndez et al. (2017), who reported that biofilm development on stainless steel and polystyrene is strongly shaped by environmental conditions and available nutrients. The clear separation of biofilm and planktonic clusters in dendrograms already after three days is consistent with Caputo et al. (2018), who demonstrated that MALDI-TOF MS reliably discriminates biofilm-producing and non-producing strains of *S. epidermidis*. The observed spectral divergence is consistent with known differences between biofilm and planktonic cells. Biofilms consist of cells embedded in an extracellular polymeric matrix that enhances tolerance to antimicrobials. Biofilm-associated gene expression shifts toward stress-response pathways (Hernández-Jiménez et al., 2013). These physiological shifts are fully compatible with the gradual, time-dependent spectral changes we observed in CMEO-treated biofilms on both wood and stainless steel. Among the tested constituents, β-pinene showed the weakest antibiofilm activity, with MIC_{50} and MIC_{90} values nearly twice as high (4.39 and 4.70 mg/mL). α-Terpineol showed intermediate antibiofilm activity ($MBIC_{50}$ = 2.64 mg/mL; $MBIC_{90}$ = 2.89 mg/mL), substantially closer to CMEO than to β-pinene, borneol ($MBIC_{50}$ = 4.66 mg/mL; $MBIC_{90}$ = 4.96 mg/mL), or camphor ($MBIC_{50}$ = 4.83 mg/mL; $MBIC_{90}$ = 5.19 mg/mL), consistent with its documented role as the most potent oxygenated constituent of CMEO in disrupting membrane integrity and interfering with biofilm formation in foodborne pathogens (Yang et al., 2023). The weaker antibiofilm activity of borneol and camphor is in agreement with reports showing that while these compounds are membranolytic, their effect on established biofilm architecture is limited compared with α-terpineol-dominant EO compositions (Wang et al., 2022; Yu et al., 2022). MALDI-TOF MS profiles of biofilms exposed to individual constituents revealed milder changes: most of the original peaks remained conserved, fewer new signals appeared, and clustering distances between planktonic and biofilm forms were significantly smaller than in CMEO treatments. These findings suggest that individual constituents do not markedly disrupt the structural organization of mature *S. enterica* biofilms but rather induce limited adaptation within an otherwise relatively conserved spectral pattern. This conclusion agrees with mechanistic studies demonstrating that hydrocarbon monoterpenes exert weaker membrane-disruptive activity than oxygenated monoterpenes and require prolonged exposure or high concentrations to produce measurable effects. Furthermore, the progressive but limited shifts seen in β-pinene-treated communities correspond with findings from Tkaczyk (2025) showing that biofilm structural adaptation is robust across environmental conditions and often resilient to single-compound stressors. The comparative results between wood and stainless steel additionally highlight that biofilm architecture is strongly modulated by the physical and chemical properties of the substrate. Wood promoted more dynamic and heterogeneous spectral profiles, whereas stainless steel supported more stable patterns. Similar substrate-driven behaviour was reported in marine biofilm studies where succession dynamics overshadowed material-specific effects, yet early developmental stages remained sensitive to surface-dependent cues (Sushmitha et al., 2021). In our system, these parallels reinforce the suitability of MALDI-TOF MS for documenting time- and surface-dependent adaptation of *S. enterica* biofilms under exposure to volatile plant metabolites. Taken together, the results demonstrate that CMEO induces substantially more extensive and progressive spectral alterations in *S. enterica* biofilms than the individual constituents. The antibiofilm effects of the whole EO therefore cannot be ascribed to its major hydrocarbon component alone but are more plausibly explained by the combined contribution of several constituents, particularly oxygenated monoterpenes such as α-terpineol, camphor, and borneol.

The insecticidal assays demonstrated that CMEO possesses markedly higher toxicity toward *C. maculatus* and *M. dorsalis* compared with all individually tested constituents, indicating that the biological activity of the entire EO cannot be attributed to any single constituent alone. This pattern agrees with earlier studies on chrysanthemum-derived EOs, such as the work of Gebreil et al. (2024), who reported strong mortality of *C. maculatus* induced by *Chrysanthemum cinerariaefolium* seed EO together with the suppression of oviposition and adult emergence during storage. Their findings support the idea that complex mixtures of terpenes, even at low concentrations, can produce robust insecticidal responses that isolated terpenes do not achieve. The superior activity of CMEO is further consistent with the repellent and toxic effects observed in other plant-derived EOs. Pandey et al. (2014) showed that EOs from *Chenopodium ambrosioides* L. and *Adhatoda vasica* Nees exerted complete repellency and achieved full mortality of bruchid beetles during storage. Similarly, Ahmed et al. (2022) demonstrated that EOs from *Eruca sativa* Mill. and *Azadirachta indica* A. Juss. effectively reduced *C. maculatus* populations while maintaining seed viability and nutritional quality. These findings collectively reinforce that whole EOs generally outperform isolated monoterpenes, most likely because multiple oxygenated monoterpenes, hydrocarbons and minor phenolic constituents contribute in parallel to fumigant and contact toxicity. Our observations regarding the tested constituents align with fumigation studies by Ajayi et al. (2014), who identified monoterpene hydrocarbons such as β-pinene and α-pinene as the least toxic compounds against *C. maculatus*, in contrast to highly active compounds such as 1,8-cineole, carvacrol, and eugenol. Ajayi also showed that β-pinene fails to inhibit oviposition or adult emergence, which reflects the limited biological range of this monoterpene. Parallel results were reported by Sharma and Tiwari (2021), who found that although β-pinene is toxic to *Sitophilus oryzae*, its efficacy requires considerably higher vapor concentrations and longer exposure times compared with eucalyptol or linalool. These observations support the conclusion that individual constituents exhibit only modest insecticidal potential compared with the whole EO. The broader evidence from EO research also indicates that insecticidal potency is enhanced when multiple EO constituents act together, rather than when single compounds are applied in isolation. For example, Jayaram et al. (2022) demonstrated high fumigant mortality of *C. maculatus* using several aromatic plant EOs, with toxicity levels strongly dependent on EO composition rather than individual constituents. In line with this, Dassanayake et al. (2021) emphasized that EOs can synergistically increase the efficacy of existing pesticides or bioactive molecules, supporting the concept that complex EOs function through multi-target interference disrupting neural transmission, respiration, cuticular integrity, and detoxification pathways simultaneously. Additional insights come from studies on EOs with parallel antimicrobial and insecticidal effects. Verešová et al. (2024) recorded strong insecticidal activity of *Rosa damascena* Mill. EO against *M. dorsalis*, while Kačániová et al. (2025) showed that *Eucalyptus citriodora* Hook. EO was effective against *M. dorsalis* and simultaneously inhibited *S. enterica* biofilm formation. These findings place CMEO within a wider group of multifunctional botanical EOs capable of acting against both insect pests and foodborne pathogens, enhancing their potential applications in storage protection and food safety. Among the tested constituents, α-terpineol consistently showed the strongest insecticidal activity, with LC_{50} values of 24.74% and 32.62% against *C. maculatus* and *M. dorsalis*, respectively, followed by β-pinene, borneol, and camphor. This ranking is consistent with the known superior insecticidal potency of oxygenated monoterpenes over hydrocarbon monoterpenes, and with the documented fumigant activity of terpineol, camphor, and borneol against stored-product beetles (El Abdali et al., 2022; Karabörklü and Ayvaz, 2023). Taken together, the literature strongly supports the conclusion

that the high insecticidal potency of CMEO arises from the combined contribution of its individual constituents rather than from any single compound. While individual constituents contribute to the overall profile of the EO, their efficacy alone is limited, confirming that whole EO formulations provide far superior outcomes when targeting storage pests such as *C. maculatus* and *M. dorsalis*. CMEO therefore represents a promising botanical alternative for integrated pest management strategies, aligning with global efforts to reduce synthetic pesticide use while maintaining the protection of stored agricultural products.

5. Conclusion

This study provides the first integrated evaluation of CMEO and its major constituents α-terpineol, β-pinene, endo-borneol, and camphor across complementary experimental levels, including *in vitro* antimicrobial testing, *in situ* vapor-phase assays on food matrices, antibiofilm experiments with *S. enterica* and insecticidal trials against stored-product beetles. CMEO was chemically characterized as an α-terpineol and β-pinene-rich chemotype with an unusually high proportion of capric acid, clearly distinct from previously reported camphor-dominant *C.* × *morifolium* EO. Across all antimicrobial assays, CMEO consistently exhibited stronger and broader activity than all tested constituents, particularly against *Y. enterocolitica* and *C. albicans*, and retained high efficacy in vapor phase on apple, pear, parsley and Hokkaido pumpkin models, including against a biofilm-forming *S. enterica* strain. CMEO also showed a markedly stronger antibiofilm effect on mature *S. enterica* biofilms than the individual constituents, as confirmed by crystal violet quantification and MALDI-TOF MS profiling, which revealed more extensive, time-dependent spectral alterations in biofilms exposed to the whole EO. In parallel, CMEO demonstrated substantially higher insecticidal activity against *C. maculatus* and *M. dorsalis*, maintaining relevant mortality even at lower concentrations where the individual constituents were weak or inactive; among them, α-terpineol showed the strongest insecticidal effect, with LC_{50} values of 24.74% and 32.62% against *C. maculatus* and *M. dorsalis*, respectively. Taken together, these findings confirm that the biological activity of CMEO cannot be attributed to any single constituent alone. α-Terpineol consistently showed the strongest activity among the tested constituents in both antimicrobial and insecticidal assays, followed by β-pinene, borneol, and camphor, yet all remained substantially weaker than the whole EO. These results suggest that synergistic interactions among multiple constituents are responsible for the overall bioactivity. CMEO thus emerges as a promising candidate for further development as a natural antimicrobial and insecticidal agent, with potential applications in active food-packaging systems, biocontrol of foodborne pathogens and the protection of stored agricultural products. Future studies should evaluate the combined contributions of major constituents and reconstituted mixtures reflecting the GC-MS composition of CMEO. In addition, sensory impact, toxicity, regulatory aspects and optimization of formulation and delivery systems should be addressed.

CRediT authorship contribution statement

Miroslava Kačániová: Conceptualization, Methodology, Investigation, Writing-original draft, Formal analyses, Supervision, Project administration, Funding acquisition, Visualization. **Minhang Qiao**: Formal analyses, Writing-review & editing. Guiguo Zhang: Formal analyses, Writing-review & editing. **Alessandro Bianchi**: Data curation, Formal analyses, Methodology, Investigation, Visualization, Writing-original draft, Writing-review & editing. **Joel Horacio Elizondo-Luévano:** Formal analyses, Writing-review & editing. **Anis Ben Hsouna**: Formal analyses, Writing-review & editing. **Rania Ben Saad**: Formal analyses, Writing-review & editing. **Zhaojun Ban**: Formal analyses, Writing-review & editing. **Li Li**: Formal analyses, Writing-review & editing. **Jian Lou**: Formal analyses, Writing-review & editing. **Maciej Ireneusz Kluz**: Formal analyses, Writing-review & editing. **Stefania Garzoli**: Formal analyses, Data curation, Investigation, Methodology, Supervision, Writing-review & editing.

Funding

This research was funded by the grant APVV-20-0058 "The potential of the essential oils from aromatic plants for medical use and food preservation and by the VEGA grant 1/0059/24 titled "Chemical properties and biological activity (*in vitro*, *in vivo* and *in situ*) of plant volatile mixtures, their main components and inclusion systems.

Declaration of Competing Interest

The authors declare that they have no known competing financial interests or personal relationships that could have appeared to influence the work reported in this paper.

Acknowledgements

The author is thankful to the Deanship of Graduate Studies and Scientific Research at University of Bisha for supporting this work through the Fast-Track Research Support Program.

Appendix A. Supporting information

Supplementary data associated with this article can be found in the online version at doi:10.1016/j.indcrop.2026.123380.

Data availability

Data will be made available on request.

References

Ahmed, A.M., Khoso, F.N., Alhilfi, A.Z.A., Otho, S.A., Ali, Q., Soomro, D.M., Soomro, Z. A., 2022. Efficacy of plant seed oils against *Callosobruchus maculatus* L. on chickpea grains. SJA 38. https://doi.org/10.17582/journal.sja/2022/38.5.222.233.

Ajayi, O.E., Appel, A.G., Fadamiro, H.Y., 2014. Fumigation toxicity of essential oil monoterpenes to *Callosobruchus maculatus* (Coleoptera: Chrysomelidae: Bruchinae). J. Insects 2014, 1–7. https://doi.org/10.1155/2014/917212.

Barbosa, D.R.E.S., De Oliveira, J.V., Da Silva, P.H.S., Santana, M.F., Breda, M.O., De França, S.M., De Miranda, V.L., 2021. Lethal and sublethal effects of chemical constituents from essential oils on *Callosobruchus maculatus* (F.) (Coleoptera: Chrysomelidae: Bruchinae) in cowpea stored grains. J. Plant Dis. Prot. 128, 1575–1586. https://doi.org/10.1007/s41348-021-00543-x.

Caputo, P., Di Martino, M.C., Perfetto, B., Iovino, F., Donnarumma, G., 2018. Use of MALDI-TOF MS to discriminate between biofilm-producer and non-producer strains of *Staphylococcus epidermidis*. IJERPH 15, 1695. https://doi.org/10.3390/ijerph15081695.

Chaubey, M.K., 2014. Biological activities of *Allium sativum* essential oil against pulse beetle, *Callosobruchus chinensis* (Coleoptera: Bruchidae). Herba Pol. 60, 41–55. https://doi.org/10.2478/hepo-2014-0009.

Chen, W., Vermaak, I., Viljoen, A., 2013. Camphor—a fumigant during the black death and a coveted fragrant wood in ancient egypt and babylon—a review. Molecules 18, 5434–5454. https://doi.org/10.3390/molecules18055434.

Dassanayake, M.K., Chong, C.H., Khoo, T.-J., Figiel, A., Szumny, A., Choo, C.M., 2021. Synergistic field crop pest management properties of plant-derived essential oils in combination with synthetic pesticides and bioactive molecules: a review. Foods 10, 2016. https://doi.org/10.3390/foods10092016.

De Macêdo Andrade, A.C., Rosalen, P.L., Freires, I.A., Scotti, L., Scotti, M.T., Aquino, S. G., De Castro, R.D., 2019. Antifungal activity, mode of action, docking prediction and anti-biofilm effects of (+)-β-pinene enantiomers against *Candida* spp. CTMC 18, 2481–2490. https://doi.org/10.2174/1568026618666181115103104.

El Abdali, Y., Agour, A., Allali, A., Bourhia, M., El Moussaoui, A., Eloutassi, N., Salamatullah, A.M., Alzahrani, A., Ouahmane, L., Aboul-Soud, M.A.M., Giesy, J.P., Bouia, A., 2022. *Lavandula dentata* L.: phytochemical analysis, antioxidant, antifungal and insecticidal activities of its essential oil. Plants 11, 311. https://doi.org/10.3390/plants11030311.

Esteve-Redondo, P., Heras-Mozos, R., Simó-Ramírez, E., López-Carballo, G., López-de-Dicastillo, C., Gavara, R., Hernández-Muñoz, P., 2024. Innovative systems for the delivery of naturally occurring antimicrobial volatiles in active food-packaging technologies for fresh and minimally processed produce: stimuli-responsive materials. Foods 13, 856. https://doi.org/10.3390/foods13060856.

Et-tazy, L., Lamiri, A., Krimi Bencheqroun, S., Errati, H., Hashem, A., Avila-Quezada, G. D., Abd-Allah, E.F., Satrani, B., Essahli, M., Satia, L., 2025. Exploring synergistic insecticidal effects of binary mixtures of major compounds from six essential oils

against *Callosobruchus maculatus*. Sci. Rep. 15, 15180. https://doi.org/10.1038/s41598-025-98566-z.
Feng, X., Xiao, Z., Yang, Y., Chen, S., Liao, S., Luo, H., He, L., Wang, Z., Fan, G., 2021a. β-pinene derived products with enhanced *in vitro* antimicrobial activity. Nat. Prod. Commun. 16, 1934578X21992218. https://doi.org/10.1177/1934578X21992218.
Fernandes, L., Costa, R., Silva, S., Henriques, M., Costa-de-Oliveira, S., Rodrigues, M.E., 2023. Effect of vapor-phase oregano essential oil on resistant candida species biofilms: mechanisms of action. Microbiol Spectr. 11, e05124-22. https://doi.org/10.1128/spectrum.05124-22.
Gajbhiye, N.A., Saha, T.N., Kadam, G.B., Raju, S., Ahammed Shabeer, T.P., Karne, S., Prasad, K.V., Kumar, S.P.J., 2025. Chemoprofiling of essential oils from *Chrysanthemum morifolium* Ramat. flowers: delineation of genotypic variations for industrial applications. Ind. Crops Prod. 230, 121137. https://doi.org/10.1016/j.indcrop.2025.121137.
Gebreil, S., Mahgoub, S., Zewar, M., Gharib, D., 2024. Insecticidal efficacy of Chrysanthemum cinerariaefolium seed oil against cowpea beetle and its impact on the physicochemical and technological characteristics of cowpea during storage. Food Technol. Res. J. 3, 59–78. https://doi.org/10.21608/ftrj.2024.345942.
Ghannay, S., Aouadi, K., Kadri, A., Snoussi, M., 2022. *In vitro* and *in silico* screening of anti-*Vibrio* spp., antibiofilm, antioxidant and anti-quorum sensing activities of Cuminum cyminum L. volatile oil. Plants 11, 2236. https://doi.org/10.3390/plants11172236.
Gupta, H., Deeksha, Urvashi, Reddy, S.G.E., 2023. Insecticidal and detoxification enzyme inhibition activities of essential oils for the control of pulse beetle, *Callosobruchus maculatus* (F.) and *Callosobruchus chinensis* (L.) (Coleoptera: Bruchidae). Molecules 28, 492. https://doi.org/10.3390/molecules28020492.
Hadizadeh, H., Samiei, L., Shakeri, A., 2022. Chrysanthemum, an ornamental genus with considerable medicinal value: a comprehensive review. South Afr. J. Bot. 144, 23–43. https://doi.org/10.1016/j.sajb.2021.09.007.
Hernández-Jiménez, E., Del Campo, R., Toledano, V., Vallejo-Cremades, M.T., Muñoz, A., Largo, C., Arnalich, F., García-Rio, F., Cubillos-Zapata, C., López-Collazo, E., 2013. Biofilm vs. planktonic bacterial mode of growth: which do human macrophages prefer? Biochem. Biophys. Res. Commun. 441, 947–952. https://doi.org/10.1016/j.bbrc.2013.11.012.
Hodaei, M., Rahimmalek, M., Arzani, A., 2021. Variation in bioactive compounds, antioxidant and antibacterial activity of Iranian *Chrysanthemum morifolium* cultivars and determination of major polyphenolic compounds based on HPLC analysis. J. Food Sci. Technol. 58, 1538–1548. https://doi.org/10.1007/s13197-020-04666-1.
Jackson-Davis, A., White, S., Kassama, L.S., Coleman, S., Shaw, A., Mendonca, A., Cooper, B., Thomas-Popo, E., Gordon, K., London, L., 2023. A review of regulatory standards and advances in essential oils as antimicrobials in foods. J. Food Prot. 86, 100025. https://doi.org/10.1016/j.jfp.2022.100025.
Jayaram, C.S., Chauhan, N., Dolma, S.K., Reddy, S.G.E., 2022. Chemical composition and insecticidal activities of essential oils against the pulse beetle. Molecules 27, 568. https://doi.org/10.3390/molecules27020568.
Jung, E.-K., 2009. Chemical Composition and antimicrobial activity of the essential oil of *Chrysanthemum indicum* against oral bacteria. J. Bacteriol. Virol. 39, 61. https://doi.org/10.4167/jbv.2009.39.2.61.
Kačániová, M., Terentjeva, M., Galovičová, L., Ivanišová, E., Štefániková, J., Valková, V., Borotová, P., Kowalczewski, P., Kunová, S., Felšöciová, S., Tvrdá, E., Žiarovská, J., Benda Prokeinová, R., Vukovic, N., 2020. Biological activity and antibiofilm molecular profile of *Citrus aurantium* essential oil and its application in a food model. Molecules 25, 3956. https://doi.org/10.3390/molecules25173956.
Kačániová, M., Galovičová, L., Valková, V., Ďuranová, H., Borotová, P., Štefániková, J., Vukovic, N.L., Vukic, M., Kunová, S., Felsöciová, S., Miklášová, K., Savitskaya, T., Grinshpan, D., 2021. Chemical composition and biological activity of *Salvia officinalis* essential oil. Acta Hortic. Regiotect. 24, 81–88. https://doi.org/10.2478/ahr-2021-0028.
Kačániová, M., Galovičová, L., Schwarzová, M., Čmiková, N., 2023a. Antimicrobial effects of Rosemary essential oil with potential use in the preservation of fresh fruits and vegetables. Acta Hortic. Regiotect. 26, 28–34. https://doi.org/10.2478/ahr-2023-0005.
Kačániová, M., Vukovic, N.L., Čmiková, N., Galovičová, L., Schwarzová, M., Šimora, V., Kowalczewski, P., Kluz, M.I., Puchalski, C., Bakay, L., Vukic, M.D., 2023b. *Salvia sclarea* essential oil chemical composition and biological activities. IJMS 24, 5179. https://doi.org/10.3390/ijms24065179.
Kačániová, M., Čmiková, N., Vukovic, N.L., Verešová, A., Bianchi, A., Garzoli, S., Ben Saad, R., Ben Hsouna, A., Ban, Z., Vukic, M.D., 2024. *Citrus limon* essential oil: chemical composition and selected biological properties focusing on the antimicrobial (*In Vitro, In Situ*), antibiofilm, insecticidal activity and preservative effect against Salmonella enterica inoculated in carrot. Plants 13, 524. https://doi.org/10.3390/plants13040524.
Kačániová, M., Vukic, M.D., Vukovic, N.L., Terentjeva, M., Ban, Z., Li, L., Bianchi, A., Ben Saad, R., Ben Hsouna, A., Elizondo-Luévano, J.H., Čmiková, N., Garzoli, S., 2025. Chemical composition, antimicrobial, antibiofilm and insecticidal enhancing of *Eucalyptus citriodora* essential oil and its potential to shelf-life extension of pumpkin after inoculation of Salmonella enterica. Food Control 172, 111152. https://doi.org/10.1016/j.foodcont.2025.111152.
Karabörklü, S., Ayvaz, A., 2023. A comprehensive review of effective essential oil components in stored-product pest management. J. Plant Dis. Prot. 130, 449–481. https://doi.org/10.1007/s41348-023-00712-0.
Kim, K.-J., Kim, Y.-H., Yu, H.-H., Jeong, S.-I., Cha, J.-D., Kil, B.-S., You, Y.-O., 2003. Antibacterial activity and chemical composition of essential oil of *Chrysanthemum boreale*. Planta Med. 69, 274–277. https://doi.org/10.1055/s-2003-38479.
Kong, A.S.-Y., Lim, S.-H.E., Cheng, W.-H., Yuswan, M.H., Tan, N.-P., Lai, K.-S., 2025. Harnessing Monoterpenes and Monoterpenoids as Weapons against Antimicrobial Resistance. Pol. J. Microbiol. 74, 1–18. https://doi.org/10.33073/pjm-2025-010.
Kuang, C., Lv, D., Shen, G., Li, S., Luo, Q., Zhang, Z., 2018. Chemical composition and antimicrobial activities of volatile oil extracted from *Chrysanthemum morifolium* Ramat. J. Food Sci. Technol. 55, 2786–2794. https://doi.org/10.1007/s13197-018-3203-1.
Lawal, O.A., Ogunwande, I.A., Olorunloba, O.F., Opoku, A.R., 2014. The essential oils of *Chrysanthemum morifolium* Ramat. from Nigeria. Am. J. Essent. Oils Nat. Prod. 2, 63–66.
Li, L., Shi, C., Yin, Z., Jia, R., Peng, L., Kang, S., Li, Z., 2014. Antibacterial activity of α-terpineol may induce morphostructural alterations in *Escherichia coli*. Braz. J. Microbiol. 45, 1409–1413. https://doi.org/10.1590/S1517-83822014000400035.
Lin, H.-J., Hsu, P.-H., Lin, T.-C., Lu, W.-J., Lin, H.-T.V., 2024. Solid- and vapor-phase antibacterial activities and mechanisms of essential oils against fish spoilage bacteria. Antibiotics 13, 1137. https://doi.org/10.3390/antibiotics13121137.
Matos, L.F., Barbosa, D.R.E.S., Lima, E.D.C., Dutra, K.D.A., Navarro, D.M.D.A.F., Alves, J. L.R., Silva, G.N., 2020. Chemical composition and insecticidal effect of essential oils from *Illicium verum* and *Eugenia caryophyllus* on *Callosobruchus maculatus* in cowpea. Ind. Crops Prod. 145, 112088. https://doi.org/10.1016/j.indcrop.2020.112088.
Melkina, O.E., Plyuta, V.A., Khmel, I.A., Zavilgelsky, G.B., 2021. The mode of action of cyclic monoterpenes (−)-limonene and (+)-α-pinene on bacterial cells. Biomolecules 11, 806. https://doi.org/10.3390/biom11060806.
Monacci, E., Sanmartin, C., Bianchi, A., Pettinelli, S., Najar, B., Mencarelli, F., Taglieri, I., 2025. Chemical quality and characterization of essential oils in postharvest Hop cv. cascade: ventilated room temperature as a sustainable alternative to hot-stove and freeze-drying processes. Beverages 11, 54. https://doi.org/10.3390/beverages11020054.
Palomares-Navarro, J.J., Bernal-Mercado, A.T., González-Aguilar, G.A., Ortega-Ramirez, L.A., Martínez-Téllez, M.A., Ayala-Zavala, J.F., 2022. Antibiofilm action of plant terpenes in *Salmonella* strains: potential inhibitors of the synthesis of extracellular polymeric substances. Pathogens 12, 35. https://doi.org/10.3390/pathogens12010035.
Pandey, A.K., Palni, U.T., Tripathi, N.N., 2014. Repellent activity of some essential oils against two stored product beetles *Callosobruchus chinensis* L. and *C. maculatus* F. (Coleoptera: Bruchidae) with reference to *Chenopodium ambrosioides* L. oil for the safety of pigeon pea seeds. J. Food Sci. Technol. 51, 4066–4071. https://doi.org/10.1007/s13197-012-0896-4.
Paz-Méndez, A., Lamas, A., Vázquez, B., Miranda, J., Cepeda, A., Franco, C., 2017. Effect of food residues in biofilm formation on stainless steel and polystyrene surfaces by Salmonella enterica strains isolated from poultry houses. Foods 6, 106. https://doi.org/10.3390/foods6120106.
Ribeiro, J.C.S., Arantes, A.C.S., Soares, D.S., Cardoso, M.D.G., Campos, A.K., Remedio, R. N., 2025. Alpha- and beta-pinene alter the morphology of oocytes in *Rhipicephalus microplus* ticks (Acari: Ixodidae). Vet. Parasitol. 337, 110507. https://doi.org/10.1016/j.vetpar.2025.110507.
Said-Al Ahl, H.A.H., Kačániova, M., Mahmoud, A.A., Hikal, W.M., Čmiková, N., Szczepanek, M., Błaszczyk, K., Al-Balawi, S.M., Bianchi, A., Smaoui, S., Tkachenko, K.G., 2024. Phytochemical characterization and biological activities of essential oil from *Satureja montana* L., a medicinal plant grown under the influence of fertilization and planting dates. Biology 13, 328. https://doi.org/10.3390/biology13050328.
Sharma, J.H., Tiwari, S., 2021. Fumigant toxicity of alpha-pinene, beta-pinene, eucalyptol, linalool and sabinene against rice weevil, Sitophilus oryzae (L.).
Sharma, N., Radha, Kumar, M., Kumari, N., Puri, S., Rais, N., Natta, S., Dhumal, S., Navamaniraj, N., Chandran, D., Mohankumar, P., Muthukumar, M., Senapathy, M., Deshmukh, V., Damale, R.D., Anitha, T., Balamurugan, V., Sathish, G., Lorenzo, J.M., 2023. Phytochemicals, therapeutic benefits and applications of chrysanthemum flower: a review. Heliyon 9, e20232. https://doi.org/10.1016/j.heliyon.2023.e20232.
Shunying, Z., Yang, Y., Huaidong, Y., Yue, Y., Guolin, Z., 2005. Chemical composition and antimicrobial activity of the essential oils of *Chrysanthemum indicum*. J. Ethnopharmacol. 96, 151–158. https://doi.org/10.1016/j.jep.2004.08.031.
Silva, A.C.R.D., Lopes, P.M., Azevedo, M.M.B.D., Costa, D.C.M., Alviano, C.S., Alviano, D. S., 2012. Biological activities of a-pinene and β-pinene enantiomers. Molecules 17, 6305–6316. https://doi.org/10.3390/molecules17066305.
Somrani, M., Huertas, J.-P., Iguaz, A., Debbabi, H., Palop, A., 2025. Biofilm busters: exploring the antimicrobial and antibiofilm properties of essential oils against *Salmonella* Enteritidis. Food Sci. Technol. Int 31, 547–553. https://doi.org/10.1177/10820132241227004.
Sun, Q.-L., Hua, S., Ye, J.-H., Zheng, X.-Q., Liang, Y.-R., 2010. Flavonoids and volatiles in *Chrysanthemum morifolium* Ramat flower from Tongxiang County in China. Afr. J. Biotechnol. 9, 3817–3821.
Sushmitha, T.J., Rajeev, M., Sriyutha Murthy, P., Ganesh, S., Toleti, S.R., Karutha Pandian, S., 2021. Bacterial community structure of early-stage biofilms is dictated by temporal succession rather than substrate types in the southern coastal seawater of India. PLoS ONE 16, e0257961. https://doi.org/10.1371/journal.pone.0257961.
Tkaczyk, M., 2025. Biofilm as a key element in the bacterial pathogenesis of forest trees: a review of mechanisms and ecological implications. Microorganisms 13, 2649. https://doi.org/10.3390/microorganisms13122649.
Verešová, A., Vukic, M.D., Vukovic, N.L., Terentjeva, M., Ban, Z., Li, L., Bianchi, A., Kollár, J., Ben Saad, R., Ben Hsouna, A., Elizondo-Luévano, J.H., Kluz, M.I., Čmiková, N., Garzoli, S., Kačániová, M., 2024. Chemical composition, biological activity, and application of *Rosa damascena* essential oil as an antimicrobial agent in minimally processed eggplant inoculated with *Salmonella enterica*. Foods 13, 3579. https://doi.org/10.3390/foods13223579.

Vidaković Knežević, S., Knežević, S., Milanov, D., Vranešević, J., Pajić, M., Kocić-Tanackov, S., Karabasil, N., 2025. Essential oils as a novel anti-biofilm strategy against *Salmonella* enteritidis isolated from chicken meat. Microorganisms 13, 2412. https://doi.org/10.3390/microorganisms13102412.

Wang, Y., Liu, H., Zhan, F., 2022. Effects of natural borneol on germ tube formation and preformed biofilm activity in *Candida albicans*. Nat. Prod. Commun. 17, 1934578X221129128. https://doi.org/10.1177/1934578X221129128.

Xiao, S., Yu, H., Guo, Y., Cheng, Y., Yao, W., 2025. The antibacterial and anti-inflammatory potential of *Cinnamomum camphora* chvar. borneol essential oil *in vitro*. Plants 14, 1880. https://doi.org/10.3390/plants14121880.

Yang, X., Zhao, S., Deng, Y., Xu, W., Wang, Z., Wang, W., Lv, R., Liu, D., 2023. Antibacterial activity and mechanisms of α-terpineol against foodborne pathogenic bacteria. Appl. Microbiol Biotechnol. 107, 6641–6653. https://doi.org/10.1007/s00253-023-12737-4.

Youssef, F.S., Eid, S.Y., Alshammari, E., Ashour, M.L., Wink, M., El-Readi, M.Z., 2020. *Chrysanthemum indicum* and *Chrysanthemum morifolium*: chemical composition of their essential oils and their potential use as natural preservatives with antimicrobial and antioxidant activities. Foods 9, 1460. https://doi.org/10.3390/foods9101460.

Yu, H., Ren, X., Yang, F., Xie, Y., Guo, Y., Cheng, Y., Yao, W., 2022. Antimicrobial and anti-dust mite efficacy of *Cinnamomum camphora chvar. Borneol* essential oil using pilot-plant neutral cellulase-assisted steam distillation. Lett. Appl. Microbiol. 74, 258–267. https://doi.org/10.1111/lam.13610.

Zentek, J., Buchheit-Renko, S., Ferrara, F., Vahjen, W., Van Kessel, A.G., Pieper, R., 2011. Nutritional and physiological role of medium-chain triglycerides and medium-chain fatty acids in piglets. Anim. Health Res. Rev. 12, 83–93. https://doi.org/10.1017/S1466252311000089.

Zhan, J., He, F., Cai, H., Wu, M., Xiao, Y., Xiang, F., Yang, Y., Ye, C., Wang, S., Li, S., 2021. Composition and antifungal mechanism of essential oil from *Chrysanthemum morifolium* cv. Fubaiju. J. Funct. Foods 87, 104746. https://doi.org/10.1016/j.jff.2021.104746.